Kinetic radical additions are apparently controlled by the interplay between the reaction enthalpy and the charge transfer during the course of the reaction, …

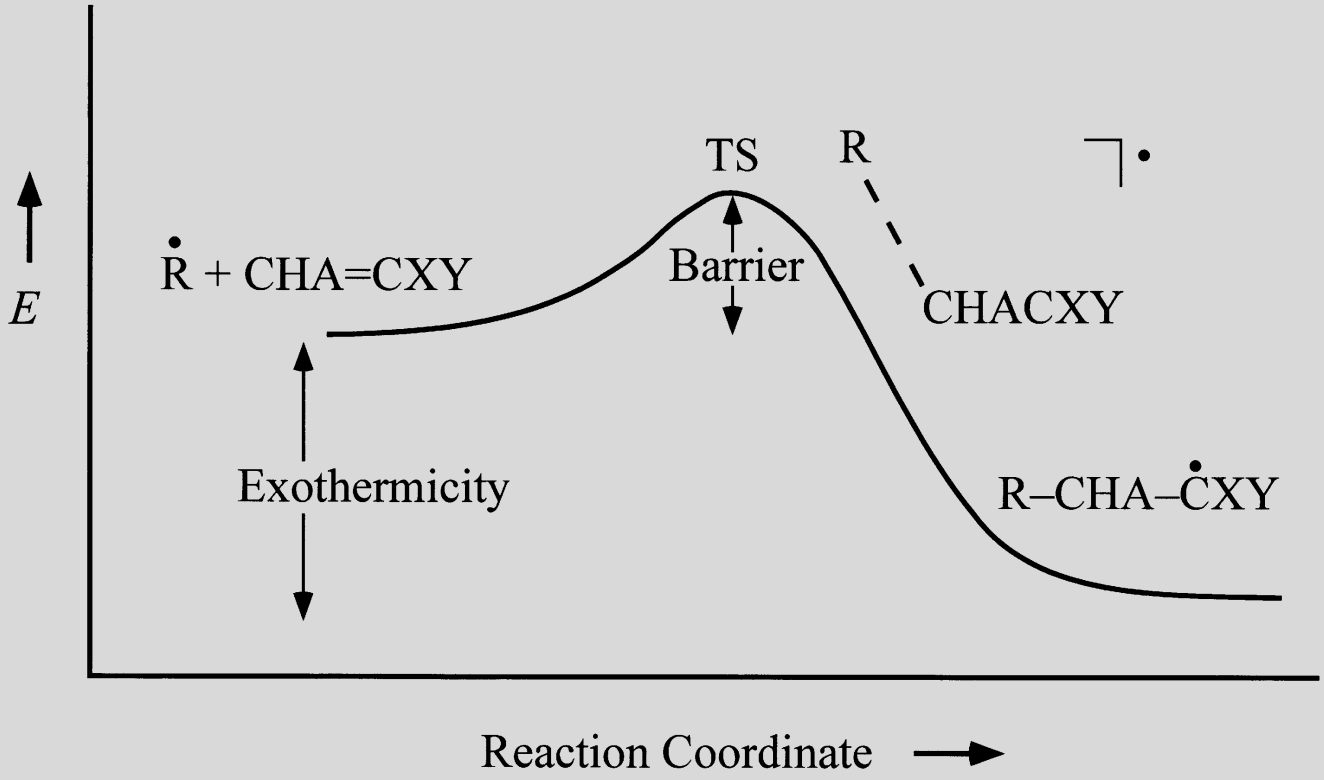

… and the nucleophilic and electrophilic polar effects of the substituents (A, X, Y). This dependency can be described accurately by new nonlinear equations.

Factors Controlling the Addition of Carbon-Centered Radicals to Alkenes—An Experimental and Theoretical Perspective

Hanns Fischer* and Leo Radom

The successful exploitation of syntheses involving the generation of new carbon–carbon bonds by radical reactions rests on some prior knowledge of the rate constants for the addition of carbon-centered radicals to alkenes and other unsaturated molecules, and of the factors controlling them. Two former classical reviews in *Angewandte Chemie* by Tedder (1982) and by Giese (1983) provided mechanistic insight and led to various qualitative rules on the complex interplay of enthalpic, polar, and steric effects. In the meantime, the field has experienced very rapid progress: many more experimental absolute rate constants have become available, and there have been major advances in the efficiency and reliability of quantum-chemical methods for the accurate calculation of transition structures, reaction barriers, and reaction enthalpies. Herein we review this progress, recommend suitable experimental and theoretical procedures, and display representative data series for radical additions to alkenes. On this basis, and guided by the pictorial tool of the state-correlation diagram for radical additions, we then offer a new and more stringent quantification of the controlling factors. Our analysis leads to a partial revision of the previous qualitative rules, and it more clearly exhibits the interplay of the reaction enthalpy effects, polar charge-transfer contributions, and steric substituent effects on the reaction energy barrier. The various contributions are cast into the form of new, simple, and physically meaningful but non-linear, predictive equations for the preestimation of rate constants. These equations prove successful in several tests but call for additional theoretical and experimental foundation. The kinetics of related reactions such as polymer propagation, copolymerization, and the addition of radicals to alkynes and aromatic compounds is shown to follow the same principles.

Keywords: ab initio calculations · additions · kinetics · radical reactions

1. Introduction

The addition of carbon-centered radicals to alkenes and other unsaturated compounds leads to the creation of new carbon–carbon σ bonds at the expense of existing π bonds. It is a very important radical reaction and has long been applied in polymer chemistry, but recent years have also seen numerous applications in the synthesis of small molecules.[1–3] The reaction rates and selectivities vary considerably, and depend on the substitution of both the substrate and the radical. For example, in liquid solution at room temperature the methyl radical adds to propene with a rate constant of $4300\,\mathrm{M^{-1}\,s^{-1}}$, while the reaction is about 100 times faster with styrene ($2.6\times10^5\,\mathrm{M^{-1}\,s^{-1}}$) and acrylonitrile ($5.4\times10^5\,\mathrm{M^{-1}\,s^{-1}}$). The addition of a simple derivative, the hydroxymethyl radical, to propene ($270\,\mathrm{M^{-1}\,s^{-1}}$) and styrene ($2.3\times10^4\,\mathrm{M^{-1}\,s^{-1}}$) is more than ten times slower than the addition of the methyl radical, but hydroxymethyl radical reacts markedly faster than the methyl radical with acrylonitrile ($1.1\times10^6\,\mathrm{M^{-1}\,s^{-1}}$). Such order-of-magnitude rate variations may result in the success or failure of syntheses, and therefore a predictive synthetic strategy relies on some prior knowledge of the rate constants for the addition, and of the factors controlling them.[2, 4]

These factors have found extensive discussion since the early days of radical chemistry[5] and were summarized some time ago in this journal, especially for the addition to alkenes, by Tedder[6] and by Giese.[7] There is a "complex interplay of polar, steric, and bond-strength effects",[6] but Tedder and Giese were able to extract several general but qualitative rules. These were subsequently supported by others,[2, 8] and have found widespread acceptance.

[*] Prof. H. Fischer
Physikalisch-Chemisches Institut der Universität Zürich
Winterthurerstrasse 190
8057 Zürich (Switzerland)
Fax: (+41) 1-6356856
E-mail: hfischer@pci.unizh.ch
Prof. L. Radom
Research School of Chemistry
Australian National University
Canberra, ACT 0200 (Australia)

  1433-7851/01/4008-1341 $ 17.50+.50/0

In the meantime, considerable progress has been made, both in accurate experimental determinations of absolute rate constants for radical reactions and their activation parameters, and in quantum-chemical calculations of transition state structures and reaction barriers. Moreover, a unifying theoretical model for the interpretation of reaction barriers has become available. Hence, a reconsideration of the controlling factors seems timely. Herein, we first outline the previous interpretations, sketch the refined rationalization concept, and summarize the progress of the experimental and theoretical methods. Then, we present and discuss absolute rate constants and activation parameters for the addition of several prototype carbon-centered radicals to a large variety of typical alkenes, explicitly covering cases mainly from our own work. These form a representative series, allow important and clarifying generalizations, and lead to a general predictive analysis which extends an earlier attempt[9] and is presented here for the first time. The experimental data have been obtained for reactions in solution, and the theoretical reaction barriers by state-of-the-art ab initio calculations. In addition to the main topic of additions to alkenes, related subjects such as additions to alkynes, aromatics, and other unsaturated compounds, as well as polymerizations, are briefly mentioned, but we will not review these fields exhaustively, nor will we cover the stereochemical aspects of additions,[10] intramolecular cyclizations, and the multitude of known synthetic applications.[2, 3]

2. Concepts for the Interpretation of Reactivities and Regioselectivities

2.1. Previous Rules for the Addition of Radicals to Alkenes

The addition of a reactive carbon-centered radical to a molecule with a multiple carbon–carbon bond is generally exothermic because a π bond is replaced by a σ bond (Figure 1). Therefore, and according to Hammond's postulate,[11] the transition state is early, that is, the cleavage of the π bond and the formation of the σ bond are far from being complete in the transition structure. Figure 2 shows the transition structure obtained from recent high-level calcula-

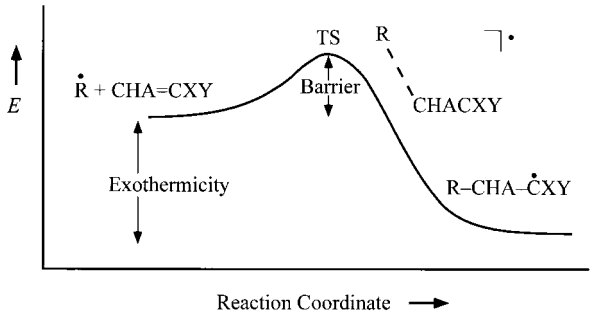

Figure 1. Schematic energy profile showing the reaction of a radical R· with an alkene CHA=CXY.

H. Fischer

L. Radom

Hanns Fischer born in 1935 started his academic career at the Technical University Darmstadt, Germany, where he obtained his Diploma (1960), Ph.D.(1963), and Habilitation (1966) all in Physics working at the Deutsches Kunststoff-Institut, mostly studying the structure and reactivity of polymer related transient carbon-centered free radicals by spectroscopic means (ESR, NMR, CIDNP). After leading a physico-chemically oriented division of this Institute, a short period at Carnegie-Mellon University Pittsburgh (USA), and teaching molecular physics at the Technical University Darmstadt he moved in 1969 to his present position as associate, then (1971) full professor for Physical Chemistry of the University of Zürich. There, he continued to work on transient organic free radicals, their structure, reaction mechanisms, and reaction kinetics in liquid solutions employing and developing ESR, CIDNP, optical spectroscopy, and muon spin rotation methods. In this field he has authored more than 200 original publications and several reviews and edited large series of tables on radical properties and kinetics in Landolt–Börnstein. Special honors include the Centenary Medal and Lectureship of the Chemical Society London and the Silver Medal of the International EPR Society.

Leo Radom was born in 1944. He studied at the University of Sydney, obtaining a B.Sc. degree and the University Medal in 1965, and a Ph.D. in 1969 in the general area of physical organic chemistry. Following a 3½ year postdoctoral period on a Fulbright Fellowship with John Pople at Carnegie-Mellon University in Pittsburgh (USA), he returned to Australia in 1972 on a Queen Elizabeth II Fellowship at the Research School of Chemistry of the Australian National University where he currently holds the position of Professor. His main research interests are concerned with the study of the structures and stabilities of molecules and the mechanisms of reactions in which they are involved by use of ab initio molecular orbital theory. His achievements have been recognized through the award of the Rennie Medal, the H. G. Smith Medal, and the Archibald Olle Prize of the Royal Australian Chemical Institute, the Schrödinger Medal of the World Association of Theoretically Oriented Chemists, and through election to the Australian Academy of Science and the International Academy of Quantum Molecular Science.

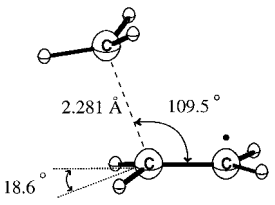

Figure 2. Transition structure for the addition of the methyl radical to ethene (QCISD(T)/6-31GT(d)). From refs. [12, 13].

tions for the addition of the methyl radical to ethene.[12, 13] As expected, the newly forming bond is still long (2.281 Å), but the angle of attack (109.5°) is already close to the corresponding angle in the product radical. There are appreciable out-of-plane deformations of the hydrogen atoms at both the α carbon atom of ethene (18.6°) and at the radical carbon (32.4°). These general features have been found for the transition structures for a large variety of addition reactions. The unsymmetrical structure means that additions to the two carbon atoms of an unsymmetrically substituted multiple bond have separate and in general different rate constants.

The temperature dependence of the rate constants is well described by the Arrhenius equation $k = A\exp(-E_a/RT)$. Thus, at a given temperature, the rate variations with radical and substrate substitution can be caused by variations in the frequency factor (A) and/or the activation energy (E_a). For polyatomic radicals, the frequency factors span a narrow range of one to two orders of magnitude ($6.5 < \lg(A/M^{-1}s^{-1}) < 8.5$).[6] Hence, the large variation in the rate constants is mainly because of variations in the activation energy.

The major factors influencing the activation energy are a) steric effects of the radical and alkene substituents, b) effects of the overall reaction enthalpy, and c) so-called polar effects. They are covered by the rules of Tedder and Giese:[6, 7]

a) Steric effects of repulsion between the radical and the alkene substituents X, Y, and A (Figure 1) decrease the rate constants and have been rationalized in terms of steric substituent parameters.[6, 7] They are thought to decrease the frequency factor and simultaneously increase the activation energy. The steric effects are in accord with the transition structure (Figure 2), in that substituents at the attacked alkene carbon atom (α substituents, A) hinder the reaction much more than substituents at the remote carbon atom (β substituents, X and Y). This explains why the addition to monosubstituted and 1,1-disubstituted alkenes occurs predominantly at the unsubstituted carbon atom, for 1,1,2-trisubstituted alkenes at the carbon with the single substituent, and for 1,2-disubstituted alkenes and alkynes at the carbon atom which carries the "smaller" group.

b) The reaction enthalpies (H_r) range from about $-180\ kJ\,mol^{-1}$ to $-20\ kJ\,mol^{-1}$ (see Sections 4.2, 4.3). The activation energies range from close to zero to about $42\ kJ\,mol^{-1}$ and show less variation than the reaction enthalpies with alkene or radical substitution, as one would expect for early transition states. Generally, they decrease with increasing exothermicity, as expressed by the Evans–Polanyi–Semenov[14] relation [Eq. (1)]. For exothermic proc-

$$E_a = \text{const} + \alpha H_r \qquad (1)$$

esses, the proportionality constant (α) is thought to be approximately 0.25,[14b] which means that about one quarter of the variation in H_r is transferred to the transition structure. H_r includes the stabilizing or destabilizing effects of substituents on the adding radical, the alkene, and the adduct radical, factors which were extensively noted in the earlier work.[6, 7]

c) Polar substituent effects reveal themselves by particularly fast additions of electron-donor-substituted radicals to electron-acceptor-substituted alkenes and of acceptor-substituted radicals to donor-substituted alkenes. In early work, they were loosely ascribed to contributions of charge-transfer resonance structures to the transition state.[5a] In the terms of frontier molecular orbital (FMO) theory,[7] the polar effects are attributed to orbital interactions. The energy of the singly occupied molecular orbital (SOMO) of an electron-donor-substituted radical is relatively high, and the energy of the lowest unoccupied molecular orbital (LUMO) of an acceptor-substituted alkene is low. Interaction of these energetically close orbitals lowers the energy of the transition state and provides a partial electron transfer from the radical to the alkene. Hence, donor-substituted radicals express a nucleophilic character, and this increases with the acceptor strength of the alkene substituent. On the other hand, the low-lying SOMO of an acceptor-substituted radical interacts favorably with the high-lying highest occupied molecular orbital (HOMO) of a donor-substituted alkene. This leads to a partial electron transfer from the alkene to the radical, and such radicals show an electrophilic addition pattern.

Evidence for the polar effects is provided by good correlations of rate data with polar σ-substituent constants, from which a nucleophilic character was deduced for the methyl radical and its alkyl- or other donor-substituted derivatives.[6, 7] On the other hand, radicals carrying fluoro substituents,[6, 15] or two cyano,[16] or two carboxy[17] groups at the radical center were recognized as electrophilic. Giese, in his review,[7] thought that the polar effects even override the influence of the enthalpy, the exception being for an attacking radical with phenyl substituents. It has also been stated[18] that monocyano- and monocarboxy-substituted radicals react fast with alkenes carrying strong electron-acceptor substituents and also with alkenes carrying strong electron-donor substituents, and hence exhibit an ambiphilic addition behavior towards alkene substitution.

Besides the steric, enthalpic (bond strength), and polar effects, other factors have also been suggested. Thus, Szwarc et al.[19] argued that the activation energy should decrease with decreasing alkene triplet-excitation energy, and this was exemplified by additions to aromatic compounds. In addition, an influence of the hybridization of the radical carbon atom has been proposed. It is known that alkyl radicals with fluoro or other lone-pair-donor substituents are pyramidally hybridized at the radical carbon, whereas methyl, benzyl, and acceptor-substituted radicals are planar or close to planar. In the transition structure, the bonds at the initial radical carbon atom adopt a pyramidal configuration (Figure 2). Intuitively,[15, 20] this seems easier to reach when it is already present in the radical, and therefore pyramidal radicals such as trifluoromethyl should have an advantage. On the other hand, radicals with extended delocalization such as the benzyl radical and cyano- or carboxy-substituted methyl radicals are expected to resist pyramidalization, which by this argument may lead to higher activation energies.[21]

2.2. The State Correlation Diagram

In the past 20 years, a more unifying theoretical framework for the discussion of reaction barriers in terms of the correlation and the interaction of reactant and product electronic configurations has been developed by Shaik and Pross.[22, 23] It extends earlier work[24] and is based on a valence-bond (VB) description of chemical reactivity. In broad terms, this approach employs qualitative energy diagrams which depict the energies of VB configurations along the reaction coordinate. The curve-crossing model, alternatively referred to as a valence-bond state correlation (VB-SC) model, configuration mixing (VB-CM) model, or state correlation diagram (SCD), has in particular been exploited to help understand the factors influencing the addition reactions of radicals to alkenes[9, 25–29] and has been theoretically supported by VBCI (CI = configuration interaction) calculations for a model system where zwitterionic states were included and substituent effects were simulated by a variation of nuclear charges.[30] Its predictive strength is further evaluated in this review.

To construct potential energy profiles for additions, one considers the four lowest doublet configurations of the three-center-three-electron system formed by the initially unpaired electron at the radical carbon atom R• and the electron pair of the attacked π bond of the alkene C=C bond. These are the reactant ground-state configuration with a singlet electron pair on the alkene ($R^{\bullet} + C{=}C^1$), the excited reactant configuration with a triplet electron pair ($R^{\bullet} + C{=}C^3$), and two polar charge-transfer (CT) configurations ($R^+ + C{=}C^-$ and $R^- + C{=}C^+$). Spin-pairing schemes and VB arguments[22–24, 30] show that the energies of the diabatic reactant configurations develop along the reaction coordinate as indicated in Figure 3. In the absence of configuration interaction (CI) and upon approach to the product geometry, the energy of the reactant ground-state configuration ($R^{\bullet} + C{=}C^1$) increases because the double bond is stretched, and because in this electronic configuration there is no bonding between the radical center and the attacked carbon atom. Hence, it leads to an excited-state configuration of the product (dotted line). On the other hand, the ground-state configuration of the product with two single bonds approaches an excited configuration of the reactant geometry, the configuration $R^{\bullet} + C{=}C^3$. At the transition geometry, the configuration mixing yields an avoided crossing and determines the reaction barrier, as indicated in Figure 3 by the heavy lines.

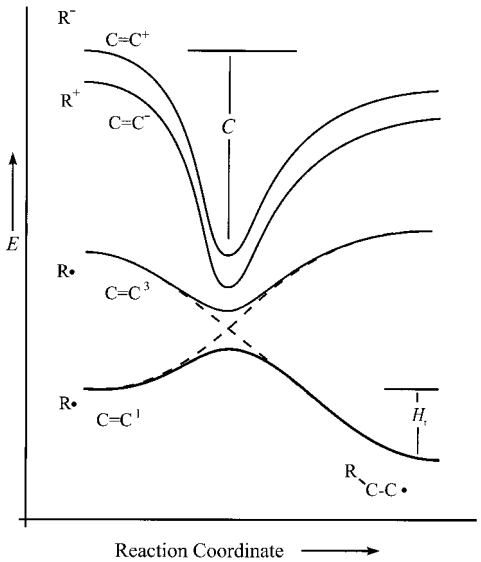

Figure 3. Schematic configuration mixing or state correlation diagram (SCD) for a radical-addition reaction showing the configuration energies as functions of the reaction coordinate.

The polar charge-transfer configurations, $R^+ + C{=}C^-$ and $R^- + C{=}C^+$ have high energies at the reactant geometry. They are stabilized as the two reactants approach one another by the Coulomb interaction (C) and can then potentially mix with the other configurations. The degree of mixing will depend on the strength of the interaction (γ) which is related to the FMO coefficients at the interacting centers. However, as long as the energies of the CT configurations remain far above the crossing region, the influence on the barrier is expected to be small. It becomes large when there is sufficient interaction and when the energy of one or both CT configurations, reduced by the Coulomb interaction, falls sufficiently close to the crossing-region of the two lower nonpolar configurations. Then, the adiabatic mixing of the nonpolar configurations with the CT configurations will lower the barrier and cause CT in the transition state.

The SCD predicts the influence of various energy parameters on the reaction barrier. Firstly, when polar effects are small or absent, the barrier should decrease with increasing exothermicity ($-H_r$), as in the Evans–Polanyi–Semenov relation [Eq. (1)]. Secondly, the barrier should decrease with a decreasing singlet–triplet energy gap ΔE_{ST} of the alkene, as suggested by Szwarc.[19] Also, with increasing exothermicity ($-H_r$) and decreasing ΔE_{ST}, the transition structure will lie earlier on the reaction coordinate, so that the distance between the reactants in the transition structure should increase. If the energies of the CT configurations are low and approach the crossing-region, polar effects will overlay the effects of the reaction enthalpy and of the singlet–triplet energy gap. Hence, the polar effects are expected to increase with decreasing energy of either of the CT configurations, namely $E_i(R) - E_{ea}(A)$ and/or $E_i(A) - E_{ea}(R)$ of the reactants reduced by the Coulomb attraction C (where E_i = ionization energy, E_{ea} = electron affinity, R = radical, A = alkene). Radicals will exhibit a nucleophilic addition pattern if $E_i(R) - E_{ea}(A) - C$ is sufficiently small, and an electrophilic reactivity pattern if $E_i(A) - E_{ea}(R) - C$ is sufficiently small. If both energies are small, the addition pattern becomes ambiphilic. However, in all cases an influence of the exothermicity and of ΔE_{ST} should remain.

A further important point, we wish to note is that the Coulomb interaction C and the interaction strength γ are expected to decrease if the radical electron spin and/or the transferred charges are delocalized over the reactants. Therefore, in comparison with less delocalizing reactants, the polar effects should be smaller in reactions involving highly conjugated radicals or alkenes, such as those carrying phenyl substituents. Also, the parameters C and γ need not be equal for nucleophilic and electrophilic contributions and may differ with radical and alkene. Finally, steric effects and/or a

resistance to pyramidalization of the radical and/or alkene may lead to a steeper increase in the ground-state energy upon approach of the reactants, and may also affect the barrier.

3. Methodology

3.1. Experimental Techniques

Up to about 25 years ago, the knowledge of radical reactivity and selectivity was essentially based only on ratios of rate constants derived from the product distributions of suitably chosen competing reactions. Since then, spectroscopic methods have become available which follow the change in the radical concentrations directly during the reactions in real time and provide absolute data. Most modern techniques employ an intermediate digital sampling and storage of the weak signals, and use digital signal processing and analysis. Hence, the methodology has enormously profited from the rapid developments in computer hardware and software. Even large sets of rate constants can now be measured within reasonable times. The reader is referred to the literature for details,[31] and we outline only a few important methods here.

Kinetic absorption spectroscopy is probably the most popular technique for determining the rates of radical reactions in solution, and it originates from the flash photolysis studies developed by Porter.[32] The radicals are generated in a photochemical reaction during a nanosecond laser pulse, and their optical absorption or that of the species formed by the addition is followed in the UV/Vis spectral range. If the reactant and product radicals do not absorb sufficiently, the reaction of interest is run in parallel to another reaction which yields a more easily followed indicator radical. The observation period lasts from about 50 ns to about 100 μs after the pulse, with the lower limit governed by the laser pulse length and luminescence disturbances. Up to about 50 to 100 μs there is usually little bimolecular radical termination so that the reactions of interest are followed under kinetic-isolation conditions. This, however, sets a lower limit to the straightforwardly accessible rate constants of about $10^5\,M^{-1}\,s^{-1}$.

In determinations of lower rate constants, the radical termination can not be avoided. It is often diffusion controlled[33] and competes with the addition process. In such cases, the rate constants can still be obtained with confidence if the radical signals are observed with sufficiently small noise levels and if all competing reactions are known. This is done by multiparameter fits of theoretical rate laws to the data. Detection by electron spin resonance[33] is advantageous because of the clear separation of interfering radical signals, and the range of accessible rate constants is about 1 to $10^6\,M^{-1}\,s^{-1}$.

Apart from these methods, pulse radiolysis initiation,[34] modulation spectroscopy,[35] and radical or product detection by muon spin rotation[35] and electron or nuclear[36] spin polarization, respectively, have also been used in time-resolving studies of absolute addition rates, and IR or Raman spectroscopy have future potential.[37] Compilations of most of the data known for low molecular weight systems are available.[31]

In the polymer domain, the determination of precise rate constants for the addition of a propagating-chain radical to its monomer has been a long-standing problem. Time-resolved techniques still await application but considerable progress has been made through the invention of laser-pulse polymerization.[38] In principle, one analyzes the distribution of the molecular weight of the polymer produced by a repetitive pulse initiation and its dependence on the time interval between the pulses. Of the many radicals formed during one pulse only a few survive. They grow by monomer addition until they are effectively scavenged by new radicals formed in the next pulse. Hence, the degree of polymerization shows a peak which depends linearly on the length of the time interval, the monomer concentration, and the propagation constant. Most often, size-exclusion chromatography is used to obtain the molecular-weight distribution, and calibrations and critical evaluations of the data are necessary.[39]

3.2. Theoretical Procedures

An alternative to experiment as a source of quantitative information about radical-addition reactions is provided by ab initio molecular orbital theory.[40, 41] Since the time of the Tedder and Giese reviews,[6, 7] there have been substantial increases in the power of computers and significant advances in the algorithms used to carry out ab initio calculations. As a result, the cost of carrying out such calculations has decreased by a factor of approximately 100 000 during this period, allowing a much greater range of systems to be examined, and providing a greater reliability in the predictions. The theoretical approach consequently represents a useful partner to experiment in the study of radical reactivity.

The ab initio calculations enable the type of information displayed in Figure 1 to be obtained. The schematic potential-energy profile in Figure 1 corresponds to the reaction between a radical R$^\bullet$ and an alkene CHA=CXY, proceeding via a transition structure (TS) to give the product radical RCHA–CXY$^\bullet$. Properties that may be calculated include complete geometries (i.e. bond lengths, bond angles, and torsional angles) and vibrational frequencies of all species including the transition structure. The vibrational frequencies rigorously characterize stationary points on the potential energy surface as minima or first-order (or higher) saddle points and they are also useful (after scaling)[42] in thermochemical and kinetic analyses. Because the determination of experimental geometries and vibrational frequencies is difficult for radicals and virtually impossible for transition structures, theory is playing a particularly useful role here. Theory can also be used to determine thermochemical quantities such as the reaction barrier and exothermicity. It also provides information on the direction and extent of charge transfer. An important feature of the ab initio calculations is that the properties of interest, for example, extent of charge transfer, reaction barrier or reaction enthalpy, can be obtained explicitly and directly.

We note that there are a broad variety of ab initio calculations, ranging from cheap and (potentially) nasty to expensive and very accurate. The quality of an ab initio calculation depends on two factors, namely the size of the basis set used in the calculation and the extent of incorporation of electron correlation. Better calculations are more expensive. In choosing the level of theory at which the calculations are to be performed, it is necessary to strike a compromise between the accuracy that is required and the computational expense that can be afforded. An important factor is that the computational cost of an ab initio calculation increases very rapidly with the size of the system that is being examined, roughly between the 2nd and 7th power of the number of electrons (for a given basis set).

It is beyond the scope of the present article to go into details concerning the theoretical procedures but it is appropriate to comment on various broad features, beginning with basis sets. Among commonly used basis sets developed by Pople and co-workers,[40] STO-3G is a small basis set, 6-31G(d) (also called 6-31G*) is a medium-sized basis set, while large basis sets have names such as 6-311 + G(3df,2p). For a given system, the cost of the ab initio calculation increases rapidly as the basis set size increases.

Theoretical procedures that are in common use, listed in order of increasingly refined treatment of electron correlation (and cost), include Hartree–Fock (HF), Møller–Plesset perturbation theory truncated at second (MP2), third (MP3), or fourth (MP4) order, quadratic configuration interaction including single, double, and (perturbatively calculated) triple excitations (QCISD(T)), and coupled cluster theory (CCSD(T)). Density functional theory (DFT)[43] is an attractive approach that is often highly cost effective, popular variants being B-LYP and B3-LYP. DFT offers the prospect of applicability to quite large systems because of the recent development of algorithms with so-called linear scaling with respect to the size of system or basis set.[44]

There is an additional degree of freedom for calculations on open-shell systems such as the radicals involved in radical-addition reactions.[45] The calculations may be carried out using either a wavefuntion restricted, in terms of the electron spins, (restricted HF; RHF) or unrestricted (unrestricted HF; UHF) starting point. In the RHF procedure, the α and β orbitals are constrained to be the same. This has the advantage that the resultant wave function is a pure doublet, characterized by the spin-squared expectation value $\langle S^2 \rangle = 0.75$. On the other hand, if the α and β orbitals are allowed to be different, leading to the UHF procedure, the energy becomes lower. However, the wave function is no longer a pure doublet but is contaminated by states of higher spin multiplicity, as reflected in an $\langle S^2 \rangle$ value greater than 0.75. It is not clear beforehand which out of RHF or UHF is better.

When electron correlation is introduced, the procedures can be based on either UHF or RHF starting points. For example, Møller–Plesset perturbation theory can be based on UHF and is then denoted UMP. If there is severe spin contamination, there can be poor convergence in the Møller–Plesset expansion so that it may be inadvisable to use the UMP procedure (see, for example, references [46, 47]). There is generally a significant improvement with the use of restricted Møller–Plesset theory (RMP)[48] or projected Møller–Plesset theory (PMP)[49] in such circumstances. For more sophisticated procedures, such as quadratic configuration interaction[50] or coupled cluster,[51] the difference between the unrestricted (UQCI, UCC) and restricted (RQCI, RCC) approaches is generally much smaller.[52] DFT calculations also appear to show less spin contamination in the wave function.[53] It has been argued that calculations using DFT should be carried out in the unrestricted form, for example, UB-LYP and UB3-LYP.[54]

An ab initio calculation requires the specification of a correlation procedure and a basis set, and this defines the level of theory that is being used. For example, HF/STO-3G represents a very low level of theory. B3-LYP/6-31G(d) or MP2/6-31G(d) represent intermediate levels of theory while QCISD(T)/6-311+G(3df,2p) and CCSD(T)/6-311+G(3df,2p) represent high levels of theory. The ultimate level of theory, yielding the exact solution to the nonrelativistic Schrödinger equation, corresponds to full electron correlation with an infinite basis set. Unfortunately, this is not accessible in practice for normal systems, so an appropriate compromise is therefore necessary. In this connection, an essential element in the application of ab initio procedures is to assess the performance of a particular method in cases where the answer is known (either from experiment or high-level theory) before using that method to probe the unknown.

A number of theoretical methods attempt to obtain higher quality results from lower quality calculations (and hence to more closely approach the exact solution of the Schrödinger equation at lower cost) by taking advantage of additivity or extrapolation procedures. For example, the assumption of additivity of the basis set and correlation effects often holds reasonably well, and therefore lends itself to such an approach. Composite procedures of this type relevant to the present work include variants of the G2 and G3 procedures of Pople and co-workers,[55] the CBS (complete basis set) procedures of Petersson and co-workers,[56] and the extrapolation procedures (e.g. W1) of Martin.[57]

4. Monosubstituted and 1,1-Disubstituted Alkenes

4.1. Experimental Results

4.1.1. Rate Constants

As described in Section 2.2, the addition of alkyl radicals to monosubstituted and 1,1-disubstituted alkenes is directed by the substituents to occur predominantly at the unsubstituted carbon atom and therefore should not be strongly affected by the individual steric demands of the alkene substituents. Therefore, we first discuss experimental data for this simplest situation and select radicals (Figure 4) which allow a case study for the action of enthalpy and polar effects alone. Besides the methyl radical,[58] we include the resonance-stabilized benzyl radical,[21, 59] and three other primary radicals, two with an electron-acceptor substituent (cyanomethyl[60] and *tert*-butoxycarbonylmethyl[60]) and one with an electron-donor substituent (hydroxymethyl[61]), four tertiary

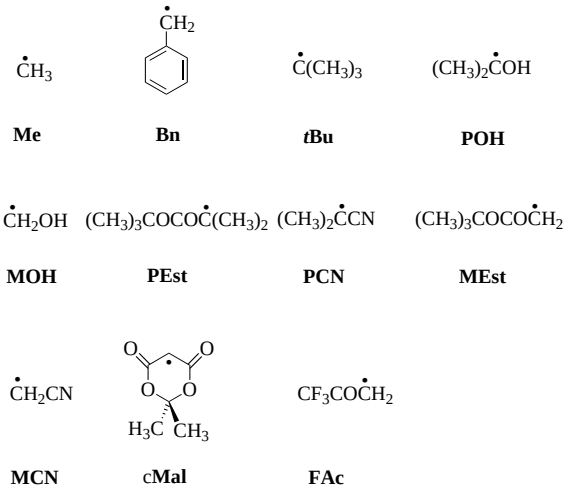

Figure 4. Radicals included in Tables 1 and 2 and in Figures 7, 8, and 12–15.

species, two with only donor substituents (*tert*-butyl[35, 36a, 62] and 2-hydroxy-2-propyl[36b, 63]) and two with two donor and one acceptor substituent (2-*tert*-butoxycarbonyl-2-propyl[64] and 2-cyano-2-propyl[65]). There are also two radicals with stronger electron-acceptor substitution, namely the cyclic malonyl radical, 2,2-dimethyl-4,6-dioxo-1,3-dioxan-5-yl, derived from Meldrum's acid,[66] and the trifluoroacetonyl radical.[64]

Table 1 gives absolute rate constants measured at or close to room temperature for the addition of these radicals to a variety of monosubstituted and 1,1-disubstituted alkenes in solution. The alkene substituents include electron-donating and electron-accepting groups with a wide range of radical-stabilizing properties, and the rate constants are believed to be accurate to better than a factor of two. For many systems, it was ascertained that the addition occurs, as expected, at the CH_2 group only. Table 1 clearly shows the enormous variability in the rate constants. They range from 14 to $2.7 \times 10^8\,\text{M}^{-1}\text{s}^{-1}$, that is, they vary by more than seven orders of magnitude. To structure the data, the alkenes are listed according to increasing rate constants for the methyl radical additions, with the exception of the phenyl-substituted alkenes which are placed at the end, and the radicals are ordered according to the different polar effects. Loosely the reactions can be characterized by the following groupings.

Methyl and benzyl radicals do not exhibit strong polar effects. With alkene substitution their rate constants vary by a factor of 200 and in a similar manner. Benzyl reacts 100–1000 times (average 470) more slowly than methyl, and much of this difference may be a result of the radical stabilizing effect of the phenyl group.

tert-Butyl, 2-hydroxy-2-propyl, and hydroxymethyl are the most selective radicals in the series, since their rate constants vary by three to five orders of magnitude. In comparison to methyl, these electron-donor-substituted species react more slowly with electron-rich alkenes but much faster with electron-deficient alkenes. Moreover, their rate constants increase strongly with the electron-accepting power of the alkene substituents. Clearly, these radicals exhibit a strong nucleophilic polar effect, and they react faster with alkenes bearing strong acceptor groups than with the phenyl-substituted alkenes, despite the exothermicity of addition being larger with the latter systems.

The radicals of the next group carry a carboxy or cyano substituent which should cause an electrophilic rate enhancement. Indeed, with most alkenes the primary species react faster than the methyl radical. Their tertiary counterparts react much more slowly (440 times for the carboxy-substituted and 210 times for the cyano-substituted radical, on average), but the reactivity pattern is similar. All four radicals are about equally selective as the methyl radical. The cyclic malonyl and trifluoroacetonyl radicals react much faster than methyl with electron-rich alkenes but slower with alkenes bearing strong electron-acceptor groups, which means that these radicals are certainly electrophilic. However, they are less selective than methyl, because their rate constants for the non-phenyl-substituted alkenes vary only by factors of 10 to 100. For the electrophilic trifluoromethyl and perfluoro-*n*-alkyl radicals, the same trends have been observed.[20, 67]

4.1.2. Frequency Factors and Activation Energies

For many but not all additions, the activation parameters have been determined from rate constants obtained at several temperatures, and the frequency factors are also presented in Table 1. For a given radical reacting with the various alkenes, these constants and factors center around a mean value. There are large deviations from the averages, but a comparison of all the data appears to show no systematic dependence on the alkene substitution. Instead, the large deviations often occur when the frequency factors and the activation energies are both either exceptionally low or high. This suggests that the scatter is mainly because of the known error correlation of the activation parameters, for which the χ^2-surface over $\lg(A)$ and E_a has an extended minimum valley. Hence, we believe that the large deviations are accidental.

The frequency factors for the primary radicals center around $\lg(A/\text{M}^{-1}\text{s}^{-1}) = 8.5$, and for the tertiary radicals they center around $\lg(A/\text{M}^{-1}\text{s}^{-1}) = 7.5$. The frequency factor for the cyclic malonyl radical is larger, $\lg(A/\text{M}^{-1}\text{s}^{-1}) = 8.7$, and the corresponding open-chain di-*tert*-butylmalonyl radical (not included in Table 1) has an intermediate value, $\lg(A/\text{M}^{-1}\text{s}^{-1}) = 8.2$.[66] Apart from this trend, there appears to be no systematic variation with specific radical substituents. The narrow ranges of the frequency factors are consistent with earlier notions[6] and with the similar transition structures obtained theoretically for various additions (Figure 2 and Section 4.2.3). Moreover, the differences in $\lg(A)$ appear qualitatively reasonable. Tertiary radicals should show lower values than the primary radicals because they experience increased hindrance of the internal methyl rotations in the transition structure. By the same reasoning, the frequency factor of the open-chain secondary malonyl radical should be intermediate and that of the more rigid cyclic malonyl should be larger. Based on these findings we suggest that average frequency factors can be used to calculate satisfactory activation energies from rate constants observed at a single temperature, though the averages adopted and given below for the different

Table 1. Absolute rate constants [$M^{-1}s^{-1}$] and experimental frequency factors (($\lg(A/M^{-1}s^{-1})$ in parentheses) for the addition of carbon-centered radicals to monosubstituted and 1,1-disubstituted alkenes CH_2=CXY in solution at or near room temperature. Radicals: Me = methyl, Bn = benzyl, *t*Bu = *tert*-butyl, POH = 2-hydroxy-2-propyl, MOH = hydroxymethyl, PEst = 2-*tert*-butoxycarbonyl-2-propyl = *iso*-butyryl, PCN = 2-cyano-2-propyl, MEst = *tert*-butoxycarbonylmethyl, MCN = cyanomethyl, cMal = 2,2-dimethyl-4,6-dioxo-1,3-dioxan-5-yl (a cyclic malonyl radical), FAc = trifluoroacetonyl (see Figure 4).

CH_2=CXY	Radical					
X,Y	nonpolar – nucleophilic	nucleophilic		ambiphilic – electrophilic		electrophilic
	Me/ Bn	*t*Bu	POH/ MOH	PEst/ PCN[a]	MEst/ MCN[b]	cMal/ FAc
H,H[c]	3500	1250 (7.9)			1.1×10^4	
			410 (7.9)		3.3×10^3	2.0×10^4
H,Me	4300	920 (7.4)			7.5×10^4 (8.9)	1.7×10^5
			270 (7.5)		1.2×10^4	1.9×10^5
H,Et[d]	7600	1100 (7.5)			5.4×10^4 (7.9)	2.2×10^5
	33		300 (7.5)	34	1.1×10^4	2.8×10^5
Me,Me	8500	740 (7.7)			1.8×10^5	3.8×10^5
			240 (8.0)		1.1×10^4	4.0×10^6
Me,OMe	1.2×10^4	220	1080	50	1.4×10^5 (8.1)	4.0×10^5 (8.6)
	21 (8.9)		230 (8.1)	82	3.5×10^4 (8.9)	
Me,OAc	1.2×10^4	1700	4850	58	8.8×10^4 (9.1)	5.8×10^5 (8.7)
	46 (7.7)		680 (7.4)	79	1.2×10^4	3.0×10^5
H,OEt	1.4×10^4	390 (7.7)	320	75	1.5×10^5 (8.3)	3.0×10^5 (8.6)
	14 (10.2)		180 (8.3)	108	4.3×10^4	
H,OAc	1.4×10^4 (8.4)	4200 (7.2)	7500	18	6.5×10^4 (8.1)	4.0×10^5 (8.8)
	15 (5.9)		590 (7.7)	41	1.3×10^4	2.0×10^5
H,Cl	2.0×10^4	1.6×10^4			7.1×10^4 (8.4)	1.1×10^5
			5000 (8.3)		1.2×10^4	9.5×10^4
H,$SiMe_3$	2.3×10^4 (8.1)	9600 (7.0)	2.5×10^4	75	8.9×10^4 (8.3)	2.2×10^5 (8.5)
	33 (8.4)		2060 (7.8)	75	1.3×10^4 (8.4)	1.0×10^5
Me,Cl	3.5×10^4	1.1×10^4	2.2×10^4	150	1.6×10^5 (8.4)	9.2×10^5 (8.8)
	43		2110 (7.9)	120	1.6×10^4 (8.9)	5.0×10^5
Cl,Cl	3.2×10^5 (8.9)	3.5×10^5 (8.0)	1.3×10^6	1170 (6.9)	2.7×10^5	3.9×10^5 (8.9)
	460 (8.5)		5.3×10^4 (8.1)	603	3.3×10^4 (8.8)	3.3×10^5
H,CO_2Me	3.4×10^5	1.1×10^6	3.5×10^7	1150 (6.6)	4.9×10^5	1.1×10^5 (8.7)
	430 (7.7)		7.1×10^5 (8.7)	370	1.1×10^5	1.3×10^5
Me,CO_2Me	4.9×10^5 (8.9)	6.6×10^5	1.6×10^7 (9.0)	3710	1.3×10^6	1.1×10^6 (8.9)
	2100 (8.1)		6.0×10^5 (8.6)	1590	2.4×10^5	1.2×10^6
H,CN	6.1×10^5	5.2×10^6	1.5×10^8	2640 (7.2)	5.4×10^5	1.5×10^5 (8.9)
	2200 (8.9)		1.1×10^6 (8.3)	2020	1.1×10^5 (8.4)	3.5×10^4
H,CHO	7.4×10^5	2.8×10^6	2.7×10^8	1810	3.8×10^5	1.1×10^5 (8.5)
	2500 (8.5)		2.1×10^6 (8.4)	1200	2.5×10^4 (8.5)	6.4×10^4
Me,CN	7.9×10^5 (8.9)	1.7×10^6	4.5×10^7 (8.9)	4460	9.1×10^5	6.0×10^5 (8.7)
	6600 (8.4)		6.7×10^5 (8.2)	1060	1.7×10^5	1.9×10^5
H,Ph	2.6×10^5 (8.9)	1.3×10^5 (7.6)	7.3×10^5 (7.5)	5500 (6.7)	1.9×10^6	1.2×10^6 (8.8)
	1100 (8.6)		2.3×10^4 (8.4)	2410 (7.7)	3.8×10^5	6.3×10^6
Me,Ph	3.1×10^5 (8.8)	5.9×10^4	2.0×10^5 (7.5)	6030	3.9×10^6	1.3×10^6 (8.7)
	850 (9.6)		2.8×10^4 (8.6)	2310	6.6×10^5	7.7×10^6
Ph,Ph	7.8×10^5 (7.9)	1.0×10^6	7.1×10^5 (6.9)	1.0×10^4 (7.0)	1×10^7	2.4×10^6 (8.6)
	4100 (8.5)		1.4×10^5 (8.3)	7010	2.4×10^6	6.9×10^6
$\lg(A)_{av}$[e]	8.6 ± 0.4	7.3 ± 0.4	8.0 ± 0.9	6.9 ± 0.3	8.4 ± 0.3	8.7 ± 0.1
	8.6 ± 0.3		8.1 ± 0.1	7.7	8.7 ± 0.3	

[a] 315 K. [b] 278 K. [c] Per CH_2 group, that is, the measured rate constants are divided by 2. [d] Also valid for H, *n*-alkyl. [e] Average including data for other alkenes not listed in the Table.

classes of radicals clearly need further experimental and theoretical verification.

Table 2 shows the activation energies for the reactions listed in Table 1, as calculated from the rate constants using the average values of $\lg(A/M^{-1}s^{-1}) = 8.5$ for methyl, benzyl, *tert*-butoxycarbonylmethyl, cyanomethyl, and trifluoroacetonyl, = 8.2 for hydroxymethyl and di-*tert*-butylmalonyl, = 8.5 for the cyclic malonyl radical, and = 7.5 for all tertiary radicals. The activation energies range from about 42 kJ mol^{-1} down to values close to or set to zero.[68] For the later analysis and for comparisons with theoretical data, we also display the ionization energies (E_i) and the electron affinities (E_{ea}) of the radicals and the alkenes, taken from refs. [58, 66], the reaction enthalpy (H_r(Me)) for the addition of the methyl radical to each alkene and the differences (ΔH_r) between the reaction enthalpies for the addition of methyl and for the other radicals. The reaction enthalpies H_r(Me) are only available for a very few methyl additions. Hence, the data given in Table 2 were deduced from other known quantities[69, 70] and have considerable uncertainties[58] because of the

Table 2. Activation energies E_a [kJ mol^{-1}] for the addition of carbon-centered radicals to monosubstituted and 1,1-disubstituted alkenes CH_2=CXY in solution, ionization energies E_i [eV], and electron affinities E_{ea} [eV] of radicals and alkenes, heats of addition H_r(Me) [kJ mol^{-1}] for the methyl radical, and differences $\Delta H_r = H_r(R) - H_r(Me)$ for the addition of the other radicals R to ethene. All activation energies were calculated from the rate constants of Table 1 using average frequency factors (see text). For radical abbreviations, see Table 1 and Figure 4.

	Radical							
	nonpolar-nucleophilic		nucleophilic		ambiphilic-electrophilic		electrophilic	
	Me	Bn[a]	*t*Bu	POH/ MOH	PEst/ PCN	MEst/ MCN	cMal[b]	FAc
E_i(R)	9.8	7.2	6.7	6.5/7.6	7.7[c]/8.5	9.8[c]/10.3	11[d]	10.9[c]
E_{ea}(R)	0.1	0.9	0.0	0.3/0.1	1.3[c]/1.0	1.7[c]/1.5	1.8[d]	2.63
ΔH_r(R)	0	56	16	18/14	32/55	26/30	42	40
X,Y $E_i/E_{ea}/H_r$(Me)								
H,H	28.2		25.3			24.8		24.0
10.5/ – 1.8/ – 99				33.6		26.5		
H,Me	27.7		26.1			20.2	19.8	18.4
9.7/ – 2.0/ – 97				34.6		23.5		
H,Et[f]	26.3	39.4	25.6			21.0	19.2	17.4
9.6/ – 1.9/ – 99				34.4	35.2	23.7		
Me,Me	26.0		26.6			18.1	17.8	10.9
9.2/ – 2.2/ – 98				34.9		23.7		
Me,OMe	25.1	40.5	29.6	25.3	33.1	18.7	17.7	
8.6/ – 2.5/ – 94				35.0	33.0	21.1	14.8	
Me,OAc	25.1	38.6	24.5	21.7	32.7	19.8	16.8	15.6
9.1/ – 1.5/ – 109				32.3	33.1	20.1		
H,OEt	24.8	41.5	28.2	28.4	32.1	18.5	18.4	
8.8/ – 2.2/ – 100				35.6	32.3	20.6		
H,OAc	24.8	41.4	22.3	20.6	35.6	20.5	17.7	18.3
9.2/ – 1.2/ – 101				32.7	34.7	23.3		
H,Cl	23.9		18.9			20.3	20.9	20.1
10.0/ – 1.3/ – 106				27.4		23.5		
H,$SiMe_3$	23.5	39.4	20.2	17.7	32.1	19.8	19.2	18.1
9.5/ – 1.1/ – 101				29.6	33.2	23.3	16.5	
Me,Cl	22.5	38.8	19.8	17.9	30.4	18.3	15.6	
9.8/ – 1.4/ – 99				29.5	32.0	22.9		
Cl,Cl	17.0	33.0	11.2	9.4	25.3	17.1	17.7	17.0
9.8/ – 0.8/ – 125				21.5	27.9	21.2		
H,CO_2Me	16.9	33.1	8.4	0[e]	25.3	15.6	20.9	19.4
9.9/ – 0.5/ – 117		26.0		15.1	29.1	18.4	16.7	
Me,CO_2Me	16.0	29.2	9.7	2.6	22.4	13.3	15.2	13.8
9.5/ – 0.4/ – 119		23.0		15.5	25.4	16.6		
H,CN	15.4	29.1	4.5	0[e]	23.3	15.4	20.1	22.6
10.9/ – 0.2/ – 139		23.5		14.0	24.8	18.4	16.3	
H,CHO	15.0	28.8	6.0	0[e]	24.2	16.2	20.9	21.1
10.1/0.0/ – 122				12.4	26.1	21.8	15.3	
Me,CN	14.9	26.4	7.3	0[e]	22.0	14.1	16.7	18.4
10.3/ – 0.2/ – 130				15.3	26.4	17.4		
H,Ph	17.5	30.8	13.7	10.2	21.5	8.3	15.0	9.7
8.4/ – 0.3/ – 150		25.0		23.6	24.3	15.5		
Me,Ph	17.1	31.5	15.7	13.1	21.2	10.6	14.8	9.2
8.2/ – 0.2/ – 144				23.1	24.4	14.3		
Ph,Ph	14.8	28.9	8.6	7.4	20.0	14.5	13.2	9.5
8.0/0.4/ – 153		22.1		19.1	21.6	11.3		

[a] Where two values are given, the second refers to the cumyl radical (rate constants not included in Table 1).[59] [b] Where two values are given, the second refers to the di-*tert*-butylmalonyl radical (rate constants not included in Table 1).[66] [c] Calculated values, A. P. Scott, personal communication. References to all other ionization energies and electron affinities are given in ref. [58 – 66]. [d] Data for the di-*tert*-butylmalonyl radical. [e] The rate constants are higher than the average frequency factor of A ($10^{7.5}$ M^{-1} s^{-1}) for tertiary alkyl radicals. Hence, the activation energy of the addition step was set to zero.[68] [f] Also valid for H, *n*-alkyl.

imprecision in the available C–H bond dissociation energies. The increments ΔH_r[71] are also subject to uncertainties, and their use for all alkenes assumes that the effect of γ substituents on the bond dissociation energies is independent of the α substituents.

4.1.3. Phase and Solvent Effects

In the course of this review, we will compare experimental activation energies with theoretical reaction barriers. The experimental data refer to liquid solution at ambient pressure

while the theoretical results are obtained for isolated reaction systems. Hence, a consideration of possible phase and solvent effects is appropriate.

Table 3 shows experimental rate constants and activation parameters for several addition reactions in the liquid and in the gas phase. The gas-phase data were obtained at pressures high enough to disperse the excess heat of reaction very rapidly. At room temperature, all listed gas-phase rate constants are smaller than the liquid-phase values, by an average factor of ten, but the variation with radical and substrate structure are generally rather similar. As in the liquid phase (Table 1), the frequency factors of the gas-phase reactions scatter considerably, which again suggests effects of the error correlation of the activation parameters. Interestingly, for the additions of the methyl radical to monosubstituted and 1,1-disubstituted alkenes, the average gas-phase frequency factor is $\lg(A/\text{M}^{-1}\text{s}^{-1}) = 8.50 \pm 0.75$, and practically identical to the mean reaction-in-solution value. On average, the experimental gas-phase activation energies are higher than their solution counterparts by 2.1 kJ mol^{-1}, however, when considered in detail larger differences are noticed. The close similarity of the mean frequency factors suggests that the average values found above for solutions may be adopted also for the gas phase. Using these, the reported rate constants lead to somewhat more unified gas-phase activation energies which are also shown in Table 3. Their variation with radical and substrate structure closely parallels that established for solutions.

On average, the recalculated activation energies are larger by 6.5 ± 2.3 kJ mol^{-1} for the gas than for the liquid phase, and the same trend was previously recognized in the analysis of a larger data set.[58] However, the straightforward conclusion that there is a significant, general difference, between gas-phase and liquid-phase rate constants caused mainly by different activation energies, not frequency factors, is subject to considerable uncertainty. Firstly, all gas-phase data date back many years and have been determined relative to other rate constants that are not yet firmly established.[73] Secondly, the difference is also not explained easily because there is no generally accepted theory which relates gas-phase to liquid-phase rate data. A simple explanation of a larger gas-phase activation energy is based on the Eyring equation and the difference of the thermal expansion coefficients of the two phases.[74, 75] It leads to the prediction that reaction barriers calculated for isolated systems should be larger than liquid-phase activation energies by $RT = 2.5$ kJ mol^{-1} at room temperature and the frequency factors should also be higher so that the rate constants remain equal. This is not the case in practice. Another possible explanation is suggested by the negative activation volume of the addition reactions ($\Delta V^{\neq} = -11$ to -17 cm^3 mol^{-1}). This is known from polymerizations in solution[76] and leads to an increase in the rate constants with increasing pressure, as expected from Le Chatelier's principle.[77] In liquids the molecules are held together by cohesive forces, and these will operate on the reactants and the transition state. These forces are equivalent to considerable internal liquid pressures of many thousand bars, and it has been suggested that this internal pressure influences the reaction rates as an external pressure.[78b,c] With this assumption, a general difference of the activation energies between the gas and liquid phase can, in fact, be obtained, and it is even of the correct order of magnitude.[77]

Further evidence for effects of molecular interactions, in the liquid phase, on rate constants of radical addition reactions is given by the small but noticeable dependence of these constants on solvent polarity.[79] An increase in the rate constant with increasing solvent polarity would generally be expected if the transition structure is more polar than the parent reactants. This pattern is observed for the addition of the hex-5-enyl radical to the electron-deficient alkenes, methylacrylate and acrylonitrile,[80a] and to nitroso and nitrone spin traps,[80b] and for the addition of the *tert*-butyl radical to acrylonitrile.[80c] These alkyl radicals exhibit some nucleophilic character in such reactions so that there is charge transfer in the transition state. For the addition of the *tert*-butyl radical to acrylonitrile, the rate constant increases by a factor of 3.6 upon replacement of the nonpolar solvent tetradecane by the much more polar solvent acetonitrile, from this result the transferred charge was estimated as 0.23 elementary charges.[80c] For the addition of thiyl radicals to alkenes, opposite solvent polarity effects are known, and these are presumably because of the partial loss of the large radical dipole moment during formation of the transition state.[80d]

Table 3. Rate constants k [M^{-1}s^{-1}] at 298 K,[a] frequency factors A [M^{-1}s^{-1}], and activation energies E_a [kJ mol^{-1}][b] for the addition of carbon-centered radicals to unsaturated molecules in the liquid (l) and the medium-pressure gas phase (g).[c]

Reaction	k^l	k^g	k^l/k^g	$\lg(A^l)$	$\lg(A^g)$	E_a^{l}[b]	E_a^{g}[b]
$^{\cdot}CH_3 + CH_2{=}CH_2$	7000[58b]	850[72]	8.2	9.0[d]	8.0[d]	31.4/28.2	30.8/33.5
$^{\cdot}CH_3 + CH_2{=}CHCH_3$	4300[58b]	500[73]	8.6	9.3	7.9	32.3/27.7	29.7/33.1
$^{\cdot}CH_3 + CH_2{=}CHC_2H_5$	7600[58b]	530[73]	14	7.8	8.0	22.5/26.3	30.1/33.0
$^{\cdot}CH_3 + CH_2{=}C(CH_3)_2$	8500[58b]	1400[73]	6.1	8.9	8.2	28.1/26.0	28.9/30.5
$^{\cdot}CH_3 + CH_2{=}CHF$	4600[58b]	560[73]	8.2	–	9.2	–/27.6	36.8/32.8
$^{\cdot}CH_3 + CH_2{=}CHCl$	20000[58b]	1100[72]	18	–	9.7	–/23.9	38.1/31.1
$^{\cdot}CH_3 + CH{\equiv}CH$	4800[58b]	1400[72]	3.4	9.4[d]	8.5[d]	34.3/33.2	32.2/36.2
$^{\cdot}CH_3 + CH{\equiv}CCH_3$	2200[58b]	180[73]	12	8.8	8.7	31.1/33.4	36.8/39.6
$^{\cdot}C(CH_3)_3 + CH_2{=}CH_2$	2500[62a]	30[73]	83	7.9[d]	7.0[d]	27.6/25.1	33.4/36.1

[a] Liquid-phase values were taken from Table 1 or calculated from the activation parameters. For vinyl fluoride and vinyl chloride, k_{338} was converted into k_{298} using the recommended frequency factor $\lg(A/[\text{M}^{-1}\text{s}^{-1}]) = 8.5$ for additions of primary alkyl radicals to CH_2 groups (see text). Gas-phase values were calculated from the reported activation parameters. [b] The first entry is the reported experimental activation energy. The second value was calculated from the rate constants of columns 3 and 4 with the frequency factors recommended in this work of $\lg(A/[\text{M}^{-1}\text{s}^{-1}]) = 8.5$ for additions of primary alkyl radicals to individual $CH_2{=}$ groups, $\lg(A/[\text{M}^{-1}\text{s}^{-1}]) = 9.2$ for additions of primary alkyl radicals to individual $CH{\equiv}$ groups, and $\lg(A/[\text{M}^{-1}\text{s}^{-1}]) = 7.5$ for additions of tertiary alkyl radicals to individual $CH_2{=}$ groups (see text). [c] Where more than one set of gas-phase data are available, the most recent data are used. For vinyl chloride, a second available data set[73] gives an unreasonably large ratio $k^l/k^g = 1800$. [d] Per $CH_2{=}$ or $CH{\equiv}$ group.

In summary, radical addition rate constants appear to be about one order of magnitude larger in solution than in the gas phase, probably because of a smaller activation energy. However, the rate constants and activation energies in the two phases vary similarly with radical and substrate structure. Changes in solvent polarity cause only small rate variations. Hence, theoretical reaction barriers which are calculated for isolated systems may exceed the barriers of liquid-phase reactions by a few kJ mol^{-1}.

4.2. Theoretical Results

4.2.1. Reaction Barriers

A number of studies have shown that it is not straightforward to obtain a reliable theoretical description of radical addition.[81] It is important therefore to assess which theoretical methods are suitable for studying such reactions.[12, 13, 82, 83]

The pattern of results obtained is exemplified by the barriers for methyl radical addition to ethene, calculated with a wide variety of theoretical procedures (Table 4).[12, 13, 82] The experimental barriers with which to make comparison, obtained from the observed activation energies after back-correcting for temperature and zero-point energy effects,[82, 84] are either 25.7 kJ mol^{-1} from the gas-phase studies[72] or 21.3 kJ mol^{-1} from the liquid phase results.[58] The calculated barriers show a massive dependence on the level of theory used. They range from 7 kJ mol^{-1} for the widely used AM1 semiempirical procedure to nearly 90 kJ mol^{-1} for RHF. The commonly used UMP2 procedure also gives a very high barrier of 60 kJ mol^{-1}. The best levels of theory include variants of the G2(MP2,SVP),[85] G3,[86] G3(MP2),[87, 88] CBS-RAD,[89] CBS-QB3,[90] and W1[57] procedures and give barriers in the range 20.5 – 28.6 kJ mol^{-1}, respectably close to the experimental values. The UB3-LYP DFT procedure also gives satisfactory results, including values of 18.3 kJ mol^{-1} (UB3-LYP/6-31G(d)) and 25.0 kJ mol^{-1} (UB3-LYP/6-311+G(d,p)) for small- to moderate-sized basis sets that would be practical to use for calculations on large systems. We note that UB3-LYP and other DFT procedures are found to be less successful in describing hydrogen-addition reactions, significantly underestimating the reaction barriers.[12, 81o]

Table 4. Effect of level of theory on calculated barriers E_a [kJ mol^{-1}] for the addition of a methyl radical ($^{\bullet}CH_3$) to ethene ($CH_2{=}CH_2$).[a]

Level	E_a	Level	E_a
AM1	7.1	UB3-LYP/6-311+G(d,p)[d,e]	25.0
UHF	39.4	UQCISD(T)/6-311+G(d,p)[c,d]	30.0
UMP2	60.1	UCCSD(T)/6-311+G(d,p)[c,d]	30.8
UMP4	53.7	URCCSD(T)/6-311+G(d,p)[c,d]	29.5
PMP2	20.1	UMP2/6-311+G(3df,2p)[e,f]	57.5
PMP4	21.5	PMP2/6-311+G(3df,2p)[e,f]	20.9
RHF	89.7	RMP2/6-311+G(3df,2p)[e,f]	34.4
RMP2	40.3	UB-LYP/6-311+G(3df,2p)[b,e]	20.7
RMP4	38.2	UB3-LYP/6-311+G(3df,2p)[d,e]	25.6
UB-LYP[b]	13.2	G2(MP2,SVP)[e,f]	28.6
UB3-LYP[c]	14.6	G3(MP2)//B3-LYP[c,d]	28.3
UB3-LYP[d,e]	18.3	G3(MP2)-RAD[c,d]	27.2
UQCISD	35.5	G3//B3-LYP[c,d]	26.6
UQCISD(T)	31.7	CBS-RAD[c,d]	20.5
UQCISD(T)[e,f]	33.8	CBS-RAD[e,f]	20.9
UCCSD(T)[c,d]	32.7	CBS-QB3[c,g]	20.7
URCCSD(T)[c,d]	31.4	W1[c,h]	27.0
URCCSD(T)[c,f]	33.7	exp.[i]	21.3
		exp.[j]	25.7

[a] 6-31G(d) basis set, UHF/6-31G(d) geometries, from ref. [12], unless otherwise specified. Calculated in all cases without the inclusion of zero-point vibrational energies. [b] UB-LYP/6-31G(d) geometry. [c] From ref. [13]. [d] UB3-LYP/6-31G(d) geometry. [e] From ref. [82]. [f] UQCISD/6-31G(d) geometry. [g] UB3-LYP/6-311G(2d,d,p) geometry. [h] UB3-LYP/cc-pVTZ+1 geometry. [i] Solution-phase value at 298 K (28.2 kJ mol^{-1}) from ref. [58], back-corrected to 0 K (+2.2 kJ mol^{-1}) and for zero-point vibrational energy (ZPVE ; 9.1 kJ mol^{-1}). Corrections from ref. [82]. [j] Gas-phase value at 403 K (33.1 kJ mol^{-1}) from ref. [72], back-corrected to 0 K (+1.7 kJ mol^{-1}) and for ZPVE (9.1 kJ mol^{-1}). Corrections from ref. [82].

The results in Table 4 indicate that the calculated barriers are very sensitive to the choice of theoretical procedure but less sensitive to the choice of basis set. Changes in going from the smallest (6-31G(d)) to the largest (6-311+G(3df,2p)) basis set are typically less than 7 kJ mol^{-1}. Barone and co-workers[81t] have reported that the B3-LYP results with small basis sets can be further improved by consideration of basis set superposition errors (BSSEs). The effect of the different choice of geometries in the calculations is also relatively small, generally amounting to less than 5 kJ mol^{-1}, though some instances have been encountered where there are larger variations, with UMP2 geometries in particular giving poor results.[12] Use of the B3-LYP procedure, even with a basis set as small as 6-31G(d), is very cost-effective for geometry and frequency calculations.

The theoretical results do not fully answer the question of whether or not there is a systematic difference between the gas-phase and condensed-phase barriers beyond the correction factor of RT (that has been applied here for back-correction purposes). Some of the high-level theoretical procedures (G2(MP2,SVP), G3(MP2)//B3-LYP, G3(MP2)-RAD, G3//B3-LYP, and W1) give barriers in the range 26.6 – 28.6 kJ mol^{-1}, close to the value of 25.7 kJ mol^{-1} derived from older gas-phase experimental data.[72] On the other hand, other high-level theoretical procedures (CBS-RAD and CBS-QB3) give barriers in the range 20.5 – 20.9 kJ mol^{-1}, close to the barrier of 21.3 kJ mol^{-1} derived from recent condensed-phase experimental data.[58] Although it is not possible to settle on a precise gas-phase barrier at the present time, it is satisfying that all the high-level theoretical barriers and the experimental barriers lie within the relatively narrow range of 20 – 29 kJ mol^{-1}.

Because the primary interest in chemical studies is often concerned with trends rather than absolute quantities, it is desirable to examine whether trends are predicted well with the simpler levels of theory. A selection of the results that enable us to examine the performance of theory in predicting relative barriers is shown in Table 5.[12, 82] The results obtained with the CBS-RAD method are taken to be the most reliable and the substituents are arranged in Table 5 with the CBS-RAD calculated barriers in decreasing order. We can then examine results at the other levels to see how they compare. AM1 is very poor. UMP2 is also very poor. The trend, that is, steadily decreasing barriers, is not reproduced at all. If anything, it goes the other way. The results from UHF

Table 5. Effect of level of theory on calculated activation energy barriers [kJ mol^{-1}] for the addition of a methyl radical ($^{\bullet}CH_3$) to alkenes (CH_2=CHX).[a]

X	AM1	UHF	UB-LYP[b]	UB3-LYP[c,d]	UMP2	PMP2	RMP2	UQCISD	UQCISD(T)	CBS-RAD[d,e]
OH	3.3	50.3	13.1	20.0	62.8	24.7	40.4	36.5	32.2	21.7
F	0.3	43.6	13.2	19.1	62.4	22.2	40.8	35.8	31.8	21.4
H	7.1	39.4	13.2	18.3	60.1	20.1	40.3	35.5	31.7	20.9
CH_3	5.5	42.2	13.4	18.8	60.6	21.0	38.3	34.8	30.7	19.9
NH_2	0.3	48.2	9.9	16.9	59.4	21.9	37.1	33.7	29.2	19.1
SiH_3	7.3	36.9	9.6	14.7	55.6	17.2	33.5	29.4	25.6	14.9
Cl	2.9	34.5	9.0	13.9	56.6	15.8	33.3	29.4	25.5	13.8
CHO	2.5	21.6	1.3	6.4	73.8	9.6	23.7	23.3	18.8	7.5
CN	2.1	19.9	1.1	5.4	68.6	6.8	21.3	20.6	16.7	6.6
R^2[f]	0.02	0.89	0.95	0.98	0.35	0.96	0.98	0.99	0.99	1.00

[a] 6-31G(d) basis set, UHF/6-31G(d) geometries, from ref. [12], unless otherwise specified. Calculated without the inclusion of ZPVEs. [b] UB-LYP/6-31G(d) geometries. [c] UB3-LYP/6-31G(d) geometries. [d] From ref. [82]. [e] UQCISD/6-31G(d) geometries. [f] The R^2 values refer to the correlation with CBS-RAD calculated activation energy barriers.

calculations are not particularly good but are much better than those from UMP2. The other procedures—UB-LYP, UB3-LYP, PMP2, RMP2, UQCISD, and UQCISD(T)—are very respectable in reproducing the trends, even though the absolute values are sometimes quite poor. These qualitative observations are mirrored in calculated correlation coefficients, also included in Table 5. The regression factor values (R^2) listed are for correlations of barriers calculated with the simpler methods against barriers calculated by CBS-RAD. QCISD and QCISD(T) are very good with R^2 values above 0.99. RMP2, UB3-LYP, PMP2, and UB-LYP are all reasonably good,[91] with R^2 values in the 0.95 – 0.98 range while AM1 is hopeless, with a correlation coefficient of 0.017. UMP2 is also very bad.

The assessment work touched-on here but described in detail elsewhere,[12, 13, 82] suggests standard levels of theory that might be useful in theoretical studies of radical-addition reactions and it suggests other levels of theory that should be avoided. For small systems, CBS-RAD and G3(MP2)-RAD are attractive levels of theory, while for larger systems, B3-LYP/6-31G(d), B3-LYP/6-311+G(d,p), or B3-LYP/6-311+G(3df,2p) would all be expected to perform satisfactorily. B3-LYP/6-31G(d) geometries and (scaled) vibrational frequencies (for calculating zero-point energies and thermal enthalpy corrections) are recommended for general use. At the other end of the scale, the UMP2 procedure can be very unreliable because of spin contamination.

The performance of some of the preferred levels of theory can be tested against the experimental results from Table 2 in cases for which both theoretical and experimental data are available (Table 6). The experimental liquid phase barriers at 298 K are back-corrected to 0 K in these comparisons. It can be seen that CBS-RAD and UB3-LYP/6-31G(d) give results in good agreement with experiment barriers, with mean absolute deviations from experiment of 1.7 and 2.6 kJ mol^{-1}, respectively. G3(MP2)-RAD, UB3-LYP/6-311+G(d,p), and

Table 6. Comparison of theoretical[a] and experimental activation energy barriers [kJ mol^{-1}] at 0 K for the addition of a methyl radical ($^{\bullet}CH_3$) to alkenes (CH_2=CXY).

X	Y	UB3-LYP/ 6-31G(d)	UB3-LYP/ 6-311+G(d,p)	UB3-LYP/ 6-311+G(3df,2p)	CBS-RAD	G3(MP2)-RAD	exp.[b]
H	H	27.4[c]	34.1[c]	34.7[c]	29.7	36.2	30.4
H	Me	27.0[c]	33.7[c]	34.5[c]	27.6	34.8	29.0
H	Et	26.9	33.6	34.4	26.8	34.5	27.5
Me	Me	26.2	32.3	33.2	25.3	32.8	26.8
Me	OMe	29.5	35.6	36.7		36.8	28.2
H	OEt	30.0	36.5	37.4		38.3	28.3
H	OAc	24.6	30.3	31.3		32.4	29.9
H	Cl	22.2[c]	28.3[c]	29.3[c]	22.2	29.2	25.2
H	SiH_3	23.1	29.9	30.2	23.1	29.9	24.8[d]
Me	Cl	22.2	28.0	28.7	20.4	27.8	23.1
Cl	Cl	17.3	22.7	23.2	16.7	22.2	17.4
H	CO_2Me	14.5	20.5	21.0		21.1	17.6
H	CN	13.1[c]	18.9[c]	19.5[c]	13.8	21.1	16.4
H	CHO	14.3[c]	20.1[c]	20.7[c]	14.6	22.6	16.0
Me	CN	14.2	19.8	20.5		20.7	15.3
MOH[e]		25.8[c]	34.2[c]	35.4[c]	27.6	34.1	36.9
MCN[f]		32.3[c]	39.6[c]	40.4[c]	28.8	35.7	30.0
MAD[g]		2.6	4.7	5.3	1.7	5.4	
R^2[h]		0.77	0.81	0.83	0.87	0.82	

[a] UB3-LYP/6-31G(d) geometries, from ref. [13] unless otherwise specified. [b] Experimental values from Table 2, back-corrected to 0 K using thermal temperature corrections from refs. [13, 82]. [c] From ref. [82]. [d] Experimental barrier is for the $SiMe_3$ substituent. [e] Barrier for the addition of MOH ($^{\bullet}CH_2OH$) to ethene. [f] Barrier for the addition of MCN ($^{\bullet}CH_2CN$) to ethene. [g] MAD = mean absolute deviations from experiment. [h] The R^2 value refers to the correlation with experimental barriers.

UB3-LYP/6-311+G(3df,2p), on the other hand, appear to overestimate the liquid-phase barriers but the differences appear to be quite systematic, and the R^2 correlation coefficients when compared with the experimental barriers are 0.82, 0.81, and 0.83, respectively. That the B3-LYP deviations from experiment increase with increasing basis-set size indicates that the very good agreement observed for B3-LYP/6-31G(d) is partly fortuitous. Although the B3-LYP/6-31G(d) method seems to represent a potentially very cost-effective means of obtaining satisfactory barriers for radical-addition reactions, further work is required to see whether the good performance holds more generally.

4.2.2. Reaction Enthalpies

The calculated reaction enthalpies for the addition of methyl radical to ethene are less sensitive than the barriers to the level of theory used (Table 7). The high-level procedures give values from -105.6 to -111.5 kJ mol^{-1}, compared with the corrected experimental value of -113.1 kJ mol^{-1}. The UB3-LYP/6-311+G(3df,2p) method gives one of the poorest results of -99.0 kJ mol^{-1}.

The variation in reaction enthalpy with substitution on the alkene is examined in Table 8. Assuming again that the CBS-RAD results are the most reliable, we can see that AM1 is very poor, UMP2 is also poor in several instances while the other procedures give quite reasonable results. UHF and B3-LYP underestimate the exothermicity while the other methods, particularly RMP2, overestimate the exothermicity. The deviations in the calculated reaction enthalpies from the experimental estimates are, however, quite systematic and the correlation coefficients with CBS-RAD are very reasonable (for methods other than AM1 and UMP2), with R^2 values of 0.93 for UHF and in the range 0.98–0.99 for the other procedures.[91]

The performance of the standard procedures in calculating reaction enthalpies is compared in Table 9 with the estimates derived from experimental data (taken from Table 2 and back-corrected to 0 K). As has been pointed out above, there are considerable uncertainties in the experimental values because of the imprecision of the C–H bond dissociation energies and possible deviations from additivity assumed in their derivation. We can see that B3-LYP/6-31G(d) systematically overestimates the exothermicity while the larger basis set B3-LYP procedures significantly underestimate the exothermicity. G3(MP2)-RAD generally slightly underestimates the exothermicity while CBS-RAD appears to perform best. The differences between theory and experiment are quite systematic again for all five procedures, with correlation coefficients in the range 0.91–0.93.

Table 7. Effect of level of theory on calculated reaction enthalpies [kJ mol^{-1}] for the addition of a methyl radical ($^{\bullet}CH_3$) to ethene (CH_2=CH_2).[a]

Level	Enthalpy	Level	Enthalpy
AM1	−157.5	UB3-LYP/6-311+G(d,p)[d,e]	−101.5
UHF	−107.7	UQCISD(T)/6-311+G(d,p)[c,d]	−110.5
UMP2	−123.6	UCCSD(T)/6-311+G(d,p)[c,d]	−110.4
UMP4	−116.9	URCCSD(T)/6-311+G(d,p)[c,d]	−110.5
PMP2	−123.8	UMP2/6-311+G(3df,2p)[e,f]	−116.4
PMP4	−117.0	PMP2/6-311+G(3df,2p)[e,f]	−116.9
RHF	−107.4	RMP2/6-311+G(3df,2p)[e,f]	−117.0
RMP2	−124.2	UB-LYP/6-311+G(3df,2p)[b,e]	−85.5
RMP4	−117.0	UB3-LYP/-311+G(3df,2p)[d,e]	−99.0
UB-LYP[b]	−107.1	G2(MP2,SVP)[e,f]	−106.5
UB3-LYP[c]	−120.1	G3(MP2)//B3-LYP[c,d]	−105.6
UB3-LYP[d,e]	−119.8	G3(MP2)-RAD[c,d]	−105.7
UQCISD	−115.6	G3//B3-LYP[c,d]	−107.4
UQCISD(T)	−114.4	CBS-RAD[c,d]	−111.0
UQCISD(T)[e,f]	−112.7	CBS-RAD[e,f]	−111.5
UCCSD(T)[c,d]	−112.8	CBS-QB3[c,g]	−111.2
URCCSD(T)[c,d]	−112.9	exp.[h]	−113.1
URCCSD(T)[c,f]	−112.7		

[a] 6-31G(d) basis set, UHF/-31G(d) geometries, from ref. [12], unless otherwise specified. Calculated in all cases without the inclusion of ZVPEs. [b] UB-LYP/6-31G(d) geometry. [c] From ref. [13]. [d] UB3-LYP/6-31G(d) geometry. [e] From ref. [82]. [f] UQCISD/6-31G(d) geometry. [g] B3-LYP/6-311G(2d,d,p) geometry. [h] Gas-phase value at 298 K (-99 kJ mol^{-1}) from Table 2, back-corrected to 0 K ($+5.7$ kJ mol^{-1}) and for ZPVE (-19.8 kJ mol^{-1}). Corrections from ref. [82].

4.2.3. Geometries

One of the properties that is not accessible from experiment, at least at the present time, is the geometry of the transition structure for the radical-addition reactions (Figure 2). On the other hand, this can be obtained straightforwardly by ab initio methods and we comment here on some of the more interesting findings.

The first point is that the angle of approach (ϕ) of the radical to the alkene lies within a narrow band of values for a

Table 8. Effect of level of theory on calculated reaction enthalpies [kJ mol^{-1}] for the addition of a methyl radical ($^{\bullet}CH_3$) to alkenes (CH_2=CHX).[a]

X	AM1	UHF	UB-LYP[b]	UB3-LYP[c,d]	UMP2	PMP2	RMP2	UQCISD	UQCISD(T)	CBS-RAD[d,e]
OH	−168.5	−101.8	−106.7	−118.0	−122.5	−121.7	−123.7	−118.8	−117.6	−115.2
F	−185.1	−109.9	−111.6	−123.4	−127.6	−126.7	−128.5	−121.7	−120.4	−116.2
H	−157.5	−107.7	−107.1	−119.8	−123.6	−123.8	−124.2	−115.6	−114.4	−111.5
CH_3	−166.1	−105.6	−106.8	−118.7	−122.0	−122.4	−123.0	−116.7	−115.6	−113.4
NH_2	−185.1	−107.0	−115.4	−127.1	−129.9	−129.3	−131.4	−126.3	−125.6	−123.6
SiH_3	−156.5	−113.7	−118.5	−130.1	−130.2	−130.1	−131.4	−126.3	−124.8	−121.8
Cl	−172.0	−118.9	−121.5	−134.2	−135.1	−135.7	−136.7	−130.4	−129.5	−129.9
CHO	−169.1	−144.1	−142.8	−154.2	−123.1	−153.1	−157.5	−152.2	−151.3	−148.4
CN	−172.3	−143.7	−147.6	−158.1	−122.6	−154.8	−160.0	−153.0	−151.4	−150.5
R^2[f]	0.02	0.93	0.98	0.98	0.00	0.98	0.98	0.99	0.99	1.00

[a] 6-31G(d) basis set, UHF/6-31G(d) geometries, from ref. [12], unless otherwise specified. Calculated without the inclusion of ZPVEs. [b] UB-LYP/6-31G(d) geometries. [c] UB3-LYP/6-31G(d) geometries. [d] From ref. [82]. [e] UQCISD/6-31G(d) geometries. [f] The R^2 values refer to the correlation with the calculated CBS-RAD reaction enthalpies.

Table 9. Comparison of theoretical[a] and experimental reaction enthalpies [kJ mol^{-1}] a 0 K for the addition of a methyl radical ($^{\bullet}CH_3$) to alkenes (CH_2=CXY).

X	Y	UB3-LYP/ 6-31G(d)	UB3-LYP/ 6-311+G(d,p)	UB3-LYP/ 6-311+G(3df,2p)	CBS-RAD	G3(MP2)-RAD	exp.[b]
H	H	−100.0[c]	−81.7[c]	−79.3[c]	−91.3	−86.3	−93.3
H	Me	−100.8	−82.5	−80.1	−93.6	−86.7	−92.2
H	Et	−100.8	−82.8	−80.4	−94.6	−87.1	−94.2
Me	Me	−96.5	−78.6	−75.7	−91.6	−82.9	−93.6
Me	OMe	−89.6	−72.0	−68.7			−89.2
H	OEt	−99.8	−83.0	−80.0		−86.7	−95.1
H	OAc	−105.7	−89.1	−86.0		−92.7	−95.9
H	Cl	−112.3[c]	−93.9[c]	−92.0[c]	−107.1	−98.8	−100.8
H	SiH_3	−108.5	−90.6	−88.5	−100.6	−95.0	−95.8[d]
Me	Cl	−110.5	−91.8	−89.7	−108.3	−96.9	−93.6
Cl	Cl	−127.7	−109.0	−107.5	−124.6	−114.1	−119.6
H	CO_2Me	−123.7	−105.8	−103.3		−107.4	−111.5
H	CN	−136.3	−117.5	−115.4	−130.4	−118.7	−133.3
H	CHO	−131.1[c]	−112.7[c]	−110.1[c]	−122.9	−112.4	−116.0
Me	CN	−138.1	−120.0	−117.6		−120.7	−125.0
H	Ph	−134.5	−116.4				−144.0
MOH[e]		−80.0	−64.7	−61.2	−82.6	−79.6	−81.5
MCN[f]		−57.6	−44.4	−41.4	−69.1	−64.7	−65.7
MAD[g]		8.0	10.9	12.9	4.3	5.6	
R^2[h]		0.91	0.92	0.93	0.93	0.93	

[a] UB3-LYP/6-31G(d) geometries, from ref. [13] unless otherwise specified. [b] Experimental estimates from Table 2, back-corrected to 0 K using thermal temperature corrections from refs. [13, 82]. [c] From ref. [82]. [d] Experimental value is for the $SiMe_3$ substituent. [e] Reaction enthalpies for the addition of MOH ($^{\bullet}CH_2OH$) to ethene. [f] Reaction enthalpies for the addition of MCN ($^{\bullet}CH_2CN$) to ethene. [g] MAD = mean average deviation from experimental values. [h] The R^2 value refers to the correlation with experimental reaction enthalpies.

wide variety of radical additions. Thus, for the additions of the methyl, hydroxymethyl, cyanomethyl, and *tert*-butyl radicals to a variety of substituted alkenes, ϕ lies between 106° and 112° (UHF/6-31G(d)).[26–29] Calculations show that ϕ is not particularly sensitive to the level of theory, with the range of ϕ values for methyl additions changing from 107.5–111.0° (UHF/6–31G(d)) to 109.2–111.0° (UB3-LYP/6-31G(d)) and 108.2–110.6° (QCISD/6–31G(d)).[82]

The second geometric parameter of particular interest is the length of the partially formed C–C bond. This lies between 2.173 and 2.313 Å (UHF/6-31G(d)) and is found to correlate very nicely with the reaction enthalpy across a wide variety of radical-addition reactions (Figure 5).[26–29, 81t] This result has been rationalized, using the curve-crossing model, as indicating that the *location* of the transition structure is determined primarily by the intersection of reactant and product configurations while the *energy* of the transition structure may be strongly influenced by contributions from charge-transfer configurations.[28] This then leads to the observation of a good correlation between r(C–C) with the reaction enthalpy for a range of radicals and alkenes but not for the barrier with the reaction enthalpy. Calculations at other levels of theory show that there is a small but not negligible dependence on the level of theory for this bond length. Thus for the methyl radical plus ethene reaction, r(C–C) takes the values 2.246 Å (UHF), 2.261 Å (UMP2), 2.365 Å (UB3-LYP), 2.273 Å (UQCISD), and 2.281 Å (QCISD(T) (all with the 6–31G(d) basis set).[12] An even larger variation of r(C–C) is found for the methyl radical plus acrylonitrile reaction.[12]

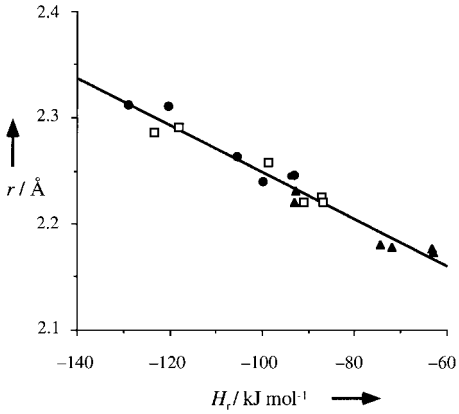

Figure 5. Plot of C–C bond length r [Å] in the transition structure (UHF/6-31G(d)) against reaction enthalpy H_r [kJ mol^{-1}] (QCISD/6-311G(d) + ZPVE,) for the addition of $^{\bullet}CH_3$ (●), $^{\bullet}CH_2OH$ (■), and $^{\bullet}CH_2CN$ (▲) radicals to alkenes CH_2=CHX (X = H, NH_2, F, Cl, CHO, CN). Taken from ref. [28]. The solid regression line is given by r [Å] = 2.03 − 2.21 × 10^{-3} H_r [kJ mol^{-1}] with R^2 = 0.953.

4.2.4. Charge Transfer

Another property that is more directly accessible from theoretical calculations than from experiment is the direction and extent of CT in the transition structure (Table 10).[26] This is clearly useful in assessing the amount of polar character in a radical-addition reaction. A direct theoretical measure of CT comes from the calculated charges in the transition structures, while a less direct measure, which is also available from experimental data, is the relative energy of the CT states, for example, CH_3^+/CH_2=CHX^- and CH_3^-/CH_2=CHX^+. In the case of the addition of the methyl radical to alkenes, it is found that for most substituents (including H) the methyl radical carries a negative charge. It carries a positive charge only for X = CHO, NO_2, and CN. In addition, in most cases (H again included), the energy of the CT state CH_3^-/CH_2=CHX^+ is

Table 10. Energies E_{CT} of CT states and the charge q on CH_3 in the transition state of the reaction of a methyl radical ($^{\bullet}CH_3$) with alkenes (CH_2=CHX).[a]

X	E_{CT} [eV][b]		q[c]
	CH_3^+/CH_2=CHX^-	CH_3^-/CH_2=CHX^+	
F	11.4	10.3	−0.012
H	11.6	10.5	−0.017
OH	11.5	9.2	−0.029
CH_3	11.6	9.8	−0.024
NH_2	11.7	8.1	−0.039
SiH_3	10.7	10.1	−0.009
Cl	11.0	9.9	0.000
CHO	9.7	10.2	+0.006
NO_2	9.0	11.8	+0.030
CN	10.0	10.9	+0.012

[a] From ref. [26]. [b] G2(MP2) values. [c] Bader charges calculated at the UHF/6-31G(d) level.

lower than the CT state CH_3^+/CH_2=CHX^-, once again showing that methyl generally prefers to be an electron acceptor rather than an electron donor. It is an electron donor only when there are strong electron-withdrawing substituents on the alkene. Thus the calculations indicate that methyl radical does not display general nucleophilic behavior, in contrast to previous conventional wisdom. It is nucleophilic only with alkenes such as acrolein and acrylonitrile that bear strong π-electron-withdrawing substituents.

The calculated energies for the possible CT states formed from the radicals (R) $^{\bullet}CH_2OH$ and $^{\bullet}CH_2CN$ with a number of alkenes (A) is shown in Table 11.[28] It can be seen that the

Table 11. Calculated energies [eV] of CT states related to the addition of $^{\bullet}CH_2OH$ and $^{\bullet}CH_2CN$ to alkenes (CH_2=CHX).[a]

X	$^{\bullet}CH_2OH$		$^{\bullet}CH_2CN$	
	R^+A^-	R^-A^+	R^+A^-	R^-A^+
F	9.1	10.5	11.8	8.8
H	9.3	10.7	12.0	9.0
NH_2	9.4	8.3	12.1	6.6
Cl	8.7	10.1	11.4	8.4
CHO	7.5	10.4	10.1	8.6
CN	7.7	11.1	10.4	9.4

[a] G2(MP2) values from ref. [28].

$^{\bullet}CH_2CN$ radical is always electrophilic, the R^-A^+ state being low in energy in an absolute sense and always lying below the R^+A^- state. On the other hand, $^{\bullet}CH_2OH$ is generally nucleophilic, the CT R^+A^- state being low in energy in an absolute sense and lying below the R^-A^+ state. The CT states involving the methyl radical (Table 10) are considerably higher in energy. In agreement with experiment, these results suggest that polar effects in the addition reactions of the $^{\bullet}CH_2OH$ and $^{\bullet}CH_2CN$ radicals should be considerably greater than for the methyl radical, where they might generally be expected to be relatively unimportant.

4.2.5. Solvent Effects

Because the ab initio calculations refer to isolated molecules in the gas phase whereas most of the experiments with which comparisons are being made were carried out in solution, for example 1,1,2-trichloro-1,2,2-trifluoroethane ($\varepsilon = 2.4$, $^{\bullet}CH_3$ additions), methanol ($\varepsilon = 32.6$, $^{\bullet}CH_2OH$ additions), or acetonitrile ($\varepsilon = 37.5$, $^{\bullet}CH_2CN$ additions), it is of interest to examine the effect of solvent.[81t, 82] This has been achieved by using the self-consistent isodensity polarizable continuum model (SCIPCM)[92] with dielectric constants (ε) of 2 (for a nonpolar solvent) and 40 (for a polar solvent) for a selection of radical-addition reactions.[82]

The predicted effect of solvent is generally not large, leading generally to small increases in the barrier (+0.5 to +1.1 kJ mol^{-1} for $\varepsilon = 2$, +1.1 to +2.8 kJ mol^{-1} for $\varepsilon = 40$) except for the CN and CHO substituents (in the alkene or the radical) for which there are small decreases in the activation energy (−0.2 to −1.1 kJ mol^{-1} for $\varepsilon = 2$, −0.6 to −3.0 kJ mol^{-1} for $\varepsilon = 40$). There predicted lowering of the activation barrier in solvent is a larger (4.7 kJ mol^{-1}; $\varepsilon = 40$) for $^{\bullet}CH_2OH$ + CH_2=CHCN relative to $^{\bullet}CH_2OH$ + CH_2=CH_2, which is consistent with the significant polar character predicted for the $^{\bullet}CH_2OH$ + CH_2=CHCN reaction (Table 11).

It is found that the effect of solvent (with $\varepsilon = 40$) on reaction enthalpy lies between +2.4 and +4.3 kJ mol^{-1} for methyl radical additions, except for X = NH_2 (+5.9 kJ mol^{-1}).[82] Larger effects are seen for the $^{\bullet}CH_2OH$ additions. For nonpolar solvents ($\varepsilon = 2$) the solvent effect is reduced by about 60%.

4.3. Discussion

4.3.1. General Aspects and Linear Correlations

In general, the trends associated with changing the radical and alkene substitution obtained with the more advanced theoretical procedures agree well with those observed experimentally. Therefore, the two sets of data do not justify separate discussions of the substituent effects, and we base the following analysis of the factors influencing the addition rates on the experimental data only. The possible, but small, phase and solvent effects are ignored. Furthermore, the analysis is restricted to the activation energies because the frequency factors have already been covered in Section 4.1.2.

4.3.1.1. Steric Effects of β and Radical Substitution

The data in tables 1 and 2 nicely confirm the earlier view[5–7] that bulky alkene β substituents (X,Y, Figure 1) have little effect on the rate constants. In fact, for all the radicals the addition to the very bulky 1,1-diphenylethene is always one of the fastest reactions. Also, depending on the radical and the other β substituent, the replacement of a β-hydrogen atom by a methyl group changes the rate constant in either direction but not greatly, and seldom by more than a factor of two. Primary and tertiary radicals behave similarly, that is, there is also no clear indication of hindering steric interactions between the methyl substituents of the radicals and the alkene β groups. Two methyl groups at the radical center decrease the rate constants markedly if the third radical substituent is a cyano or a carboxy group but lead to an increase for the hydroxy-substituted radical. Furthermore, the *tert*-butyl radical reacts faster than the methyl radical with all

strongly acceptor-substituted alkenes. Clearly, any steric retardation of the rates by β-alkene or radical substituents must be so small that it is completely masked by the other more dominating factors.

4.3.1.2. Characteristic Energy Quantities

Guided by the state correlation diagram (Figure 3) we now seek correlations between the activation energies for the addition with the energy quantities which change with the substitution pattern of the alkenes and the radicals, namely, the reaction enthalpy, the alkene triplet energy, and the relative energies of the CT configurations and the strength of the interactions with these.[93]

The reaction enthalpy for the addition of a specific radical R to an alkene A follows from the data in Table 2 as $H_r(R,A) = H_r(Me,A) + \Delta H_r(R)$.

Triplet excitation energies ΔE_{ST} are known for only a few monosubstituted and 1,1-disubstituted alkenes.[94] They range from 2.55 eV for diphenylethene to 3.65 eV for ethene, and correlate very well linearly with the differences in the vertical alkene ionization energies and electron affinities. Since the latter are more widely known (Table 2), this correlation was used to predict ΔE_{ST} for the other alkenes. They fall between $\Delta E_{ST} = 2.55 - 2.80$ eV for phenyl-substituted alkenes and $\Delta E_{ST} = 3.10 - 3.65$ eV for all other species.[95]

According to the discussion in Section 2.2, polar effects should become important when the energy of at least one of the CT configurations for the separated reactants is reduced by the Coulomb interaction C in the transition structure, that is, when $E_i(R) - E_{ea}(A) - C$ or $E_i(A) - E_{ea}(R) - C$ lies near or below ΔE_{ST}. For two point charges at the theoretical reaction distance of about 2.2 Å (Figure 5), the Coulomb attraction energy is 6.5 eV. This is an upper limit since in many cases the charges will be delocalized to some extent over both the radical and the alkene substitutents. Estimates based on semiempirical calculations lead to values for C between 2.8 eV (for benzyl reacting with phenyl-substituted alkenes, i.e. a system in which a large charge delocalization is expected) and 5.3 eV (for hydroxymethyl with ethene, a system with small charge delocalization).[62c] Hence, one may expect considerable polar effects if the energy gaps $E_i(R) - E_{ea}(A)$ or $E_i(A) - E_{ea}(R)$ are smaller than about 7–8 eV. However, the interaction parameters γ between the various configurations are also important, and a large γ value will increase the polar effects. Unfortunately, there is presently no means to address this aspect with any confidence.

4.3.1.3. Enthalpic Effects

A natural and frequently used procedure to search for specific correlations is the construction of plots of the activation energies against the characteristic energy quantities. An E_a versus H_r plot is given in Figure 6 for the addition of methyl and benzyl radicals to a variety of alkenes.[96] For both radicals the data are reasonably well described by one linear Evans–Polanyi–Semenov relation, and this is not unexpected: methyl has a high ionization energy and a low electron affinity, which yields large energy gaps of $E_i(R) - E_{ea}(A) > 9.5$ eV and $E_i(A) - E_{ea}(R) > 8$ eV for all alkenes

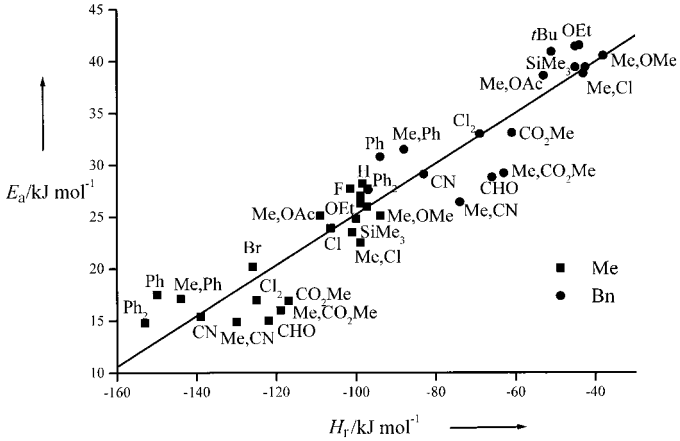

Figure 6. Activation energies for the addition of methyl (■) and benzyl (●) radicals versus the reaction enthalpy. The solid regression line is given by $E_a = 49.7(1.3) + 0.244(0.013)\,H_r$ with (errors are given in parenthesis, $R^2 = 0.89$).

(Table 10). Therefore, the polar effects should be of minor importance in methyl additions. The benzyl radical has a low ionization energy and a substantial electron affinity. Nucleophilic polar effects could consequently be expected. However, they should be diminished by the lower Coulomb term and the lower interaction strength. Hence, for both radicals a dominant influence of the reaction enthalpy is quite natural. Moreover, the common regression of benzyl and methyl means that the lower reactivity of benzyl is because of the lower exothermicity which is caused by resonance stabilization. Hence, a previous explanation of the low benzyl reactivity[21] as being the result of a particularly large resistance to pyramidalization is now abandoned.

However, Figure 6 also shows some noticeable deviations from the linear regression: for methyl additions to several electron-deficient alkenes the activation energies lie below the line. In agreement with the direction of the charge transfer given in Table 10, methyl seems to exhibit a noticeable nucleophilic polar effect in these cases, and earlier it was precisely the high reactivity of methyl towards such alkenes which led to its classification as nucleophilic.[4, 6] For benzyl, small accelerating nucleophilic polar effects towards strongly electron-deficient alkenes are also visible. These are also suggested by the extremely facile addition to the very electron-deficient superalkene C_{60} ($E_{ea} = 2.65$ eV, $k_{298} = 1.4 \times 10^7\,M^{-1}s^{-1}$, $E_a = 13.5$ kJ mol^{-1}).[97] Overall, however, the nucleophilicity of benzyl is also rather modest, and this explains why *para* substitution of the benzyl group by electron-donor or -acceptor groups does not change the addition behavior of benzyl markedly, even though these substitutions strongly affect the E_i of the radical.[21] Hence, one would conclude from Figure 6 that for the additions of methyl and benzyl radicals the reaction enthalpy is the dominating factor, and the slope of the linear regression is also close to the generally accepted $\alpha \approx 0.25$.

Interestingly, but also disturbingly, reasonable linear correlations between the activation energies and the reaction enthalpy are also found for radicals which are thought to have electrophilic or ambiphilic character, such as *tert*-butoxycar-

bonylmethyl ($E_a = 32.4 + 0.17 H_r$, $R^2 = 0.67$), cyanomethyl ($E_a = 35.1 + 0.17 H_r$, $R^2 = 0.73$), 2-*tert*-butoxycarbonyl-2-propyl ($E_a = 47.9 + 0.24 H_r$, $R^2 = 0.80$), and 2-cyano-2-propyl ($E_a = 43.3 + 0.21 H_r$, $R^2 = 0.87$). Linear E_a versus H_r relations also hold even for the strongly nucleophilic radicals hydroxymethyl ($E_a = 82.5 + 0.59 H_r$, $R^2 = 0.82$), *tert*-butyl ($E_a = 74.5 + 0.60 H_r$, $R^2 = 0.77$), and 2-hydroxy-2-propyl ($E_a = 78.0 + 0.69 H_r$, $R^2 = 0.72$), but not for the strongly electrophilic radicals cyclic malonyl ($E_a = 18.0 - 0.01 H_r$, $R^2 = 0.01$) and trifluoroacetonyl ($E_a = 12.0 - 0.07 H_r$, $R^2 = 0.02$).

The comparison of all these Evans–Polanyi–Semenov relations reveals remarkable trends. For the donor-substituted hydroxymethyl, *tert*-butyl, and 2-hydroxy-2-propyl radicals, both the intercepts and gradients are much larger than for methyl and benzyl, whereas for the acceptor-substituted *tert*-butoxycarbonylmethyl, cyano-methyl, 2-*tert*-butoxy-carbonyl-2-propyl, and 2-cyano-2-propyl radicals the gradients are smaller. For cyclic malonyl and trifluoro-acetonyl they are even negative. Clearly, the correlations found so far point to an influence of the reaction enthalpy on the activation energies but do not allow the specification of a general dependence which could be valid for all radicals and alkenes.

4.3.1.4. Nucleophilic Polar Effects

The nucleophilic polar effect should be large for the *tert*-butyl, hydroxymethyl, and 2-hydroxy-2-propyl radicals which have very small ionization energies (Table 2). For these radicals $\Delta H_r(R)$ is similar, and thus the enthalpic effects should also be similar. For nearly all the alkenes examined, the activation energies decrease in the order hydroxymethyl > *tert*-butyl > hydroxypropyl. This agrees with the order of the radical ionization energies and supports the importance of nucleophilic polar factors. Also, for most of the alkenes the energy $E_i(R) - E_{ea}(A)$ of the CT configuration R^+A^- is smaller than 8 eV. The energy of the second CT configuration R^-A^+ is greater than 8 eV for all the alkenes, and this renders electrophilic polar effects for these radicals unlikely.

Figure 7 shows that the activation energies of the three radicals correlate in a common way with the energy differences $E_i(R) - E_{ea}(A)$, and this correlation is even better than that with the reaction enthalpy. The alkenes form two classes: the activation energies of alkenes without phenyl substituents fall into a rather narrow band (width < 7 kJ mol^{-1}) and decrease from high values when the $E_i(R) - E_{ea}(A)$ energy difference is high (9–10 eV) to values close to zero for $E_i(R) - E_{ea}(A) \approx 6.0$–$6.5$ eV. The latter value is close to the Coulomb interaction $C \approx 5$–6 eV estimated above for non-delocalized systems and, according to Figure 3, $E_i(R) - E_{ea}(A) \approx C$ could mean very low or even vanishing activation energies. For the phenyl-substituted alkenes, the activation energies are higher but they also decrease with decreasing energy gap and tend to zero at $E_i(R) - E_{ea}(A) \approx 5$ eV. This is reasonable, because the Coulomb term should be smaller for the phenyl-substituted alkenes as a result of the delocalization effect. Hence, one can conclude that for the donor-substituted radicals the nucleophilic polar effect is important, at least for

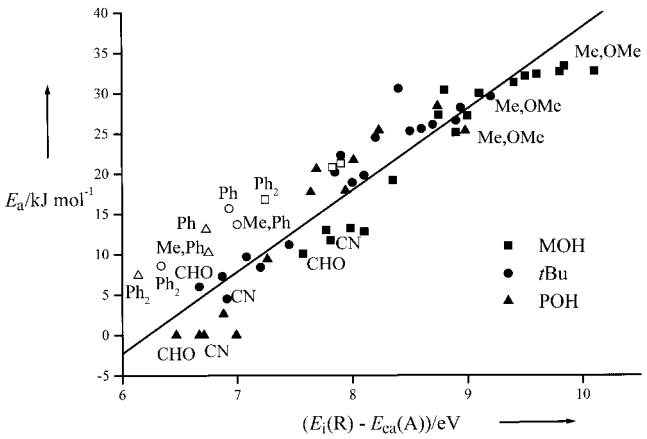

Figure 7. Activation energies for the addition of hydroxymethyl, *tert*-butyl, and 2-hydroxy-2-propyl radicals versus the relative energies of the CT configurations R^+A^- (measured by $E_i(R) - E_{ea}(A)$). Several data points are labeled with the corresponding alkene substituents. The solid regression line is given by E_a [kJ mol^{-1}] = $-63.0(4.6) + 10.1(0.6)(E_i(R) - E_{ea}(A))$ [eV] (errors are given in parenthesis, $R^2 = 0.86$).

energy differences $E_i(R) - E_{ea}(A) < 9$ eV, and that in Figure 7 the influence of the reaction enthalpy is masked.

Surprisingly, however, radicals such as methyl and benzyl with small nucleophilic polar effects also give rise to reasonable correlations of the activation energies with the energy gap $E_i(R) - E_{ea}(A)$ and/or with the alkene electron affinity ($R^2 = 0.86$ and $R^2 = 0.84$, respectively). Even the electron-acceptor-substituted radicals, 2-cyano-2-propyl ($R^2 = 0.76$), 2-*tert*-butoxycarbonyl-2-propyl ($R^2 = 0.75$), *tert*-butoxycarbonylmethyl ($R^2 = 0.51$), and cyanomethyl ($R^2 = 0.52$), behave similarly, only cyclic malonyl and trifluoroacetonyl do not. Hence, as noted for the enthalpy effect, linear correlations such as those presented in Figure 7 seem not to be of general and predictive significance.

4.3.1.5. Electrophilic Polar Effects

The trifluoroacetonyl and cyclic malonyl radicals have large electron affinities (Table 2). This suggests searching for a correlation of the activation energies with the energy $E_i(A) - E_{ea}(R)$ for the CT configuration R^-A^+. Figure 8 shows that the $E_i(A) - E_{ea}(R)$ values are indeed low for most alkenes, so that electrophilic polar effects are likely. As expected, the activation energies are lower at lower $E_i(A) - E_{ea}(R)$ energies. However, the gradient of the common correlation is much smaller than that found for the nucleophilic radicals (Figure 7), and very low activation energies are approached only for $E_i(A) - E_{ea}(R) < 6$ eV.

For all the other potentially electrophilic radicals, the plots of the activation energies versus the energy separation $E_i(A) - E_{ea}(R)$ and/or the alkene ionization energies $E_i(A)$ show large scatter and negative gradients. An electrophilic behavior should give a positive slope since the activation energies should decrease with decreasing alkene ionization energy, so that at first sight all four monocyano and monocarboxy substituted radicals appear not to be electrophilic. This is not consistent with intuition and the theoretical results (Table 11) nor with the low activation energies of the primary species, and suggests that other forces are at work.

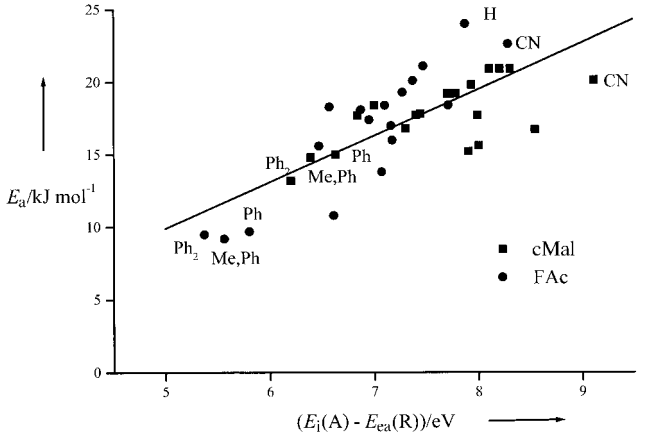

Figure 8. Activation energies for the addition of cyclic malonyl (■) and trifluoroacetonyl (●) radicals versus the relative energy of the CT configuration $R^{\cdot}A^{+}$ (determined by $E_i(A) - E_{ea}(R)$). The solid regression line is given by E_a [kJ mol^{-1}] $= -6.1(3.4) + 3.1(0.5)(E_i(A) - E_{ea}(R))$ [eV] (errors are given in parenthesis, $R^2 = 0.57$).

4.3.1.6. Correlations With the Alkene Triplet Energy

We have also searched for linear correlations of the activation energies with the alkene triplet energy ΔE_{ST}. Except for the radicals with the strongest polar effects, 2-hydroxy-2-propyl, cyclic malonyl, and trifluoroacetonyl, all species give reasonable correlations with the expected positive slopes but the scatter is large.

4.3.1.7. Interrelation of Energy Parameters and Limits of Linear Correlations

As is evident from the discussion above, linear correlations of the activation energies for individual radicals or specific radical groups with the reaction enthalpy, the energies of the CT configurations and the triplet energy appear to point to important factors but do not lead to their specification and straightforward separation. In the course of this analysis, we have recognized that the energy parameters are themselves significantly interrelated, that is, they depend on one another.

Firstly, the reaction enthalpy correlates strongly with the triplet excitation energy: H_r [kJ mol^{-1}] $= -309 + 0.62\Delta E_{ST}$ [kJ mol^{-1}], with $R^2 = 0.68$. The large and positive slope means that the effects of H_r and ΔE_{ST} are not separable by linear correlations of the activation energies or of the rate constants with either parameter. In fact, a linear dependence on one parameter will automatically lead to a linear dependence on the other, even if the latter would have no effect if it were operating alone. Despite an extensive search for specific influences of the alkene triplet energy, such influences have not been found. Therefore, we conclude that the correlations with H_r always include the effects of ΔE_{ST}.

Secondly, there is a correlation between H_r and the alkene electron affinity, H_r [kJ mol^{-1}] $= -136 - 0.20\,E_{ea}(A)$ [kJ mol^{-1}] with $R^2 = 0.77$. The negative slope means that many of the alkene substituents that make the alkene more electron deficient, and hence increase E_{ea}, also stabilize the newly formed radical, and hence decrease H_r. Therefore, for a given radical, the nucleophilic polar effect increases with decreasing H_r, that is, favorable influences of the enthalpy and the alkene electron affinity reinforce one another.

Thirdly, with the exception of the phenyl-substituted alkenes, the addition exothermicities ($-H_r$) increase with increasing alkene ionization energies, H_r [kJ mol^{-1}] $= 35 - 0.16\,E_i(A)$ [kJ mol^{-1}] with $R^2 = 0.42$. This correlation is less significant than that of H_r with E_{ea}, but it means that the electrophilic polar substituent effect which increases with decreasing alkene E_i and the enthalpy substituent effect which increases with increasing exothermicity partly cancel one another in the individual plots of the activation energies versus H_r and $E_i(A)$.

In total, these interrelations of the parameters shed considerable doubt on the meaning of the individual correlations and call for a more refined analysis.

4.3.2. Refined Analysis and Predictions

We start with the Evans–Polanyi–Semenov premise, supported by the state correlation diagram, that the reaction barriers should always decrease with decreasing reaction enthalpy (increasing exothermicity). We note in addition that any polar effects that are present can only serve to *decrease the barriers* beyond that indicated by the enthalpy effect. If the dependence of the activation energy on the reaction enthalpy is the same for all radicals and if this is described by a common Evans–Polanyi–Semenov relation, then the interrelations between H_r and the alkene E_{ea} and E_i described in Section 4.3.1.7 suggest alkene specific trends of the data in plots of the activation energies versus the reaction enthalpy if polar effects do operate. These trends are quite different for nucleophilic, electrophilic, and ambiphilic radicals, and this allows a discrimination.

4.1.3.2.1. Nucleophilic Polar Effects

Figure 9 represents in a pictorial way the variation in the activation energy with the reaction enthalpy expected from Equation (1) and from the corresponding changes resulting from accompanying additional nucleophilic polar effects

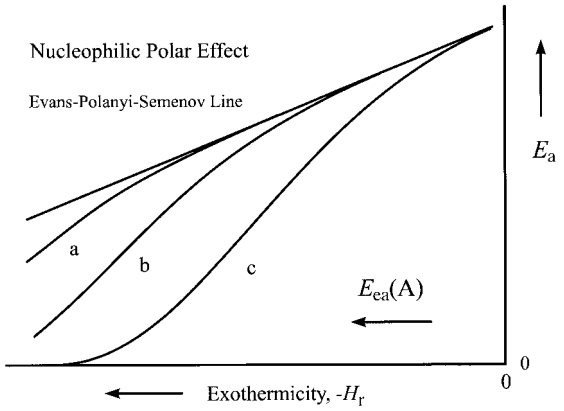

Figure 9. Schematic plot of the activation energy versus reaction exothermicity ($-H_r$) for systems showing negligible polar effects and increasing nucleophilic polar effect (increases from a to b to c).

which increase from curve a to curve c. The lines were drawn with the restriction that activation energies can not become negative but will approach zero if $E_i(R) - E_{ea}(A) - C$ becomes sufficiently small. Because $E_{ea}(A)$ generally increases with decreasing H_r, the deviations from pure enthalpy control will be larger for additions with higher exothermicity. They will set in when $E_i(R) - E_{ea}(A) - C$ falls below a critical value, and they are also influenced by the strength (γ) of the interaction between the CT configurations and the nonpolar configurations. From Figure 9 one predicts that radicals exhibiting both enthalpic effects and nucleophilic polar effects are *generally more selective and more reactive* than radicals lacking the polar effects. Normally, the accessible range of H_r is limited, and, under such circumstances, this will lead to a more or less linear dependence of the activation energies on the reaction enthalpy. Then, as seen in Figure 9, the slopes of the linear correlations are expected to be particularly large for radicals with considerable nucleophilicity. Indeed, this is observed for the nucleophilic hydroxymethyl, *tert*-butyl, and 2-hydroxy-2-propyl radicals.

4.3.2.2. Electrophilic Polar Effects

For electrophilic radicals, the expected variation in the activation energy with the reaction enthalpy is schematically displayed in Figure 10. The deviations from the Evans–Polanyi–Semenov line are largest for small $E_i(A)$, and since

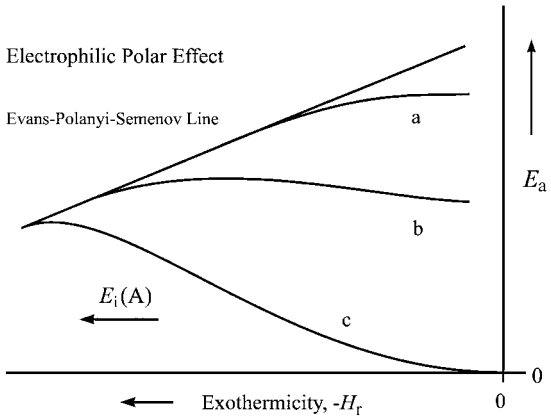

Figure 10. Schematic plot of the activation energy versus reaction exothermicity ($-H_r$) for systems showing negligible polar effects and increasing nucleophilic polar effect (increases from a to b to c).

$E_i(A)$ and the exothermicity are positively correlated, the deviations are largest for additions with low exothermicities. Hence, one predicts from Figure 10 that radicals exhibiting enthalpic and electrophilic effects are *generally more reactive but may be less selective* than radicals without electrophilicity. Again, the limited range of H_r will lead to a more or less linear dependence of the activation energies on the enthalpy, and now the slopes of the correlations will be smaller than that given by the enthalpy effect alone. For very large electrophilicity even a negative slope can result (line c). Small slopes are, in fact, encountered for the acceptor-substituted radicals *tert*-butoxycarbonylmethyl, cyanomethyl, 2-*tert*-butoxy-carbonyl-2-propyl, and 2-cyano-2-propyl, and for cyclic malonyl and trifluoroacetonyl the slopes are negative. Hence, all these acceptor-substituted radicals do show an appreciable electrophilicity.

4.3.2.3. Ambiphilic Polar Effects

For radicals with sufficiently low ionization energies and sufficiently large electron affinities, the energy of the CT configuration R^+A^- is small for reactions with strongly electron-deficient alkenes, and the energy of the other CT configuration R^-A^+ is small for additions to electron-rich alkenes. In this case, one expects an ambiphilic reaction behavior. It gives rise to the deviations from the enthalpy correlation shown in Figure 11. One now predicts that

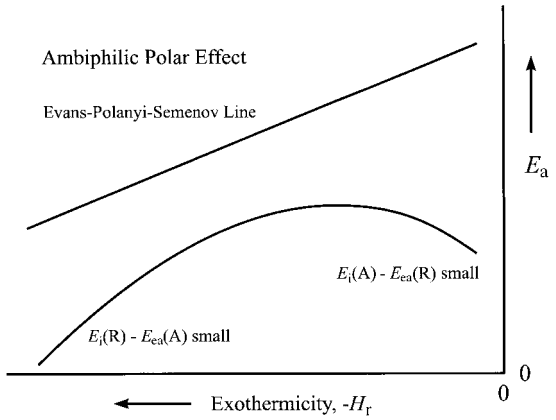

Figure 11. Schematic plot of the activation energy versus reaction exothermicity ($-H_r$) for an ambiphilic reactivity.

ambiphilic radicals will be *rather reactive but not very selective*. In these cases, the linear correlation of the activation energy with the reaction enthalpy may show nearly the correct slope but it gives an intercept that is too low. Hence, the effects of the reaction enthalpy can become more evident for ambiphilic radicals than for purely nucleophilic or electrophilic species, and this was noticed earlier by Giese[18a]. It will be seen later that several of the radicals we employed are indeed ambiphilic.

4.3.2.4. Consequences

The interrelation of the energy parameters explains the observation of linear correlations of the activation energies with the polar energy quantities for cases where such correlations should not exist, this was noted in Section 4.3.1. If the additions are mainly controlled by the reaction enthalpy, the activation energies will always seemingly decrease with increasing alkene electron affinity as if the radicals were substantially nucleophilic. This deceptive tendency holds for the carboxy- and cyano-substituted species but was not recognized in earlier work. On the other hand, because of the enthalpy effect the slopes of the correlations between E_a and $E_i(A)$ for electrophilic radicals will always appear too small, and they may even become negative. The latter is contrary to intuition, but it is observed for some acceptor-substituted species. However, a correlation of E_a

with E_i(A) with a positive slope always means an electrophilic addition behavior, especially if the radical follows line c in the E_a versus H_r plot of Figure 10.

4.3.2.5 Predictive Equations for the Activation Energy: A Common Evans – Polanyi – Semenov Relation

Our considerations, which, for the first time, include a detailed analysis of the mutual interdependence of the energy parameters, have implicitly assumed the existence of a common dependence of the reaction barriers on the reaction enthalpy. From the sizes of the energy gaps it can be concluded that most of the radicals reported herein should exhibit only weak or negligible polar effects with at least a few alkenes. Therefore, a plot of *all* the activation energy data against the reaction enthalpy should lead to an *upper limiting* line. This line should represent the true enthalpy dependence from which the polar effects are expected to cause only negative deviations. Figure 12 demonstrates that the upper limit does exist. It is even close to linear and thus provides strong support for the Evans – Polanyi – Semenov relation.

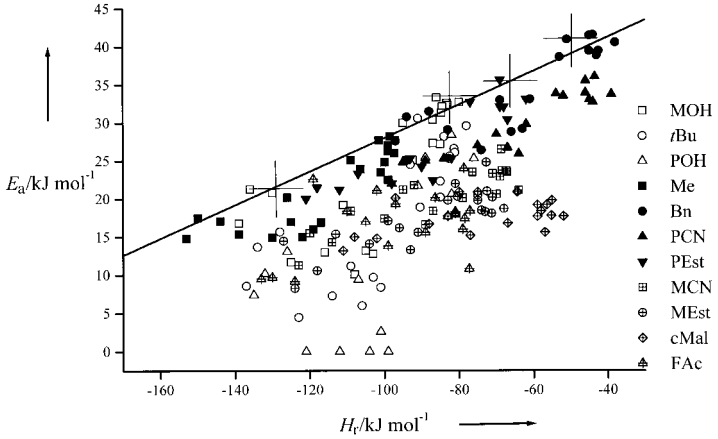

Figure 12. Activation energies for the full set of reactions versus the reaction enthalpy. The solid line is given by $E_a = 50.0 + 0.22\,H_r$.

The line is described by Equation (2). With very few exceptions, the activation energies for all radicals approach

$$E_a = 50 + 0.22\,H_r \quad (2)$$

the upper limit for specific alkenes, and this further rules out significant steric effects of the radical substituents on the activation energies. The line in Figure 12 [Eq. (2)] accommodates the experimental errors in the activation energies and in the estimated reaction enthalpies, and the resulting parameters are reasonable. Not unexpectedly, they are very similar to those given in Figure 6 for the rather nonpolar methyl and benzyl radicals. A closer inspection of Figure 12 also reveals that the deviations from the upper limiting line for methyl, benzyl, and the strongly donor-substituted radicals increase with increasing exothermicity, as expected from Figure 9, that is, the nucleophilicity of these radicals with electron-deficient alkenes is confirmed. The other radicals conform as expected to Figures 10 and 11, that is, all acceptor-substituted radicals show an electrophilic to ambiphilic behavior.

4.3.2.6. Effects of Polar Interactions on the Activation Energy

The new general Evans – Polanyi – Semenov relation allows a more quantitative analysis of the effects of polar interactions on the activation energies. We propose that the enthalpy effects are covered by Equation (2) and that the polar effects are described by superimposing *multiplicative polar factors* and not additive terms on this equation. Hence, we write the activation energies as Equation (3).[98, 99] The nucleophilic

$$E_a = (50 + 0.22\,H_r)F_nF_e \quad (3)$$

factor F_n depends on $E_i(R) - E_{ea}(A) - C_n$ and an interaction parameter γ_n, and its electrophilic counterpart F_e depends on $E_i(A) - E_{ea}(R) - C_e$ and a corresponding interaction parameter γ_e. Both F_n and F_e are restricted to values between 0 and 1. Figure 13 shows a plot of the activation energies E_a divided by the enthalpic term $(50 + 0.22\,H_r)$ for the radicals methyl, hydroxymethyl, *tert*-butyl, and 2-hydroxy-2-propyl versus the energy of the charge-separated configuration R^+A^-, $E_i(R) - E_{ea}(A)$. These radicals should exhibit only nucleophilic polar effects, and hence the ratio $E_a/(50 + 0.22\,H_r)$should represent F_n.

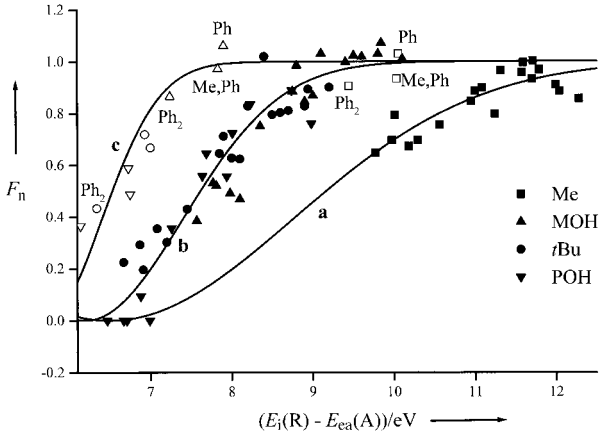

Figure 13. Nucleophilic polar factors for the methyl (■), hydroxymethyl (▲), *tert*-butyl (●), and 2-hydroxy-2-propyl (▼) radicals. Open symbols (□, △, ○, ▽) refer to the same radicals reacting with phenyl-substituted alkenes. The solid lines correspond to a) $F_n = 1 - \exp(-((x - 6.5)/3.2)^2)$, b) $F_n = 1 - \exp(-((x - 6.2)/1.7)^2)$, and c) $F_n = 1 - \exp(-((x - 5.7)/1.0)^2)$.

Also displayed are *heuristic* functions of the type (4) which accommodate the data. The term C_n is the value of $E_i(R) - E_{ea}(A)$ for which the activation energy reaches zero, and γ_n

$$F_n = 1 - \exp(-[(E_i(R) - E_{ea}(A) - C_n)/\gamma_n)^2] \quad (4)$$

denotes the value of $E_i(R) - E_{ea}(A) - C_n$ where the nucleophilic factor F_n reduces the activation energy by a factor of $1 - e^{-1}$, that is, to 63% of the value given by the enthalpy effect alone. As is evident from Figure 13, with the exception of phenyl-substituted alkenes, the polar effects of the strongly nucleophilic radicals can be described by one common F_n with a reasonable Coulomb attraction (6.2 eV) and one interaction term (1.7 eV). The nucleophilic effect of methyl requires the insertion of a larger Coulomb term (6.5 eV) and a larger interaction term (3.2 eV). For the phenyl-substituted alkenes,

the Coulomb and interaction parameters of all four radicals appear to be smaller ($C_n = 5.7$ eV, $\gamma_n = 1.0$ eV), and this also holds for the benzyl radical (not shown, $C_n = 6.0$ eV, $\gamma_n = 1.0$ eV). Clearly and as expected, the parameters C_n and γ_n are related to the charge and spin delocalization in the transition state.

Similar functions F_e accommodate the polar effects of the strongly electrophilic cyclic malonyl and the trifluoroacetonyl radical. This is shown in Figure 14 for the non-phenyl-substituted alkenes. Though the variations are less convincing

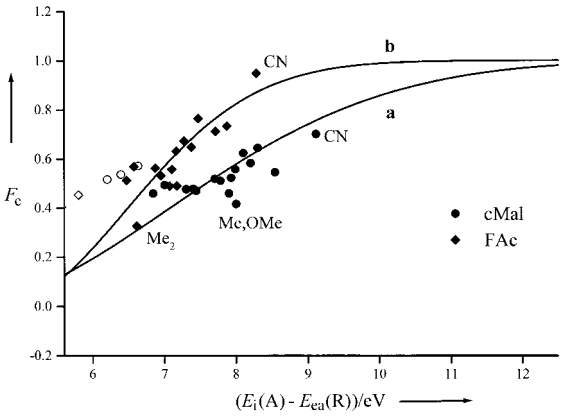

Figure 14. Electrophilic polar factors for the cyclic malonyl (●) and trifluoroacetonyl (◆) radicals. Open symbols (○, ◇) refer to the same radicals reacting with phenyl-substituted alkenes. The solid lines correspond to a) $F_e = 1 - \exp(-((x-4)/4.3)^2)$, and b) $F_e = 1 - \exp(-((x-4)/2)^2)$.

than those in Figure 13, the phenyl-substituted species are again the exceptions and call for weaker polar effects. In comparison to the values given above for the nucleophilic radicals, the Coulomb terms in Figure 14 are smaller, possibly because the carboxy- and cyano-acceptor substituents delocalize charge more easily than methyl or hydroxy groups, yet the interaction parameters of these strongly electrophilic radicals appear to be relatively large.

The activation energies of the remaining *tert*-butoxycarbonylmethyl, cyanomethyl, 2-*tert*-butoxycarbonyl-2-propyl, and 2-cyano-2-propyl radicals are smaller than those given by the general Evans – Polanyi – Semenov relation, and this holds both for the electron-deficient and for the electron-rich alkenes. This suggests an ambiphilic reaction behavior, that is, both polar factors are important. A detailed analysis shows similar parameters to those found for the purely nucleophilic and purely electrophilic radicals, and again smaller values for C and γ are needed for the phenyl-substituted alkenes.

To provide an overview of the results of our approach, in Figure 15 we compare the experimental activation energies (Table 2) with values calculated from Equations (3) and (4) and with a unified set of polar Coulomb and interaction parameters.[100] The agreement is very satisfying and lends support to the interpretation and to Equation (3). The deviations between experimental and calculated data obey the most probable Gaussian distribution, and the largest deviations of 7 kJ mol^{-1} may even be a result of the experimental errors. Of course, the polar parameters and Equation (4), especially the interactions γ and their variation with radical structure, call for theoretical explanations.

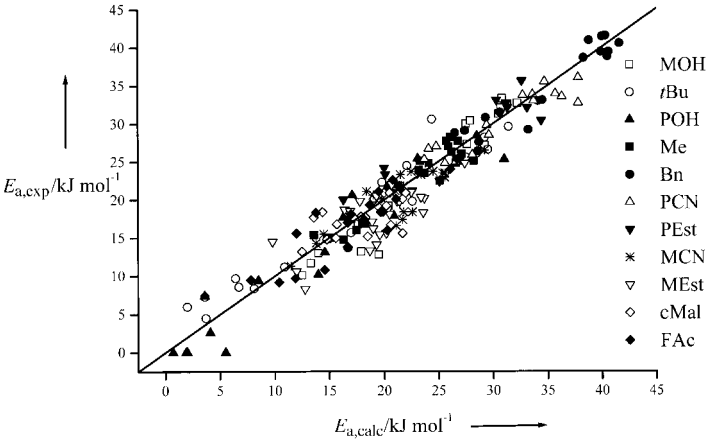

Figure 15. Experimental versus calculated activation energies for the addition reactions covered in Table 2, except cumyl and di-*tert*-butylmalonyl additions, with different symbols for different radicals. The solid line corresponds to $E_{a,exp} = E_{a,calcd}$ and describes the 206 data points with the standard deviation of 2.4 kJ mol^{-1}.

4.3.2.7. Tests of the Predictions

The polar parameters used for Figure 15 depend on the structures of the radicals and on the alkenes but do not vary extensively.[100] Therefore, they should allow the prediction of unknown activation energies for additions of similar species. Unfortunately, there are not many absolute rate constants against which such predictions can be checked. However, amongst some other scattered single values, the absolute rate constants are available for the addition of trifluoromethyl and perfluoro-*n*-alkyl radicals,[20, 67] the *n*-hexenyl and *n*-heptyl radicals,[101] the cumyl radical,[59] and various *p*-substituted benzyl radicals[21] to several alkenes at room temperature. These serve as test cases here. Using the general Evans – Polanyi – Semenov relation with estimated reaction enthalpies, and the average frequency factors and polar parameters which are close to or equal to those found for the related radicals from our series,[102–106] we arrive at the comparison of experimental and predicted rate constants shown in Figure 16.

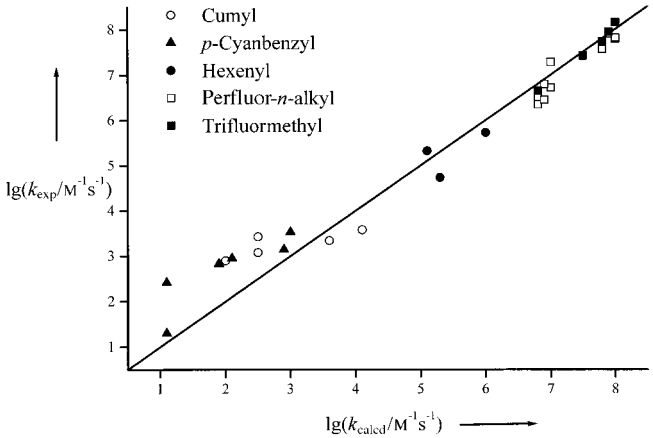

Figure 16. Experimental versus predicted rate constants for the addition of several radicals to alkenes in solution at room temperature with different symbols for different radicals. The solid line corresponds to $\lg(k_{exp}) = \lg(k_{calcd})$ and describes the 29 data points with the standard deviation of 0.54.

The data cover about seven orders of magnitude. There are a few deviations of about one order of magnitude, but the average standard deviation between the experimental and the predicted rate constants is only 0.54 units of $\lg(k/M^{-1}s^{-1})$, which means a factor of 3.5 for the rate constants. Hence, our refined analysis of the experimental data has not only provided additional insight on the action of the enthalpic and polar factors but also appears to allow predictions of rate constants for the addition of carbon-centered radicals to monosubstituted and 1,1-disubstituted alkenes to within one order of magnitude. We show in Section 5 that the operating principles also hold for related addition reactions. The most serious limitation to a widespread application of our predictive equations is currently the restricted availability of reliable reaction enthalpies.

5. Related Addition Reactions

5.1. 1,2-Disubstituted and 1,1,2-Trisubstituted Alkenes—The Steric Factor

5.1.1. General Observations

It is well established[3–9] that substitution of one or both methylene hydrogen atoms of a monosubstituted or 1,1-disubstituted alkene CH_2=CXY by other atoms or groups changes the overall rate constant of a radical addition considerably and can also change the regioselectivity of the attack. In most cases, substitution at the attacked site (named C_α) lowers the rate constants. This is commonly attributed to a steric substituent effect which hinders the approach of the radical. As a rule, the effect increases with the steric demand of the substituent and of the attacking radical but it depends also on the size of the substituents at the nonattacked carbon. It may be diminished by favorable polar α-substituent effects.

In terms of activation parameters, a pure steric substituent effect should diminish the frequency factor because it means additional motional constraints on the transition structure. Further, both for bulky radicals R$^\bullet$ and bulky α-substituents A, the newly formed C–C bond of the adduct radical R-CHA-CXY$^\bullet$ will be strained, that is, upon substitution of H by A the reaction should generally become less exothermic and have a higher activation energy. There are not enough experimental data currently available for a large-scale analysis. Therefore, we address here only some of the more important points for a representative reaction series.

Table 12 allows a comparison of the absolute rate constants and the activation parameters for the addition to alkenes CHA=CXY and CH_2=CXY. In the chosen examples, the attack at the less-substituted carbon atom is always strongly preferred. As expected, α substitution lowers the rate constants for most additions, and the decrease is larger for bulkier vicinal substituents (A and X,Y) and it is larger for the bulkier *tert*-butyl radical than for the smaller methyl radical. Moreover, the frequency factors for addition to the 1,2-disubstituted and 1,1,2-trisubstituted alkenes are lower than the average frequency factors established in Section 4.1.2 for CH_2=CXY, namely $\lg(A/M^{-1}s^{-1}) = 8.5$ for methyl and $\lg(A/M^{-1}s^{-1}) = 7.5$ for *tert*-butyl additions, and this decreases the rate constants by a factor of about 5 to 15. With few exceptions, the activation energies are larger for the α-substituted alkenes than for the unsubstituted alkenes, and this suggests a lower exothermicity for the former reaction.[107] As is evident from the Table 12 this effect of the steric strain on the activation energy may lead to an additional rate decrease by a factor similar to that originating from the frequency factor difference.[108]

Table 12. Rate effects of α-alkene substituents. Ratios of absolute rate constants per CH_2 group of monosubstituted and 1,1-disubstituted alkenes CH_2=CXY, or per CH group of 1,2-disubstituted and 1,1,2-trisubstituted alkenes CHA=CXY at 298 K, frequency factors A^A [$M^{-1}s^{-1}$] for the addition to CHA=CXY per CH group and differences in activation energies $E_a^A - E_a^H$ [kJ mol^{-1}] for the addition of methyl (Me) and *tert*-butyl (*t*Bu) radicals.

Radical	X	Y	A	k^A/k^H	$\lg(A^A)$	$E_a^A - E_a^H$
Me[58]	H	Me	(*E*)-Me[a]	0.21	7.4	−2.4
	H	Me	(*Z*)-Me[a]	0.11	7.1	−2.6
	Me	Me	Me	0.29[b]		
	H	Ph	(*E*)-Me	0.12[b]		
	H	Ph	(*Z*)-Me	0.055[b]		
	H	Ph	(*E*)-Ph	0.069	8.0	3.9
	H	Ph	(*Z*)-Ph	0.018	7.9	6.6
	Ph	Ph	Ph	46	7.4	3.3
	H	CO_2Me	(*E*)-Me	0.022[b]		
	H	CO_2Et	(*E*)-CO_2Et	2.2[c]	6.6	−12.8
	H	CO_2Et	(*Z*)-CO_2Et	0.22[c]	7.4	−2.5
*t*Bu[36c, 62]	H	Me	(*Z*)-Me	0.033	6.1	−5.3
	Me	Me	Me	0.11	7.1	2.8
	H	Cl	(*E*)-Cl	0.23	7.0	0.6
	H	Cl	(*Z*)-Cl	0.085	7.4	5.3
	Cl	Cl	Me	0.005	6.0	5.1
	Cl	Cl	Cl	0.048	7.3	6.6
	H	Ph	(*E*)-Me	0.014		
	H	Ph	(*E*)-CO_2Me	1.1		
	H	Ph	(*E*)-CN	2.8		
	H	CO_2Me	(*E*)-CO_2Me	0.18		
	H	CO_2Me	(*Z*)-CO_2Me	0.070		

[a] *E* and *Z* isomers. [b] 338 K. [c] Calculated using $k(CH_2$=$CHCO_2Me)$.

Polar effects of α-substituents are also noticed. Firstly, in comparison the addition to methylacrylate, the additions of the methyl radical to diethylfumarate and to diethylmaleate are considerably faster than expected from the rate-diminishing steric substituent effect, and have lower activation energies. As shown before (Figure 6), the addition of the methyl radical to strongly acceptor-substituted alkenes such as methylacrylate is facilitated by the nucleophilic polar effect, and for diethylfumarate and diethylmaleate this appears to be enhanced by the second ester group. Secondly, the *tert*-butyl radical adds faster to 2-carboxystyrene and 2-cyanostyrene than to styrene, thus, in these cases the polar effect of the α substituent even overrides the steric substituent effect. In this context, it has to be mentioned that the somewhat lower activation energies for additions to 2-butene, when compared with propene, may not be significant and may be a result of error compensation effects in the activation parameters. For methyl additions the difference is small, and for *tert*-butyl the experimental frequency factor is suspiciously low.

5.1.2. The Isomer Effect

Generally, *Z*-1,2-disubstituted alkenes react considerably more slowly than *E*-1,2-disubstituted alkenes (Table 12). The different reactivity of isomers was noticed long ago,[109] and constituted very early evidence for the now established transition structure in which the alkene moiety in the transition state resembles the parent alkene (Figure 2). However, the direction of the effect is not easily explained. One contribution to different reactivities is likely to come from enthalpy effects because the different isomers have different enthalpies of formation whereas the product radicals that result from additions are energetically identical. However, the direction of the effect is often contra to thermodynamics. In the case of the stilbenes, the relative reactivities were attributed to the *E* isomer having a structure closer to planarity than the *Z* isomer, and it was suggested that these arrangements could be retained in the transition structure. Hence, the newly-formed benzyl-type radical could gain some of its resonance stabilization for the *E* but not for the *Z* isomer already at an early stage of the reaction, and this would lower the barrier for the former compound.[109] The same reasoning may also explain the higher reactivity of fumarates compared with maleates. An additional possibility is that, because the isomers have different ionization energies and electron affinities, different polar effects may operate. In fact, this isomer effect has been found to explain the addition of the strongly nucleophilic *tert*-butyl radical to the 1,2-dichloroethenes.[62a,b] It seems that the isomer effect may have different origins for different cases, and the very limited amount of data currently available precludes a closer analysis.

5.1.3. Regioselectivity

For a multiply substituted alkene C(1)AB = C(2)XY, the regioselectivity of addition is given by the ratio of the rate constants for addition to C(1) and C(2), k_1/k_2, and this is strongly dependent on all the factors mentioned before. Firstly, for different motional constraints on the different transition structures, the frequency factors of k_1 and k_2 will be different, and addition to the less-crowded carbon atom should be favored. Secondly, the reaction enthalpies of the two additions differ by the difference in the enthalpies of formation of the adduct radicals R−CAB−CXY$^{\bullet}$ and R−CXY−CAB$^{\bullet}$. Therefore, from the enthalpy effect one expects the lower activation energy and a higher rate constant for the addition leading to a new R−C bond that is stronger or less strained, and to a more stabilized radical. Thirdly, it has been argued that radical attack is directed towards the alkene carbon which possesses the highest spin population in the alkene triplet state.[25] This effect normally favors attack at the less substituted carbon, and thus coincides with predictions from steric considerations. Finally, for reactions with polar effects, the correction factors F_n and F_e of the activation energies involve the same energy gaps to the CT configurations $E_i(R) - E_{ea}(A)$ and $E_i(A) - E_{ea}(R)$ for both pathways. However, the Coulomb and the interaction terms may differ, that is, the polar effects may also not be equal for the additions to C(1) and C(2). When the enthalpy and spin population or steric effects reinforce one another, addition at the less substituted carbon ensues. However, when they oppose one another, a regioselectivity crossover, as in the case of methyl radical addition to $CHF{=}CF_2$, may be observed.[25]

The experimental data indicate that the decrease in the frequency factor caused by increasing steric substituent effects often goes in parallel with an increase in the activation energy but there are noteworthy exceptions. Tedder et al.[6, 110] have shown that a variety of fluorine-substituted methyl radicals add preferentially to the less-substituted carbon atom of fluoroethenes. The frequency factors are larger and the activation energies are smaller than for the addition to the more-substituted site, and from the above arguments this is as expected. In contrast, the methyl radical adds preferentially at the disubstituted carbon atom of trifluoroethene, and this reaction has a lower activation energy than the addition to the monosubstituted site. For 1,1-difluoroethene, the regioselectivity of methyl addition is also relatively low. The seemingly anomalous behavior of the methyl radical towards these compounds can simply be explained in terms of the enthalpic effect. It is known that $CH_n{-}CF_m$ bonds are unusually strong ($n, m \geq 2$),[20] and this facilitates the addition of methyl to the substituted carbon of $CH_2{=}CF_2$[81b, 111] whereas for trifluoromethyl and other fluorine-substituted radicals it facilitates the addition to the less-substituted site.[112] The same should also hold for trifluoroethene and would lead to the anomalous regioselectivity for methyl and the lower activation energy for addition to the more-substituted site. This explanation has also been offered by others and is supported by ab initio calculations.[25, 81b, 112]

5.2. Homopolymerization Rate Constants, Copolymerization Parameters, and the Penultimate Unit Effect

In radical polymerizations, the repeated addition of alkyl radicals to alkene monomers gives rise to the polymer chains. Hence, one might expect that the rate constants of chain propagation should be subject to the same factors that control the rates of addition of small radicals to alkenes.[7] This is supported by the following comparisons.

5.2.1. Homopolymerization

Table 13 lists recent homopolymerization rate constants and their activation parameters, together with the corresponding rate data for reactions of structurally related small radicals as taken from Tables 1 and 2. With the exception of ethene propagation, for which the addition of the methyl radical to ethene may not be an adequate model, the propagation constants are about 10- to 60-fold smaller than the rate constants for the model systems. Both sets of constants vary with radical and alkene substitution by nearly three orders of magnitude and in a similar way. The activation energies of the propagations are generally slightly higher. This may be a result of a slightly larger steric effect for the polymeric species which should decrease the reaction enthalpy and increase the activation energy (see Section 5.1.1).

Table 13. Rate data for the homopolymerization of vinyl monomers and for the corresponding addition of small alkyl radicals. For radical notation, see Table 1 and Figure 4.

Homopolymerization monomer model Reaction	k_{300} [$M^{-1}s^{-1}$]	$\lg(A/M^{-1}s^{-1})$	E_a [kJ mol^{-1}]
ethene[113a]	20	7.27	34.3
Me + ethene	7000	8.5[a]	28.2
methacrylonitrile[113b]	18	6.43	29.7
PCN + methacrylonitrile	1060	7.5[a]	26.4
styrene[39a]	93	7.63	32.5
Bn + styrene	1100	8.5[a,b]	30.8
methylmethacrylate[39b]	345	6.43	22.4
PEst + methylmethacrylate	3710	7.5[a]	22.4
methylacrylate[113c]	19000	7.3	17.0
MEst + methylacrylate	490000	8.5[a,b]	15.6

[a] Average frequency factors, see text. [b] For a secondary radical, $\lg(A/M^{-1}s^{-1}) = 8.0$ is expected, see text.

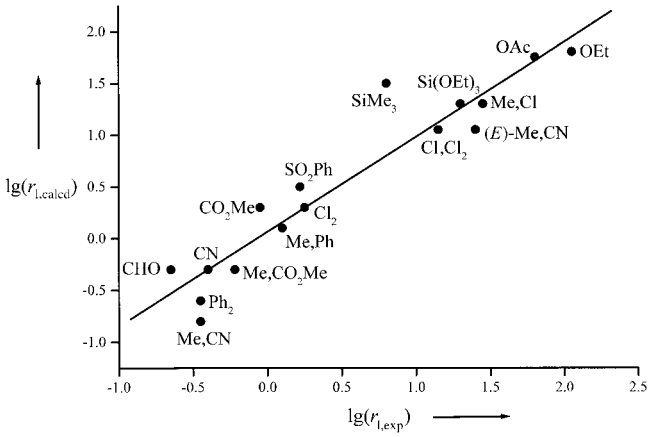

Figure 17. Experimental and predicted copolymerization parameters for styrene. The solid regression line corresponds to $\lg(r_{1,calcd}) = 0.07 + 0.92 \times \lg(r_{1,exp})$ and describes the 16 data points with $R^2 = 0.90$.

However, the similarity in the activation energies strongly suggests that the major influences of the enthalpic and polar substituent effects on the addition rates are similar for long- and short-chain carbon-centered radicals. On the other hand, the frequency factors of the propagation constants are considerably smaller than those established for the model systems. In view of the larger conformational and motional complexity of the propagating species and the constraints on the transition structure, this is not surprising. In total, the lower frequency factor lowers the rate constant by a factor of about ten for polymeric radicals in comparison with related small-radical additions, and an additional smaller decrease may be a result of the increased activation energy. Probably the same factors explain why propagation rate constants tend to decrease with the increasing chain length of the polymeric radicals.[114–116]

5.2.2. Copolymerization

As a further test for the similarity of the dominant factors, we compare copolymerisation parameters with ratios of rate constants of model systems. For a propagating radical R adding to its parent monomer M and a second monomer M′, the copolymerization parameter r_1 is defined as $r_1 = k_{RM}/k_{RM'}$, and for a given monomer feed such ratios determine the copolymer composition. Figure 17 shows experimental copolymerization parameters for styrene[117] and ratios of rate constants, $r_{1(calc)}$, of the model benzyl radical adding to styrene relative to the addition to other alkenes calculated from our absolute data.[59] The frequency factor difference between the secondary polystyryl and the primary benzyl radical should not affect the ratios, and therefore one expects a good correlation between the observed copolymerization parameters and those calculated from rate constants for the small radical if the additions of polymeric and small radicals experience similar enthalpic and polar factors. Figure 17 shows an excellent linear correlation, with a slope close to one and a small intercept value, and this confirms the similarity of the operating factors. Excellent correlations were also found for the cyanomethyl radical as a model for the propagation radical of acrylonitrile,[60] for the *tert*-butoxycarbonyl methyl radical as a model for methylacrylate,[60] and for the methoxycarbonyl-2-propyl radical as a model for methylmethacrylate.[65]

5.2.3. The Penultimate Unit Effect

Studies of copolymerization rates have recently revealed that the rate constant for the addition of a polymeric radical to a monomer does not only depend on the monomer and on the terminal structure of the radical but also to some extent on its penultimate unit[118] and possibly on even more remote groups. That is, the rate constants k_{iii} for the addition of a radical type P-M_i-$M_i^{\bullet}$, where P is a polymer chain, to the monomer M_i is different from the rate constant k_{jii} for the addition of the radical P-M_j-$M_i^{\bullet}$ to the same monomer. The selectivity ratio $s_i = k_{iii}/k_{jii}$ is difficult to determine from the polymerization rates and depends on the analysis method. Values ranging from about 0.2 to about 5 have been extracted, and they agree with the results of selectivities obtained for small model systems.[119] Hence, the penultimate unit effect is small, and this complicates its explanation. Ab initio studies indicate[120] that modest changes in the reaction enthalpy and in polar effects may be involved and affect the activation barriers, but changes in the frequency factors could also play a role.[116c, 121]

A recent detailed analysis has compared alternative models for free-radical copolymerization kinetics.[122] The simplest "terminal" model assumes that the reactivity is determined entirely by the nature of the monomer and the terminal unit of the polymeric radical. In the "implicit penultimate" model, it is assumed that the penultimate unit of the polymeric radical also plays a role but that it affects the composition but not the rate of the copolymerization processes. The most general "explicit penultimate" model assumes that both the composition and the rate of copolymerization are affected by the penultimate unit. The recent theoretical study concludes that the explicit penultimate model should be adopted as the basis for analyzing free-radical polymerization kinetics.[122]

Table 14 shows experimental absolute rate constants[123a] for the addition of radicals R–CH_2–CXY$^{\bullet}$, derived by reaction of small radicals R$^{\bullet}$ with methylmethacrylate and methylacry-

Table 14. Absolute rate constants for the addition to monomers CH_2=CXY and ESR hyperfine coupling constants (±0.05 G) of radicals R–CH_2–CXY$^\bullet$ at 295 K. MA = methylacrylate, MMA = methylmethacrylate, *t*Bu = *tert*-butyl, POH = 2-hydroxy-2-propyl, Ph = phenyl, MOH = hydroxymethyl.

Reaction	k [$M^{-1}s^{-1}$]	$3H_\beta$, H_α [G]	$2H_\beta$ [G]	$3H_\gamma$(CO_2Me) [G]
*t*Bu-MMA$^\bullet$ + MMA[a]	600	21.88	11.71	1.32
POH-MMA$^\bullet$ + MMA[a]	1205	22.09	11.93	1.35
Ph-MMA$^\bullet$ + MMA[b]	2640	22.05	14.03	1.29
MOH-MMA$^\bullet$ + MMA[c]	3290	22.17	14.43	1.36
*t*Bu-MA$^\bullet$ + MA[c]	6120	19.83	21.09	1.50
POH-MA$^\bullet$ + MA[a]	3290	20.03	21.28	1.55
Ph-MA$^\bullet$ + MA[b]	22400	20.34	21.44	1.40
MOH-MA$^\bullet$ + MA[c]	18110	20.41	22.32	1.50

[a] Solvent: 2-propanol. [b] Solvent: 1,1,2-trifluoro-1,2,2-trichloroethane. [c] Solvent: methanol.

late, to their monomers, that is, for the second step in a polymerization. The rate constants do depend on the penultimate unit (R), that is, there is a significant γ-substituent effect. They represent the first direct kinetic data providing evidence for the penultimate effect, and they support the explicit penultimate model. In particular, for methylmethacrylate, the second-step additions are faster than the homopropagation ($345\,M^{-1}s^{-1}$), and they decrease with the increasing steric demand of R (primary alkyl < phenyl < tertiary alkyl) by a factor of about five. The adducts of tertiary radicals R$^\bullet$ also add to methylacrylate more slowly, by up to a factor of seven, than the adducts of the sterically less-demanding hydroxymethyl and phenyl radicals. However, adducts of tertiary radicals add more slowly to this monomer than its homopropagation radical ($19000\,M^{-1}s^{-1}$). Thus, in these cases, the propagation constant does not decrease but increases with increasing chain length. For both monomers, the reactivity ratios s_i are in the usual range.

Table 14 also presents hyperfine coupling constants for the adduct radicals. In accord with abundant ESR studies[124] on radicals of the type R–CH_2–CXY$^\bullet$ with polyatomic groups R, they indicate planar radical centers with very similar spin populations and two equivalent equilibrium conformations with non-zero dihedral angles $\phi < 45^\circ$ between the C_β–R bond and the $2p_z$ axis of the radical center (Figure 18). The equilibrium angle ϕ is smaller for the methacrylate than for the acrylate-derived radicals and decreases with the increasing size of R. There is an exchange between the equilibrium conformations, and line-broadening effects point to a faster exchange for the acrylate than for the methacrylate radicals and a slower exchange for bulkier groups R. This all means that the radicals with smaller groups R have more rotational freedom about the C_β-R bond, and that this motion is less hindered for acrylate than for methacrylate radicals, as might have been expected from simple steric considerations.[125]

These structural features provide some indications as to the origin of the penultimate unit effect.[126] We first note that, according to the theoretical calculations, the dihedral angle must be close to zero in the transition structure (Figure 2); for the radicals presented here this is not the case. Hence, upon

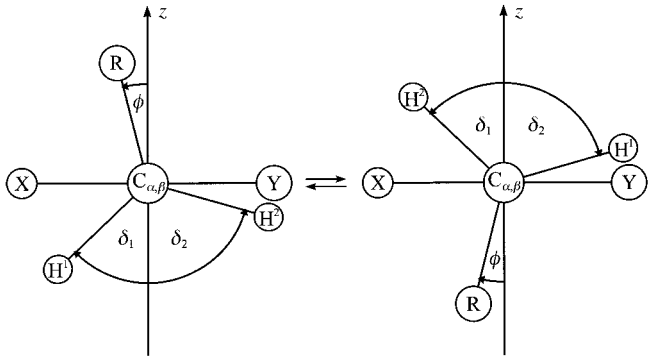

Figure 18. Equilibrium conformations of adduct radicals R–CH_2–CXY$^\bullet$.

approach to the transition structure for the next addition they have to reach higher energy conformations and will lose motional freedom. This will be energetically and entropically more costly for the radicals with bulkier groups R, and will increase the activation energy and lower the frequency factor of the addition. Both effects lead to a decrease in the rate constants with increasing size of R, as is observed. They also explain why the methacrylate radicals with tertiary penultimate groups R add more slowly to their monomer than the homopropagation radical for which R is a less sterically demanding secondary group. Moreover, the attacking radical, as suggested by the theoretical findings, is bent considerably in the transition structure (Figure 2). For the radicals R–CH_2–CXY$^\bullet$, this bending requires an approach of the α-substituents X and Y to the β-substituent R which will again be more costly for the larger groups R. Calculations are under way which should allow the importance of these effects to be addressed.[123b]

5.3. Other Unsaturated Compounds

In addition to the rate data discussed so far, there are numerous individual absolute and relative rate constants and activation parameters for additions of carbon-centered radicals to other molecules with unsaturated carbon–carbon bonds such as polyenes, allenes, alkynes, aromatic compounds, and heteroaromatic compounds, both for the liquid and for the gas phase.[31, 72, 73, 127] Of particular diagnostic value are the large series of so-called radical affinities reported by Szwarc and others.[127] These are ratios of the addition constants versus the rate constants for hydrogen abstraction by the same radical from suitable solvents. The methyl affinities were recently converted into absolute constants.[58b] A complete analysis is not yet possible because the heats of reaction and the energies of the CT configurations which determine the enthalpic and polar factors can not be reliably estimated for most cases. However, for a few examples predictions are possible.

Table 15 lists experimental rate parameters[58b] for the addition of the methyl radical to 1,3-butadiene, 1,2-butadiene (i.e. an allene), benzene, and ethyne in solution. They should not be subject to strong polar effects, and hence the activation

Table 15. Experimental and predicted rate constants at room temperature, frequency factors, and activation energies for the addition of the methyl radical to several unsaturated molecules. Predicted rate data are given in italics.

Compound	k_{300} [$M^{-1}s^{-1}$]	$\lg(A/M^{-1}s^{-1})$	E_a [kJ mol^{-1}]
1,3-butadiene	6.4×10^5/*1.1×10^5*	9.6/*8.5*[a]	21.8/*20.0*[b]
1,2-butadiene	4.3×10^3/*2.8×10^3*	8.3/*8.5*[a]	26.8/*29.0*[b]
benzene	46/*34*	8.2/*8.5*[c]	37.2/*40.0*[b]
ethyne	5.3×10^3/*1.1×10^5*	9.7/*9.4*[d]	34.3/*25.0*[b]

[a] As for the addition of the methyl radical to monosubstituted and 1,1-disubstituted alkenes. [b] Estimated as described[69] from reaction enthalpies derived from available heats of formation and bond dissociation energies and using Equation (3). [c] Estimated from $\lg(A/M^{-1}s^{-1}) = 8.5$ for the addition of the methyl radical to monosubstituted and 1,1-disubstituted alkenes with a downward correction of about 0.5 for the steric effect of α substitution and an upward correction for the increased number of addition sites. [d] As for the addition of various radicals to other alkynes, see text.

energies should follow an Evans – Polanyi – Semenov relation. Using the best available enthalpies of formation and bond-dissociation energies to estimate the reaction enthalpies as before,[69] and applying Equation (2), we arrive at the predicted activation energies which are also listed in Table 15. The frequency factors should not vary grossly, and therefore they can be estimated from the values observed for other reactions presented above. The activation energies and frequency factors then yield the predicted rate constants. As is evident from Table 15, the agreement between the experimental and predicted rate parameters is very satisfactory for the first three cases, where the observed and predicted rate constants agree within one order of magnitude. This indicates that the basic Evans – Polanyi – Semenov relation is also valid for more than just the monosubstituted and 1,1-disubstituted alkenes, at least approximately, and it supports the general and strong influence of the reaction enthalpy on the activation energies. A consideration of the terms leading to the reaction enthalpy reveals that, in comparison with ethene, the methyl radical adds faster to 1,3-butadiene because a more stabilized radical is formed. It adds faster to allene because the parent compound is less stabilized than the products, and to benzene it adds more slowly because the aromatic resonance stabilization is lost. Data for additions to electron-acceptor-substituted polyenes, benzenes, condensed aromatic compounds, and heterocycles also clearly confirm the weak nucleophilicity of the methyl radical.[58b]

For ethyne, the prediction is not satisfactory because the estimated activation energy is too low by nearly 10 kJ mol^{-1}, and the estimated rate constant exceeds the experimental value by more than one order of magnitude. Of course, this may be because of a failure in our enthalpy estimation procedure. However, methyl adds more slowly to ethyne than to ethene (Table 16), even though the reaction is more exothermic by an estimated 15 kJ mol^{-1}, an ab initio calculation gave an increased exothermicity of 34 kJ mol^{-1}.[128] Hence, additions to alkynes deserve special discussion. In fact, the slower addition of carbon-centered radicals to alkynes in comparison with similarly substituted alkenes is a general feature,[2–4, 127] and it is again demonstrated by the results given in Table 16. The rate constants for the addition of the three radicals to alkynes are all lower than for the addition to the corresponding alkenes. Also, the substituent effects appear to be less pronounced, that is, the enthalpic and the polar substituent effects are smaller though they show the same direction for alkenes and alkynes. For the alkynes the frequency factors are higher, and from a larger series an average $\lg(A/M^{-1}s^{-1}) = 9.2 \pm 0.4$ was deduced.[62d] Presumably, this is because of the linear alkyne structure and the correspondingly missing degree of freedom of rotation about the alkyne triple bond. The lower alkyne entropy suggests a smaller entropy loss upon formation of the transition structure for the alkynes than for the alkenes, and this is confirmed by calculations.[128] Since the frequency factors are higher, the lower rate constants are caused by the considerably higher activation energies. The additions to alkynes are more exothermic than the additions to alkenes, thus the higher activation energies are contra thermodynamics. A consideration of the state correlation diagram points to possible reasons. Firstly, for alkynes the electron affinities are smaller and the ionization energies are larger than for the corresponding alkenes. This diminishes the polar effects, and makes the alkyne reactions less selective and increases the activation energies. Secondly, the triplet energies are higher for alkynes than for alkenes, and this should also increase the barriers. In Sections 4.3.1.6 and 4.3.1.7 for the additions to alkenes we did not find a clear influence of the location of the triplet state, and thought it was incorporated in the enthalpic effect. However, in principle, variations of the triplet energy should cause changes in the activation energy independent of the reaction enthalpy, and we suggest that the slower additions to alkynes are partly a manifestation of this effect. It implies that the parameters in the Evans – Polanyi – Semenov relation [Eq. (2)] are smaller for alkyne additions than for alkene and other closely related additions.

Table 16. Rate constants at room temperature, frequency factors, and activation energies for the addition of methyl (Me),[58b] *tert*-butyl (*t*Bu),[62d] and *tert*-butoxycarbonyl methyl[62d] (MEst) radicals to alkynes and alkenes.

Reaction	k_{300} [$M^{-1}s^{-1}$]	$\lg(A/M^{-1}s^{-1})$	E_a [kJ mol^{-1}]
Me + HC≡CH	5.3×10^3	9.7	34.3
Me + H_2C=CH_2	7.0×10^3	8.5	28.2
Me + HC≡CCH_3	2.4×10^3	8.8	31.1
Me + CH_2=$CHCH_3$	4.3×10^3	8.5	27.7
Me + HC≡CPh	4.9×10^4	9.2	25.9
Me + CH_2=CHPh	2.6×10^5	8.5	17.5
Me + PhC≡CPh	1.5×10^3	10.5	42.1
Me + (*E*)-PhCH=CHPh	9.7×10^3	8.2	24.2
*t*Bu + HC≡$CSiMe_3$	2.4×10^3	8.9	30.8
*t*Bu + CH_2=$CHSiMe_3$	9.6×10^3	7.5	20.2
*t*Bu + HC≡CPh	2.1×10^4	8.7	23.8
*t*Bu + CH_2=CHPh	1.3×10^5	7.5	13.7
*t*Bu + HC≡CCO_2Me	1.8×10^5		
*t*Bu + CH_2=$CHCO_2Me$	1.1×10^6		
MEst + HC≡$CSiMe_3$	2.2×10^4	9.4	31.7
MEst + CH_2=$CHSiMe_3$	8.9×10^4	8.5	19.8
MEst + HC≡CCO_2Et	5.1×10^4	8.5	21.6
MEst + CH_2=$CHSiMe_3$	4.9×10^5	8.5	15.6

6. Synopsis and Perspective

Rate constants for the addition of carbon-centered radicals to alkenes and other compounds with unsaturated carbon–carbon bonds can presently be measured to rather high precision, that is, with errors $< 50\,\%$. They vary with radical and substrate substitution by many orders of magnitude from values close to zero to the upper diffusion- or collision-controlled limit of about $10^9 - 10^{10}\,M^{-1}s^{-1}$. Because of error correlation, the frequency factors are usually precise only within a factor of two and the activation energies to ± 4–$6\,kJ\,mol^{-1}$.

The frequency factors for additions to structurally related systems span a limited range, and the often much larger rate variations are primarily because of variations in the activation energy associated with radical and substrate substitution. Excursions of the frequency factors from the established ranges often go parallel with unusual activation energies. This deviation points to error compensation effects of the Arrhenius parameters and calls for advanced error analyses.[129] Both for the gas and the liquid phase, the frequency factors of radical addition to monosubstituted and 1,1-disubstituted alkenes $CH_2{=}CXY$ are insensitive to the β-alkene substituents X and Y, are in the range $6.5 < \lg(A/M^{-1}s^{-1}) < 9.0$ and decrease with the increasing steric demand of the attacking radical. As a rule, one has $\lg(A/M^{-1}s^{-1}) = 7.0 \pm 0.5$ for polymeric, 7.5 ± 0.5 for tertiary, 8.0 ± 0.5 for secondary and 8.5 ± 0.5 for primary small alkyl radicals. Because of steric effects, alkene substitution at the attacked carbon atom lowers the frequency factor by about one order of magnitude. For the addition to polyenes, allenes, and aromatic compounds, similar frequency factor ranges and steric substituent effects apply but for alkynes a larger frequency factor of $\lg(A/M^{-1}s^{-1}) = 9.2 \pm 0.5$ is recommended. If the reaction rate approaches that for diffusion-controlled reactions, the frequency factor increases to $\lg(A/M^{-1}s^{-1}) = 9$–10. Enthalpic, polar, and solvent effects appear to have only a minor influence on the frequency factors.

The activation energies of additions follow the same pattern for gas and liquid phase systems but, in general, the gas-phase activation energies seem to be higher by several $kJ\,mol^{-1}$ which leads to rate constants that are about ten times lower. *High-level ab initio calculations* can provide barriers and reaction enthalpies within the experimental precision, if the phase effect is taken into account. Suitable high-level theoretical methods include CBS-RAD and G3(MP2)-RAD, while less costly techniques like B3-LYP/6-31G(d) can still be usefully employed for larger systems. The popular UMP2 procedure often gives quite unreliable results.

The *state correlation diagram* provides an excellent basis for the discussion of the activation energies which, depending on the reaction, are dominated by enthalpic and polar substituent effects. *Steric effects on the activation energies* should generally be considered as part of the enthalpic effect, and it should be noticed that diffusion sets a lower limit to the activation energy of about $10\,kJ\,mol^{-1}$.

The reaction enthalpy H_r has a *general and often dominating influence* on the activation energy which for many alkyl radical additions to monosubstituted and 1,1-disubstituted alkenes is well described by a linear Evans–Polanyi–Semenov relation, specifically $E_a\,[kJ\,mol^{-1}] = 50 + 0.22\,H_r\,[kJ\,mol^{-1}]$. This relation is also approximately valid for other additions. The enthalpy contribution seems to incorporate an expected effect from the location of the excited triplet state of the reactants, with the possible exception of additions to alkynes where a higher constant term in the Evans–Polanyi–Semenov relation may apply. Hence, the reactivities of alkynes are remarkably low.

Polar substituent effects reflect contributions of the CT configurations to the transition state. They become noticeable when the energies of the CT configurations are less than about 10 eV higher than the reactant ground-state energy. For nucleophilic radicals with low ionization energies ($E_i < 8$–9 eV) this is the case for additions to electron-deficient alkenes, while for electrophilic radicals with high electron affinities ($E_{ea} > 2$ eV) it holds for additions to electron-rich alkenes. Radicals with borderline ionization energies and electron affinities often show an ambiphilic behavior.

The polar substituent effects decrease the activation energies below the enthalpy contribution by *multiplicative factors* ($0 < F_p < 1$). Besides depending on the energy location of the CT configurations, these depend also on the Coulomb attraction and the strength of the interaction between the polar and nonpolar configurations at the transition structure. The polar factors can not be separated into radical and alkene contributions.[130] As a rule, substituents which are capable of strongly delocalizing the transferred charges lead to smaller decreases in the activation energies by polar effects. Because of the combination of enthalpy and polar effects, nucleophilic radicals are usually more selective and more reactive in reactions with different substrates than non-nucleophilic radicals, electrophilic radicals are less selective but more reactive, and ambiphilic radicals are as selective as radicals without polar effects but more reactive. Recommended ranges for the Coulomb and the interaction parameters are given in the text and footnotes for the additions to monosubstituted and 1,1-disubstituted alkenes. For other additions, the same principles operate but accurate parameters can not yet be given.

To predict the magnitude of the enthalpy contribution to the activation energies, one needs to know the reaction enthalpy H_r. This can either be calculated by quantum chemical methods or estimated. The latter procedure requires the knowledge of the enthalpies of formation and bond dissociation energies for the molecule and radical. To predict the size of the polar factors one needs CT energies and a reliable estimate of the Coulomb and interaction energies.

Linear correlations of rate constants or activation energies with energy parameters such as the reaction enthalpy and the electron affinities and ionization energies of the reactants are of limited value because these parameters are mutually interrelated, and such an approach may even lead to wrong conclusions.[132] The analysis presented herein avoids this difficulty and takes the nonadditive operation of the various effects into proper account. For a variety of cases, it has allowed the prediction of addition constants correct to within one order of magnitude of the experimental data. The predictive power of the present analysis greatly exceeds that

of the previous qualitative rules. In contrast to these, we conclude that the reaction enthalpy has a large influence in all cases. We believe that our rationalization of addition rates and the factors controlling them can be extended to many more reactions than covered so far, with the increasing availability of more reliable radical heats of formation, bond dissociation energies, molecular electron affinities and ionization energies and with a better understanding of the Coulomb and interaction terms from either experiment or theory.

We thank our co-workers named in the citations for the provision of the experimental and theoretical data and many ideas. The Zurich group gratefully acknowledges the long-lasting support by the Swiss National Foundation for Scientific Research, and the Australian National University (ANU) group thanks the ANU Supercomputer Facility for the continuing generous provision of supercomputer time. H. F. appreciates the hospitality of the Research School of Chemistry at the Australian National University where this review was initiated.

Received: June 8, 2000 [A414]

[1] B. Giese, *Radicals in Organic Synthesis: Formation of Carbon-Carbon Bonds*, Pergamon, Oxford, **1986**.
[2] D. P. Curran in *Comprehensive Organic Synthesis*, *Vol. 4* (Eds.: B. M. Trost, I. M. Fleming, M. F. Semmelhack), Pergamon, Oxford, **1991**.
[3] J. Fossey, D. Lefort, J. Sorba, *Free Radicals in Organic Chemistry*, Wiley, New York, **1995**.
[4] B. Giese, *Angew. Chem.* **1985**, *97*, 555; *Angew. Chem. Int. Ed. Engl.* **1985**, *24*, 553.
[5] a) C. Walling, *Free Radicals in Solution*, Wiley, New York, **1957**, and refs therein; b) W. A. Pryor, *Introduction to Free Radical Chemistry*, Prentice-Hall, Englewood Cliffs, **1966**.
[6] J. M. Tedder, J. C. Walton, *Acc. Chem. Res.* **1976**, *9*, 183; J. M. Tedder, J. C. Walton, *Adv. Phys. Org. Chem.* **1978**, *18*, 51; J. M. Tedder, J. C. Walton, *Tetrahedron* **1980**, *36*, 701; J. M. Tedder, *Angew. Chem.* **1982**, *94*, 433; *Angew. Chem. Int. Ed. Engl.* **1982**, *21*, 401.
[7] B. Giese, *Angew. Chem.* **1983**, *95*, 771; *Angew. Chem. Int. Ed. Engl.* **1983**, *22*, 573.
[8] F. Minisci, E. Vismara, F. Fontana, *Heterocycles* **1989**, *28*, 489.
[9] H. Fischer in *Free Radicals in Biology and Environment* (Ed.: F. Minisci), Kluwer, Dordrecht, **1997**.
[10] D. N. Curran, N. A. Porter, B. Giese, *Stereochemistry of Radical Reactions*, VCH, Weinheim, **1996**; M. P. Sibi, N. A. Porter, *Acc. Chem. Res.* **1999**, *32*, 163.
[11] G. S. Hammond, *J. Am. Chem. Soc.* **1955**, *77*, 334.
[12] M. W. Wong, L. Radom, *J. Phys. Chem.* **1995**, *99*, 8582.
[13] D. Henry, M. W. Wong, L. Radom, unpublished results.
[14] a) M. G. Evans, *Discuss. Faraday Soc.* **1947**, *2*, 271; M. G. Evans, J. Gergely, E. C. Seaman, *J. Polym. Sci.* **1948**, *3*, 866; b) N. N. Semenov, *Some Problems in Chemical Kinetics and Reactivity (Engl. Transl.)* Princeton Press, Princeton, **1958**, pp. 29–33.
[15] A. P. Stefani, L. Herk, M. Szwarc, *J. Am. Chem. Soc.* **1961**, *83*, 4732.
[16] K. Riemenschneider, H. M. Bartels, R. Dornow, E. Drechsel-Grau, W. Eichel, H. Luthe, Y. M. Matter, W. Michaelis, P. Boldt, *J. Org. Chem.* **1987**, *52*, 205.
[17] V. Diart, B. P. Roberts, *J. Chem. Soc. Perkin Trans 2*, **1992**, 1761; R. Santi, F. Bergamini, A. Citterio, R. Sebastiano, M. Nicolini, *J. Org. Chem.* **1992**, *57*, 4250; E. Baciocchi, B. Giese, H. Farshchi, R. Ruzziconi, *J. Org. Chem.* **1990**, *55*, 5688.
[18] a) B. Giese, J. He, W. Mehl, *Chem. Ber.* **1988**, *121*, 2063; b) E. Baciocchi, B. Floris, E. Muraglia, *J. Org. Chem.* **1993**, *58*, 2013.
[19] M. Levy, M. Szwarc, *J. Am. Chem. Soc.* **1955**, *77*, 1949; M. Szwarc, *J. Polym. Sci.* **1955**, *16*, 367.
[20] M. D. Bartberger, W. R. Dolbier, Jr., J. Lusztyk, K. U. Ingold, *Tetrahedron* **1997**, *53*, 9857.
[21] K. Héberger, M. Walbiner, H. Fischer, *Angew. Chem.* **1992**, *104*, 651; *Angew. Chem. Int. Ed. Engl.* **1992**, *31*, 635.
[22] a) S. S. Shaik, *Prog. Phys. Org. Chem.* **1985**, *15*, 197; b) S. S. Shaik, H. B. Schlegel, S. Wolfe, *Theoretical Aspects of Physical Organic Chemistry. The S_N2 Mechanism*, Wiley, New York, **1992**; c) S. S. Shaik, A. Shurki, *Angew. Chem.* **1999**, *111*, 616; S. S. Shaik, A. Shurki, *Angew. Chem. Int. Ed.* **1999**, *38*, 586, and refs therein.
[23] a) A. Pross, S. S. Shaik, *Acc. Chem. Res.* **1983**, *16*, 363; b) A. Pross, *Adv. Phys. Org. Chem.* **1985**, *21*, 99; c) A. Pross, *Theoretical and Physical Principles of Organic Reactivity*, Wiley, New York, **1995**.
[24] H. C. Longuet-Higgins, E. W. Abrahamson, *J. Am. Chem. Soc.* **1965**, *87*, 2045; V. Bonacic-Koutecky, J. Koutecky, L. Salem, *J. Am. Chem. Soc.* **1977**, *99*, 842.
[25] S. S. Shaik, E. Canadell, *J. Am. Chem. Soc.* **1990**, *112*, 1446.
[26] M. W. Wong, A. Pross, L. Radom, *J. Am. Chem. Soc.* **1993**, *115*, 11050.
[27] M. W. Wong, A. Pross, L. Radom, *Isr. J. Chem.* **1993**, *33*, 415.
[28] M. W. Wong, A. Pross, L. Radom, *J. Am. Chem. Soc.* **1994**, *116*, 6284.
[29] M. W. Wong, A. Pross, L. Radom, *J. Am. Chem. Soc.* **1994**, *116*, 11938.
[30] A. Salikhov, H. Fischer, *Theor. Chem. Acc.* **1997**, *96*, 114.
[31] *Radical Reaction Rates in Liquids* (Ed.: H. Fischer), Landolt-Boernstein, New Series, *Vols. II/13* and *II/18*, Springer, Berlin, **1983–97**.
[32] G. Porter, M. R. Topp, *Proc. R. Soc. London A* **1970**, *315*, 163; J. C. Scaiano, *Acc. Chem. Res.* **1983**, *16*, 234; *Handbook of Organic Photochemistry* (Ed.: J. C. Scaiano), CRC, Boca Raton, **1989**, and refs therein.
[33] H. Fischer, H. Paul, *Acc. Chem. Res.* **1987**, *20*, 200.
[34] G. V. Buxton, J. C. Green, *J. Chem. Soc. Faraday Trans. 1* **1978**, *74*, 697.
[35] F. Jent, H. Paul, E. Roduner, M. Heming, H. Fischer, *Int. J. Chem. Kinet.* **1986**, *18*, 1113.
[36] a) C. Blättler, Ph.D. Thesis, University of Zürich, **1995**; b) I. Gatlik, P. Rzadek, G. Gescheidt, G. Rist, B. Hellrung, J. Wirz, K. Dietliker, G. Hug, M. Kunz, J.-P. Wolf, *J. Am. Chem. Soc.* **1999**, *121*, 8332; c) S. N. Batchelor, H. Fischer, *J. Phys. Chem.* **1996**, *100*, 9794.
[37] a) Y. Ishikawa, P. A. Hackett, D. M. Rayner, *J. Am. Chem. Soc.* **1987**, *109*, 6644; b) G. N. R. Tripathy, R. H. Schuler, *J. Chem. Phys.* **1984**, *81*, 113.
[38] O. F. Olaj, I. Bitai, F. Hinkelmann, *Makromol. Chem.* **1987**, *188*, 1689; O. F. Olaj, I. Bitai, *Angew. Makromol. Chem.* **1987**, *155* ,177.
[39] a) M. Buback, R. G. Gilbert, R. A. Hutchinson, B. Klumperman, F.-D. Kuchta, B. G. Manders, K. F. O'Driscoll, G. T. Russell, J. Schweer, *Macromol. Chem. Phys.* **1995**, *196*, 3267; b) S. Beuermann, M. Buback, T. P. Davies, R. G. Gilbert, R. A. Hutchinson, O. F. Olaj, G. T. Russell, J. Schweer, A. M. van Herk, *Macromol. Chem. Phys.* **1997**, *198*, 1545; c) M. D. Zammit, M. D. Coote, T. P. Davies, G. D. Willett, *Macromolecules* **1998**, *31*, 955, and refs therein.
[40] W. J. Hehre, L. Radom, P. von R. Schleyer, J. A. Pople, *Ab Initio Molecular Orbital Theory*, Wiley, New York, **1986**.
[41] F. Jensen, *Introduction to Computational Chemistry*, Wiley, Chichester, **1998**.
[42] A. P. Scott, L. Radom, *J. Phys. Chem.* **1996**, *100*, 16502.
[43] W. Kohn, A. D. Becke, R. G. Parr, *J. Phys. Chem.* **1996**, *100*, 12974.
[44] See, for example, B. G. Johnson, C. A. White, Q. Zhang, B. Chen, R. L. Graham, P. M. W. Gill, M. Head-Gordon, *Theor. Comput. Chem.* **1996**, *4*, 441.
[45] For a recent review, see T. Bally, W. T. Borden, in *Reviews in Computational Chemistry*, *Vol. 13* (Eds.: K. B. Lipkowitz, D. B. Boyd), Wiley-VCH, New York, **1999**.
[46] P. J. Knowles, K. Somasundram, N. C. Handy, K. Hirao, *Chem. Phys. Lett.* **1985**, *113*, 8.
[47] a) P. M. W. Gill, L. Radom, *Chem. Phys. Lett.* **1986**, *132*, 16; b) R. H. Nobes, D. Moncrieff, M. W. Wong, L. Radom, P. M. W. Gill, J. A. Pople, *Chem. Phys. Lett.* **1991**, *182*, 216.
[48] P. J. Knowles, J. S. Andrews, R. D. Amos, N. C. Handy, J. A. Pople, *Chem. Phys. Lett.* **1991**, *186*, 130.
[49] H. B. Schlegel, *J. Chem. Phys.* **1986**, *84*, 4530.
[50] J. A. Pople, M. Head-Gordon, K. Raghavachari, *J. Chem. Phys.* **1987**, *87*, 3700.
[51] R. J. Bartlett, J. F. Stanton in *Reviews in Computational Chemistry*, *Vol. 5* (Eds.: K. B. Lipkowitz, D. B. Boyd), Wiley-VCH, New York, **1994**.

[52] J. F. Stanton, *J. Chem. Phys.* **1994**, *101*, 371.
[53] J. Baker, A. Scheiner, J. Andzelm, *Chem. Phys. Lett.* **1993**, *216*, 380.
[54] J. A. Pople, P. M. W. Gill, N. C. Handy, *Int. J. Quantum Chem.* **1995**, *56*, 303.
[55] a) L. A. Curtiss, K. Raghavachari, G. W. Trucks, J. A. Pople, *J. Chem. Phys.* **1991**, *94*, 7221; b) L. A. Curtiss, K. Raghavachari, P. C. Redfern, V. Rassolov, J. A. Pople, *J. Chem. Phys.* **1998**, *109*, 7764; c) For a recent review, see "Computational Thermochemistry": L. A. Curtiss, K. Raghavachari, *ACS Symp. Ser.* **1998**, *677*, 176.
[56] a) J. W. Ochterski, G. A. Petersson, J. A. Montgomery, Jr., *J. Chem. Phys.* **1996**, *104*, 2598; b) For a recent review, see "Computational Thermochemistry": G. A. Petersson, *ACS Symp. Ser.* **1998**, *677*, 237.
[57] J. M. L. Martin, G. de Oliveira, *J. Chem. Phys.* **1999**, *111*, 1843.
[58] a) T. Zytowski, H. Fischer, *J. Am. Chem. Soc.* **1996**, *118*, 437; b) T. Zytowski, H. Fischer, *J. Am. Chem. Soc.* **1997**, *119*, 12869.
[59] M. Walbiner, J. Q. Wu, H. Fischer, *Helv. Chim. Acta* **1995**, *78*, 910.
[60] a) J. Q. Wu, I. Beranek, H. Fischer, *Helv. Chim. Acta* **1995**, *78*, 194; b) I. Beranek, H. Fischer in *Free Radicals in Synthesis and Biology* (Ed.: F. Minisci), Kluwer, Dordrecht, **1988**.
[61] J. Q. Wu, H. Fischer, *Int. J. Chem. Kinet.* **1995**, *27*, 167.
[62] a) K. Münger, H. Fischer, *Int. J. Chem. Kinet.* **1985**, *17*, 809; b) H. Fischer in *Substituent Effects in Radical Chemistry* (Eds.: H. G. Viehe, Z. Janousek, R. Merényi), Reidel, Dordrecht **1986**; c) A. Salikhov, Ph.D. Thesis, University of Zürich, **1997**; d) H. Rubin, H. Fischer, *Helv. Chim. Acta* **1996**, *79*, 1670.
[63] a) K. Héberger, H. Fischer, *Int. J. Chem. Kinet.* **1993**, *25*, 913; b) R. Martschke, R. D. Farley, H. Fischer, *Helv. Chim. Acta* **1997**, *80*, 1363; c) R. Martschke, Ph.D. Thesis, University of Zürich, **1999**.
[64] T. Zytowski, B. Knuehl, H. Fischer, *Helv. Chim. Acta* **2000**, *83*, 658.
[65] K. Héberger, H. Fischer, *Int. J. Chem. Kinet.* **1993**, *25*, 249.
[66] M. Weber, H. Fischer, *Helv. Chim. Acta* **1998**, *81*, 770.
[67] D. V. Avila, K. U. Ingold, J. Lusztyk, W. R. Dolbier, Jr., H. Q. Pan, *J. Am. Chem. Soc.* **1993**, *115*, 1577; D. V. Avila, K. U. Ingold, J. Lusztyk, W. R. Dolbier, Jr., H. Q. Pan, M. Muir, *J. Am. Chem. Soc.* **1994**, *116*, 99; D. V. Avila, K. U. Ingold, J. Lusztyk, W. R. Dolbier, Jr., H. Q. Pan, *J. Org. Chem.* **1996**, *61*, 2027; D. V. Avila, K. U. Ingold, J. Lusztyk, W. R. Dolbier, Jr., H. Q. Pan, *Tetrahedron* **1996**, *52*, 12351.
[68] It should be kept in mind that rate constants for bimolecular reactions in solution can not exceed the diffusion-controlled upper limit. For low viscosity solvents, the limit k_{Diff} is in the range[33] of $3\times10^9\,M^{-1}s^{-1}$ to $7\times10^9\,M^{-1}s^{-1}$ at room temperature, with a frequency factor A_{Diff} of about $5\times10^{11}\,M^{-1}s^{-1}$ and an activation energy $E_{a,Diff}$ of about 10 kJ mol^{-1}. For the addition of the 2-hydroxy-2-propyl radical to acrylates, acrylonitriles, and acrolein, the rate constants given in Table 1 are close to or even exceed the frequency factor $\lg(A/M^{-1}s^{-1})=7.5$ observed for the same and other tertiary alkyl radicals in a variety of other reactions. Measured temperature dependencies of k give $\lg(A/M^{-1}s^{-1})=9.0$ and $E_a=10.4$ kJ mol^{-1} for the addition of 2-hydroxy-2-propyl to methyl methacrylate and $\lg(A/M^{-1}s^{-1})=8.9$ and $E_a=8.9$ kJ mol^{-1} for the addition to methacrylonitrile.[63c] These frequency factors and activation energies indicate the onset of diffusion control. Hence, the activation energies of the addition step itself must be smaller than the observed values.
[69] Calculated from $H_r(Me)=h_f(MeCH_2CXYH)-h_f(CH_2=CXY)-h_f(CH_4)+E_d(MeCH_2CXY\text{-}H)-E_d(CH_3\text{-}H)$ from standard molar heats of formation h_f and bond dissociation energies E_d as described earlier with error assessments.[58] Deviations from reported data are because of a reevaluation based on more recent and more reliable experimental and theoretical heats of formation and bond dissociation energies which were not available or known to us before.[70] Some deviations in the correlations of activation energies with H_r may be because of remaining errors in H_r.
[70] N. Cohen, *J. Phys. Chem. Ref. Data* **1996**, *25*, 1411; K. Rakus, S. P. Verevkin, H.-D. Beckhaus, C. Rüchardt, *Chem. Ber.* **1994**, *127*, 2225; W. V. Steele, R. D. Chirico, N. K. Smith, *J. Chem. Thermodyn.* **1995**, *27*, 671; J. A. Manion, R. Louw, *Recl. Trav. Chim. Pays-Bas* **1986**, *105*, 442; J.-L. M. Abboud, P. Jimenez, M. V. Roux, C. Turrion, C. Lopez-Mardomingo, *J. Phys. Org. Chem.* **1995**, *8*, 15; M. R. Ahmad, G. D. Dahlke, S. R. Kass, *J. Am. Chem. Soc.* **1996**, *118*, 1398; D. A. Block, D. A. Armstrong, A. Rauk, personal communication; M. J. Rossi, D. F. McMillan, D. M. Golden, *J. Phys. Chem.* **1984**, *88*, 5031.
[71] Estimated for the addition to ethene as $\Delta H_r(R)=H_r(R)-H_r(Me)=h_f(RCH_2CXYH)-h_f(MeCH_2CXYH)-h_f(RH)+h_f(CH_4)-E_d(R\text{-}H)+E_d(CH_3\text{-}H)$. The small difference between $E_d(MeCH_2CXY\text{-}H)$ and $E_d(RCH_2CXY\text{-}H)$ is neglected.
[72] J. A. Kerr in *Free Radic*als, *Vol. 1* (Ed.: J. Kochi), Wiley, New York, **1972**; P. M. Holt, J. A. Kerr, *Int. J. Chem. Kinet.* **1977**, *9*, 185; D. L.Baulch, C. J. Cobos, R. A. Cox, C. Esser, P. Frank, T. Just, J. A. Kerr, M. J. Pilling, J. Troe, R. W. Walker, J. Warnatz, *J. Phys. Chem. Ref. Data* **1992**, *21*, 411; D. L.Baulch, C. J. Cobos, R. A. Cox, C. Esser, P. Frank, T. Just, J. A. Kerr, M. J. Pilling, J. Troe, R. W. Walker, J. Warnatz, *J. Phys. Chem. Ref. Data* **1994**, *23*, 847.
[73] J. A. Kerr, S. J. Moss, *CRC Handbook of Bimolecular and Termolecular Gas Reactions*, CRC, Boca Raton, **1981**, and refs therein.
[74] The additions should obey the Eyring equation which for an addition reaction, under proper inclusion[75] of the standard concentration ($c_S=1$ M) is, $k=(k_BT/hc_S)\exp(\Delta S^{\ddagger}/R)\exp(-\Delta H^{\ddagger}/RT)$. For equal activation entropies $\Delta S^{\ddagger}$ and activation enthalpies $\Delta H^{\ddagger}$ in both phases, one can then derive the relationship for the difference of the activation energy in the gas (g) and liquid (l) state $(E_a^g-E_a^l)/RT=\ln(A^g/A^l)=1-\alpha^l/\alpha^g$. The isobaric thermal expansion coefficients α follow $\alpha^l<\alpha^g=1/T$ (perfect gas). Hence, the gas-phase activation energy should be higher than the liquid-phase value by about $RT=2.5$ kJ mol^{-1} at room temperature. For the frequency factor, a related higher gas-phase value should hold but the rate constants should be equal.
[75] P. J. Robinson, *J. Chem. Educ.* **1978**, *55*, 509; D. M. Golden, *J. Chem. Educ.* **1971**, *48*, 235.
[76] S. Beuermann, M. Buback in *High Pressure Molecular Science* (Eds.: R. Winter, J. Jonas), Kluwer Academic, Amsterdam, **1999**.
[77] For the pressure dependence of addition rate parameters, the Eyring equation gives $(\partial E_a/\partial p)_T/RT=\Delta V^{\ddagger}/RT-\Delta V^{\ddagger}\alpha_V/R+T(\partial\alpha_V/\partial p)_T$ and $(\partial\ln(A)/\partial p)_T=-\kappa-\Delta V^{\ddagger}\alpha_V/R+T(\partial\alpha_V/\partial p)_T$ where κ is the isothermal cubic compressibility, so that $(\partial\ln(k)/\partial p)_T=-\kappa-\Delta V^{\ddagger}/RT$.[78a] If the terms involving the expansion coefficient α_V are neglected and $\Delta V^{\ddagger}=-15$ cm^3 mol^{-1} and $\kappa=10^{-4}$ bar^{-1} are used, one predicts from these relations a decrease in E_a by 7.5 kJ mol^{-1}, a decrease in $\lg(A/M^{-1}s^{-1})$ by 0.2 units and an increase in the rate constant by a factor of 12 upon a pressure increase of 5000 bar.
[78] a) M. J. Pilling, P. W. Sears, *Reaction Kinetics*, Oxford Science, Oxford, **1995**, p. 160; b) K. A. Connors, *Chemical Kinetics*, VCH, Weinheim, **1990**; c) M. R. J. Dack, *J. Chem. Educ.* **1974**, *51*, 231.
[79] Effects of solvent polarity and internal pressure are difficult to separate because the internal pressure increases with increasing polarity.[78b,c]
[80] a) B. Giese, G. Kretschmar, *Chem. Ber.* **1984**, *117*, 3160; b) Y. Maeda, P. Schmid, D. Griller, K. U. Ingold, *J. Chem. Soc. Chem. Commun.* **1978**, 525; c) A. Salikhov, H. Fischer, *Appl. Magn. Reson.* **1993**, *5*, 445; d) O. Ito, M. Matsuda, *J. Phys. Chem.* **1984**, *88*, 1002, and refs therein.
[81] Recent theoretical studies on the addition reactions of alkyl radicals to alkenes include: a) K. N. Houk, M. N. Paddon-Row, D. C. Spellmeyer, N. G. Rondan, S. Nagase, *J. Org. Chem.* **1986**, *51*, 2874; b) R. Arnaud, R. Subra, V. Barone, F. Lelj, S. Olivella, A. Sole, N. Russo, *J. Chem. Soc. Perkin Trans. 2* **1986**, 1517; c) T. Clark, *J. Chem. Soc. Chem. Commun.* **1986**, 1774; d) T. Fueno, M. Kamachi, *Macromolecules* **1988**, *21*, 908; e) C. Gonzales, C. Sosa, H. B. Schlegel, *J. Phys. Chem.* **1989**, *93*, 2435; f) C. Gonzales, C. Sosa, H. B. Schlegel, *J. Phys. Chem.* **1989**, *93*, 8388; g) R. Arnaud, *New J. Chem.* **1989**, *13*, 543; h) H. Zipse, J. He, K. N. Houk, B. Giese, *J. Am. Chem. Soc.* **1991**, *113*, 4324; i) R. Arnaud, S. Vidal, *New J. Chem.* **1992**, *16*, 471; j) D. J. Tozer, J. S. Andrews, R. D. Amos, N. C. Handy, *Chem. Phys. Lett.* **1992**, *199*, 229; k) C. Schmidt, M. Warken, N. C. Handy, *Chem. Phys. Lett.* **1993**, *211*, 272; l) T. P. Davis, S. C. Rogers, *Macromol. Theory Simul.* **1994**, *3*, 905; m) V. Barone, L. Orlandini, *Chem. Phys. Lett.* **1995**, *246*, 45; n) A. Bottoni, *J. Chem. Soc. Perkin Trans. 2* **1996**, 2041; o) M. T. Nguyen, S. Creve, L. G. Vanquickenborne, *J. Phys. Chem.* **1996**, *100*, 18422; p) B. Jursic, *J. Chem. Soc. Perkin Trans. 2* **1997**, 637; q) A. K. Chandra, M. T. Nguyen, *J. Chem. Soc., Perkin Trans. 2* **1997**, 1415; r) J. Korchowiec, T. Uchimaru *J. Phys. Chem. A* **1998**, *102*, 2439; s) R. Arnaud, V. Vetere, V. Barone, *Chem. Phys. Lett.* **1998**, *293*, 295; t) R. Arnaud, N. Bugaud, V. Vetere, V. Barone, *J. Am. Chem. Soc.* **1998**, *120*, 5733.

[82] M. W. Wong, L. Radom, *J. Phys. Chem.* **1998**, *102*, 2237.
[83] "Controlled Radical Polymerization": L. Radom, M. W. Wong, A. Pross, *ACS Symp. Ser.* **1998**, *685*, 31.
[84] See, for example, J. I. Steinfeld, J. S. Francisco, W. L. Hase, *Chemical Kinetics and Dynamics*, Prentice Hall, New Jersey, **1989**.
[85] a) B. J. Smith, L. Radom, *J. Phys. Chem.* **1995**, *99*, 6468; b) L. A. Curtiss, P. C. Redfern, B. J. Smith, L. Radom, *J. Chem. Phys.* **1996**, *104*, 5148.
[86] A. G. Baboul, L. A. Curtiss, P. C. Redfern, K. Raghavachari, *J. Chem. Phys.* **1999**, *110*, 7650.
[87] L. A. Curtiss, P. C. Redfern, K. Raghavachari, V. Rassolov, J. A. Pople, *J. Chem. Phys.* **1999**, *110*, 4703.
[88] C. J. Parkinson, L. Radom, unpublished resutls.
[89] P. M. Mayer, C. J. Parkinson, D. M. Smith, L. Radom, *J. Chem. Phys.* **1998**, *108*, 604.
[90] J. A. Montgomery, Jr., M. J. Frisch, J. W. Ochterski, G. A. Petersson, *J. Chem. Phys.* **1999**, *110*, 2822.
[91] Similarly good correlations have been observed by Arnaud, Barone, and co-workers.[81t].
[92] a) "Modelling the Hydrogen Bond": T. A. Keith, M. J. Frisch, *ACS Symp. Ser.* **1994**, *569*, 22; b) K. B. Wiberg, T. A. Keith, M. J. Frisch, M. Murcko, *J. Phys. Chem.* **1995**, *99*, 9072.
[93] It has also been customary in such discussions to use various relative reactivity scales (σ scales) which are thought to reflect substituent effects on the rate constants and barriers of mechanistically similar reactions. Here, we prefer the more physically based energy quantities because they allow a more quantitative formulation.
[94] T. Ni, R. A. Caldwell, L. A. Melton, *J. Am. Chem. Soc.* **1989**, *111*, 457.
[95] K. D. Jordan, P. D. Burrow, *Acc. Chem. Res.* **1978**, *11*, 341.
[96] For theoretical plots of this type, see for example: refs. [12, 26–29, 81d, 81t, 82].
[97] M. Walbiner, H. Fischer, *J. Phys. Chem.* **1993**, *97*, 4880.
[98] In Equation (3), the enthalpy effect and the polar effects appear as multiplicative factors and not as additive terms of the activation energy. This nonlinear combination of effects evolved from considerations of the state correlation diagram (Figure 3) and the constructions of Figures 9–11. We note that other authors[99a–d] have used advanced multiple linear regressions, linear principal component analyses, and other additive schemes in previous analyses of our and related addition rate data with the aim of classifying the radical addition behavior. Apart from the questionable application of linear methods, the important interrelations of the energy parameters were not explicitly considered. Hence, some of the earlier results such as the suggested nucleophilicity of the *tert*-butoxycarbonylmethyl and the cyanomethyl radicals[99b] are now in doubt. However, in a linear analysis of activation energies for hydrogen abstraction reactions, Roberts et al.[99e] found an enthalpy dependence which is very close to that observed here.
[99] a) K. Héberger, A. Lopata, *J. Chem. Soc. Perkin Trans 2* **1995**, 91; b) K. Héberger, A Lopata, *J. Org. Chem.* **1998**, *63*, 8646; c) G. A. Bakken, P. C. Jurs, *J. Chem. Inf. Comput. Sci.* **1999**, *39*, 508; d) E. Denisov in *General Aspects of the Chemistry of Radicals* (Ed.: Z. B. Alfassi), Wiley, New York, **1999**; e) B. P. Roberts, A. J. Steel, *J. Chem. Soc. Perkin Trans 2* **1994**, 2155.
[100] Nucleophilic and electrophilic parameters C_n and γ_n, and C_e and γ_e, respectively, (all values in eV) for the polar influence (with values for phenyl-substituted alkenes given in parentheses are): methyl $C_n = 6.5$ (6.0) eV, $\gamma_n = 3.2$ (2.0), benzyl $C_n = 5.5$ (5.0), $\gamma_n = 1.5$ (0.75), hydroxymethyl, *tert*-butyl, and 2-hydroxy-2-propyl $C_n = 6.0$ (5.5), $\gamma_n = 2.0$ (1.0), 2-cyano-2-propyl $C_n = 6.0$ (5.5), $\gamma_n = 2.0$(1.0), $C_e = 4.5$ (4.2), $\gamma_e = 2.5$ (2.5), 2-*tert*-butoxycarbonyl-2-propyl $C_n = 6.0$ (5.5), $\gamma_n = 1.5$ (0.75), $C_e = 4.5$ (4.0), $\gamma_e = 2.0$ (2.0), cyanomethyl $C_n = 6.0$ (5.5), $\gamma_n = 3.0$ (2.0), $C_e = 4.5$ (4.2), $\gamma_e = 3.0$ (3.0), *tert*-butoxycarbonylmethyl $C_n = 6.0$(5.5), $\gamma_n = 3.0$ (1.5), $C_e = 4.5$ (4.0), $\gamma_e = 3.0$ (3.0), cyclic malonyl $C_e = 4.0$ (3.5), $\gamma_e = 4.3$ (3.5), trifluoroacetonyl $C_e = 4.5$ (4.0), $\gamma_e = 3.0$ (2.5).
[101] a) A. Citterio, A. Arnold,F. Minisci, *J. Org. Chem.* **1979**, *44*, 2674; A. Citterio, F. Minisci, A. Arnoldi, R. Pagano, A. Paravicini, D. Porta, J. *Chem. Soc. Perkin Trans. 2* **1978**, 519.
[102] a) For trifluoromethyl and perfluoro-*n*-alkyl radicals, lg $(A/M^{-1}s^{-1}) = 8.2$ is assumed to be larger than for other tertiary radicals because of the pyramidal radical structure. $\Delta H_r = -40$ kJ mol^{-1} is estimated from enthalpies of formation and bond dissociation energies given in refs. [20, 67, 103]. The addition is more exothermic than that of methyl because of the strong CF_n–CH_2 bond in the resulting adduct radical. $E_{ea}(R) = 2.8$ eV,[104] $C_e = 4.5$ (4.0) eV, $\gamma_e = 3.0$ (3.0) eV (cf. cyanomethyl and *tert*-butoxycarbonylmethyl), and no nucleophilic correction is applied, that is $F_n = 1$. b) For the hexenyl radical, $lg(A/M^{-1}s^{-1}) = 8.5$, as for a primary alkyl, $\Delta H_r = +5$ kJ mol^{-1}, as estimated for the addition of the ethyl radical from enthalpies of formation and bond dissociation energies given in ref. [105]. $E_i(R) = 8.5$ eV,[106] $C_n = 6.0$ (5.5) eV, $\gamma_n = 2.5$ (1.25) eV (cf. methyl and hydroxymethyl), $F_e = 1$. c) For cumyl radical, $lg(A/M^{-1}s^{-1}) = 7.5$ is applied as for a tertiary radical, $\Delta H_r = +72$ kJ mol^{-1}, $E_i(R) = 6.6$ eV,[59] $C_n = 5.5$ (5.0) eV, $\gamma_n = 1.3$ (1.3) eV (cf. benzyl), $F_e = 1$. d) For *p*-cyanobenzyl the data, $lg(A/M^{-1}s^{-1})$ and ΔH_r as for benzyl are used. $E_i(R) = 7.85$ eV,[21] polar parameters as for benzyl, $F_e = 1$.
[103] a) R. Asher, B. Ruscic, *J. Chem. Phys.* **1997**, *106*, 210; b) J. M. Martell, R. J. Boyd, Z. Shi, *J. Phys. Chem.* **1993**, *97*, 7208.
[104] J. H. Richardson, L. M. Stephenson, J. I. Brauman *Chem. Phys. Lett.* **1975**, *30*, 17.
[105] a) J. Berkowitz, G. B. Ellison, D. Gutman *J. Phys. Chem.* **1994**, *98*, 2744; b) S. G. Lias, J. E. Bartmess, J. F. Liebman, J. L. Holmes, R . D. Levin, W. G. Mallard, *J. Phys. Chem. Ref. Data* **1988**, *17*, Suppl. 1.
[106] D. V. Dearden, J. L. Beauchamp, *J. Phys. Chem.* **1985**, *89*, 5359.
[107] Using our standard estimation procedures for methyl additions,[69] we arrive at a minor (and probably insignificant) difference of $\Delta H_r = +4$ kJ mol^{-1} between 2-butene and propene and a substantial difference of $\Delta H_r = +21$ kJ mol^{-1} between stilbene and styrene. With the Evans–Polanyi–Semenov relation [Eq. (2)], these differences translate into increases in the activation energy of 1 kJ mol^{-1} and 4.6 kJ mol^{-1}, respectively. For the stilbenes, the increase is compatible with the experimental findings (Table 12).
[108] This is contrary to an earlier statement[6] that the steric hindrance manifests itself primarily in the activation energy and only to a much smaller extent in the pre-exponential factor. However, this suggestion was mostly based on data for addition rates of small radicals (methyl, trifluoromethyl etc.) to alkenes with rather small α substituents such as methyl and fluorine atoms, and may not hold more generally.
[109] A. R. Bader, R. P. Buckley, F. Leavitt, M. Szwarc, *J. Am. Chem. Soc.* **1957**, *79*, 5621; F. M. Lewis, F. R. Mayo, *J. Am. Chem. Soc.* **1948**, *70*, 1533.
[110] J. M. Tedder, J. C. Walton, K. D. R. Winton, *J. Chem. Soc. Faraday Trans. 1* **1972**, *68*, 1866; H. C. Low, J. M. Tedder, J. C. Walton, *J. Chem. Soc. Faraday Trans. 1* **1976**, *71*, 1707; J. N. Cape, A. C. Greig, J. M. Tedder, J. C. Walton, *J. Chem. Soc. Faraday Trans. 1* **1975**, *71*, 592.
[111] If one uses the absolute energies of $CH_3CF_2CH_3$ and $CH_3CH_2CHF_2$ and the C–H bond dissociation energies calculated by Dolbier et al.[20] for an estimation of reaction enthalpy, the addition of methyl to the substituted carbon of $CH_2{=}CF_2$ is enthalpy favored by about 30 kJ mol^{-1} because of the formation of the strong CH_3–CF_2 bond but disfavored by about 20 kJ mol^{-1} because of the formation of a less stabilized radical. The more facile addition of trifluoromethyl than methyl is because of more favorable enthalpic and polar factors.[102]
[112] a) M. J. Jones, G. Moad, E. Rizzardo, D. H. Solomon, *J. Org. Chem.* **1989**, *54*, 1607; b) E. Canadell, O. Eisenstein, G. Ohanessian, J. P. Poblet, *J. Phys. Chem.* **1985**, *89*, 4856.
[113] a) M. Buback, T. Dröge, *Macromol. Chem. Phys.* **1999**, *200*, 256; b) D. M. Huang, M. J. Monteiro, R. G. Gilbert, *Macromolecules* **1998**, *31*, 5175; c) M. Buback, C. H. Kurz, C. Schmaltz, *Macromol. Chem. Phys.* **1998**, *199*, 1721.
[114] a) G. Moad, D. H. Solomon, *The Chemistry of Free Radical Polymerization*, Pergamon, Oxford, **1995**; b) G. Moad, E. Rizzardo, D. H. Solomon, A. L. J. Beckwith, *Polymer Bull.* **1992**, *29*, 647.
[115] For alkyl methacrylates, the propagation constants vary by up to a factor of three with the structure of the alkyl ester residue. According to careful considerations of the error correlation of activation parameters, this effect appears mainly to be a result of variations in the frequency factor and not in the activation energy.[116]
[116] a) M. Buback, C. H. Kurz, *Macromol. Chem. Phys.* **1998**, *199*, 2301; b) R. A. Hutchison, S. Beuermann, D. A. Paquet, Jr., J. H. McMinn, *Macromolecules* **1997**, *30*, 3490; c) For first principle calculations of

activation parameters of propagation reactions, see J. P. A. Heuts, R. G. Gilbert, L. Radom, *Macromolecules* **1995**, *28*, 8771.

[117] *Polymer Handbook* (Eds.: Y. Brandrup, E. H. Immergut), Wiley, New York, **1989**. Where more than one value was available, the most recent copolymerization parameter was preferred, and the rate constants of the model reactions were taken at the polymerization temperature.

[118] T. Fukuda, Y.-D. Ma, H. Inagaki, *Macromolecules* **1985**, *18*, 17; R. A. Hutchinson, J. H. McMinn, D. A. Paquet, Jr., S. Beuermann, C. Jackson, *Ind. Eng. Chem. Res.* **1997**, *36*, 1103; M. L. Coote, L. P. M. Johnston, T. P. Davis, *Macromolecules* **1997**, *30*, 8191, and refs therein.

[119] B. Giese, R. Engelbrecht, *Polym. Bull.* **1984**, *12*, 55; S. A. Jones, G. S. Prementine, D. A. Tirrell, *J. Am. Chem. Soc.* **1985**, *107*, 5275; D. A. Cywar, D. A. Tirell, *J. Am. Chem. Soc.* **1989**, *111*, 7544.

[120] M. L. Coote, T. P. Davis, L. Radom, *Macromolecules* **1999**, *32*, 2935; M. L. Coote, T. P. Davis, L. Radom, *J. Mol. Struct. (THEOCHEM)* **1999**, *461–462*, 91; M. L. Coote, T. P. Davis, L. Radom, *Macromolecules* **1999**, *32*, 5270.

[121] J. P. A. Heuts, R. G. Gilbert, I. A. Maxwell, *Macromolecules* **1997**, *30*, 726.

[122] "Controlled/Living Radical Polymerization" (Ed.: K. Matyjaszewski): M. L. Coote, T. P. Davis, L. Radom, *ACS Symp. Ser.* **2000**, *768*, 82.

[123] a) M. Weber, Ph.D. Thesis, University of Zürich, **2000**; b) M. Weber, M. Spichty, H. Fischer, unpublished results.

[124] Landolt-Boernstein, *Magnetic Properties of Free Radicals*, New Series, Group II, *Vols. 1, 9b, 17b* (Ed.: H. Fischer), Springer, Berlin, **1967**.

[125] The decrease in the CH_2 couplings of adducts to acryl and methacryl derivatives with the increasing size of the adding radical R• was noted long ago and was interpreted in the same way: H. Fischer, *Z. Naturforsch. A* **1964**, *19*, 866; H. Fischer, G. Giacometti, *J. Pol. Sci. C* **1967**, *16*, 2763. For line-broadening effects of the propagating radical of methacrylic acid, see H. Fischer, *Polym. Lett.* **1964**, *2*, 529.

[126] Such a connection has been suggested before: H. Tanaka, K. Sasai, T. Sato, T. Oda, *Macromolecules* **1988**, *21*, 3534.

[127] M. Szwarc, *J. Phys. Chem.* **1957**, *61*, 40; M. Szwarc, J. H. Binks, *Theoretical Organic Chemistry*, Butterworth, London, **1952**, p. 262 (Kekule Symposium); "The Transition State": M. Szwarc, *Spec. Publ. R. Soc. Chem.* **1962**, *16*, 91, and refs therein. A more complete list of references to the early work has been given in ref. [58b]

[128] R. Arnaud, V. Barone, S. Olivella, A. Sole, *Chem. Phys. Lett.* **1985**, *118*, 573.

[129] K. Héberger, S. Kemény, T. Vidoczy, *Int. J. Chem. Kinet.* **1987**, *19*, 171.

[130] An example of the factorization of enthalpic and polar effects into individual contributions of the radical and the alkene is provided by the Alfrey–Price Q-e Scheme which is widely used to rationalize copolymerization parameters.[117] An improved variant, the "revised patterns" scheme, was recently applied successfully to extract alkene-independent polar radical parameters for most of our radicals from the data of Table 1.[131] The operational success of these factorization methods can not be denied. However, for suitable radical and alkene polar parameters they lead to an increase of the barrier, that is, a rate decreasing polar effect. This is at variance with the prediction of the state correlation diagram, and even the simpler FMO models, that CT interactions in the transition state can only reduce the barrier and increase the rate.

[131] A. D. Jenkins, *Polymer* **1999**, *40*, 7045.

[132] Recently, most of our rate constants (Table 1) have been analyzed using various chemometric methods,[133] and nonlinear models indeed led to better predictions than linear ones. However, the resulting parameters have no simple physical interpretation.

[133] K. Héberger, A. P. Borosy, *J. Chemom.* **1999**, *13*, 473.